UNIVERSIDAD NACIONAL AUTÓNOMA DE MÉXICO

PROGRAMA DE POSGRADO EN CIENCIAS DE LA TIERRA

INSTITUTO DE GEOLOGÍA

CIENCIAS AMBIENTALES

FORMACIÓN DEL FRAGIPÁN Y SU RELACIÓN CON LA PEDOGÉNESIS DE SUELOS QUE LO INCORPORAN EN ZONAS CLIMÁTICAS CONTRASTANTES

TESIS

QUE PARA OPTAR POR EL GRADO DE

DOCTORA EN CIENCIAS DE LA TIERRA

PRESENTA:

Lilit Pogosyan

COMITÉ TUTOR:

Dr. Sergey Sedov (tutor), Instituto de Geología, UNAM

Dra. Blanca Lucía Prado Pano, Instituto de Geología, UNAM

Dr. Pavel Vladimirovich Krasilnikov, Universidad Estatal de Moscú, Rusia

Ciudad de México, septiembre de 2021

CODIGO DE ÉTICA:

“Declaro conocer el Código de Ética de la Universidad Nacional Autónoma de México, plasmado en la Legislación Universitaria. Con base en las definiciones de integridad y honestidad ahí especificadas, aseguro mediante mi firma al calce que el presente trabajo es original y enteramente de mi autoría. Todas las citas de, o referencias a, las obras de otros autores aparecen debida y adecuadamente señaladas, así como acreditadas mediante los recursos editoriales convencionales.”

DEDICATORIA

A mi familia, que siempre me ha apoyado y nunca ha dudado de mí.

Y a todos aquellos que a lo largo de mi camino me han enseñado a hacer preguntas y buscar respuestas.

AGRADECIMIENTOS

Al Instituto de Geología UNAM y el Posgrado en Ciencias de la Tierra, por aceptarme en el programa de doctorado y dar todo el apoyo posible para realizar mi investigación y presentarla al nivel internacional.

Al CONACyT y a la UNAM, por la beca otorgada que ha hecho posible hacer mi doctorado en México con una estancia en Rusia que se necesitaba para hacer el trabajo de campo y análisis en los laboratorios.

Al Instituto de Biología del Centro de Investigación de Karelia de la Academia de Ciencias de Rusia, por el proyecto 0221-2017-0047 y el apoyo con el trabajo de campo.

A la Universidad Estatal M.V. Lomonosov de Moscú, Instituto de Geografía de la Academia de Ciencias de Rusia y el Instituto V.V. Dokuchaev de Ciencia del Suelo por todo el apoyo con los análisis en sus laboratorios y consultas, que me han ayudado a mejorar mi investigación.

A mi tutor, Dr. Sergey Sedov, le agradezco mucho por todo el conocimiento que me ha compartido, tanto sobre la ciencia como de la vida, durante estos años. Muchas gracias por ayudarme a lograr mis metas y mucho más de lo que yo podía pensar y también muchas gracias por su confianza.

Al Dr. Pavel Vladimirovich Krasilnikov, por los valiosos consejos y por haber ayudado a encontrar el tema de estudio y la manera de realizar la investigación.

A la Dra. Blanca Prado Pano, por apoyarme en las situaciones difíciles, y por ayudarme con el estudio de porosidad y el análisis tomográfico que resultó ser tan importante para toda mi investigación.

A la Dra. Elizabeth Solleiro Rebolledo, por aceptarme en el grupo de Paleosuelos, por ayudar a hacer lo imposible y lo posible también. Sin su apoyo no hubiera llegado a este momento.

A la Dra. Teresa Pi Puig, por tratarme como su alumna, por enseñarme todo lo que se puede saber sobre la mineralogía de arcillas, por siempre encontrar tiempo, por las conversaciones, por la confianza.

A María Luisa Reyes Ochoa, Araceli Chamán, Gloria Alba y Erika Ulloa por su apoyo, por aclarar todas las dudas y siempre encontrar las soluciones.

A la Dra. Annick Dannels, por su interés y por siempre ayudar a mejorar mi trabajo.

A los doctores Serafín Sánchez Pérez y Bruno Chávez Vergara, aprendí mucho de sus platicas y comentarios.

Al Maestro Jaime Díaz Ortega, por compartir con todos nosotros su talento, experiencia y buen humor.

A Fabiola Vega García y Daniel Ramos Pérez, por enseñarme a hacer los análisis químicos en el Laboratorio de Geoquímica Ambiental.

A Yaz, por su enseñanza en el laboratorio de Paleosuelos. A Gina, por siempre compartir sonrisa y ser el corazón del grupo. A Gildo, por ayudarme tantas veces. A Fer, Karla, Axel, Pamela, Sol, Ema y Eliuth, por hacerme sentir parte de un equipo. A Thania y Marta, por la bonita experiencia de compartir con ustedes una semana de la conferencia. A Manuel, Yusnier y Hugo, por su amistad.

A Reyna y Mariana, por ser mis mejores amigas. A ustedes y toda su familia, les agradezco mucho por enseñarme lo mejor de este hermoso país.

A Edy, por enseñarme quien soy, por apoyarme en mi carrera, en pandemia, por ser imparable, por darme la esperanza, por hacerme querer ser mejor y mejor cada día.

A mi familia, incluso los que ya no están. Ha sido difícil irme tan lejos, verlos tan pocos días durante estos años, pero ninguna distancia ha podido hacerme sentir sola. ¡Los quiero mucho!

Índice

Resumen

El fragipán es un horizonte subsuperficial compactado de suelo distribuido en varios países del mundo. Se caracteriza por su alta densidad y estructura de bloques poligonales, separados por grietas que sirven como conductos de agua y raíces de plantas, debido a que estas no pueden penetrar la matriz del bloque. Estando dentro del perfil de suelo, el fragipán sirve como un acuicludo y puede favorecer las condiciones *stágnicas* en las capas superiores. Su origen sigue siendo una cuestión abierta y se han desarrollado varias hipótesis. Una de la hipótesis es su desarrollo desde el permafrost de los ambientes periglaciales que supuestamente ha ocurrido al final del Pleistoceno Tardío. Esta hipótesis concuerda bien con el mapa de distribución de los fragipanes en Estados Unidos de América (EUA), donde el límite norte del área de distribución coincide con el límite de expansión máxima de la Glaciación de Wisconsin, mientras que en el oeste coincide con el límite de la distribución actual de los bosques. Sin embargo, hay fragipanes en otros países, incluso tropicales, que no han tenido glaciares durante el desarrollo del suelo. Por esta razón la hipótesis dominante es la de hidroconsolidación, la cual explica la formación del fragipán por la reorganización de las partículas tamaño arcilla de la matriz, conectando los granos gruesos y reorganizando el espacio poroso. En este trabajo se ha hecho un análisis comparativo de suelos con fragipanes desarrollados en condiciones contrastantes. Se han aplicado varias técnicas de estudio, en particular el espacio poroso se ha estudiado con los métodos de análisis en la muestra inalterada en 2D y 3D. El estudio del fragipán ha revelado el acceso a la memoria edáfica que contiene y la que se usó para la reconstrucción paleoambiental.

Como objetos de estudio se eligieron dos áreas en Rusia y México. El suelo ruso se encuentra en la región de Karelia, bajo clima húmedo y con cubierta de nieve constante desde noviembre hasta abril. El área de estudio se caracteriza como un paisaje relativamente joven donde el suelo se ha desarrollado sobre una morrena de deglaciación formada hace aproximadamente 13 mil años. Por otro lado, el objeto de estudio en México son los tepetates tipo fragipán del estado Tlaxcala, estudiados en la barranca de Santiago de Tlalpan. Las condiciones actuales son de clima húmedo templado, con la temporada de lluvias desde mayo hasta octubre. La barranca está en un bloque elevado, a una altura de 2600 m s.n.m. El tepetate se encuentra en una secuencia pedosedimentaria y está posicionado sobre un Vertisol datado a 33 mil años A.P.

La memoria edáfica contenida dentro de los horizontes *frágicos* y comparada con la memoria de los perfiles completos ha permitido acceder a la secuencia de los procesos ocurridos durante el desarrollo del suelo. En el caso de Karelia el fragipán se ha formado después de la formación de

un perfil tipo Luvisol, que probablemente ocurrió durante el Máximo del Holoceno. Después, el clima se hizo más frio y en la zona de transición de la zona eluvial hacia la iluvial se ha formado el fragipán, lo que ha restringido la iluviación de arcilla. El espacio poroso del fragipán es entre 12.5 y 15%, y consiste mayormente de poros texturales, mientras que poros de otro tipo son casi ausentes. La presencia del fragipán ha provocado el proceso *stágnico* y formación de nódulos de hierro en el horizonte E. Los procesos actuales de actividad biológica y criogénesis no han perturbado el horizonte endurecido. En el caso de Tlaxcala el tepetate tipo fragipán se ha formado de un pedosedimento saturado de agua y posteriormente se ha transformado a un horizonte *árgico* donde los cutanes de iluviación han favorecido la compactación adicional del fragipán. La porosidad total del fragipán es de 27%, constituida mayormente por poros texturales y el resto por poros-canales rellenos de arcilla iluviada. En el horizonte superior al fragipán se han formado nódulos de hierro, al igual que en Karelia. Probablemente en el perfil de Tlaxcala esto pasó durante el Pleistoceno Tardío, MIS2. Luego, el perfil se sepultó y el desarrollo de suelos superiores en el clima árido del Holoceno no perturbó al fragipán. Sin embargo, su presencia ha afectado al desarrollo del paisaje: con la actividad agrícola de los últimos 3000 años se ha formado una red de barrancas en el área y el perfil de estudio se encuentra en riesgo de desaparecer en los próximos años. De manera general en esta tesis se concluye que en condiciones contrastantes entre Karelia y Tlaxcala, a través de diferentes procesos pedogenéticos, se ha formado el fragipán, lo que es un ejemplo de isomorfismo. Además, el detallado de la memoria edáfica de los tepetates puede revelar la información de evolución del paisaje, lo que ha sido aplicado en esta investigación.

Abstract

The fragipan is a compacted subsurface soil horizon which occur in many countries around the world. It is characterized by high bulk density and polygonal blocky structure, so its structure units are divided by cracks that serves as conduct for water and roots. While being hidden in soil the fragipan function as an aquiclude and favors *stagnic* conditions in overlying horizons. Its origin is still under discussion and there are several hypotheses of its formation. One of such hypotheses is that its formation is related to permafrost of periglacial environments that occurred at the end of the Late Glacial. This hypothesis is in agreement with general map of distribution of fragipans in United States of America, where the northern limit of fragipan distribution coincide with the maximum boundary of Wisconsin Glaciation, while the western limit follows the limit of actual distribution of forest. Nonetheless, there are fragipans in other countries, including those in tropics, that did not suffer any glacial influence during soil formation. For this reason, the most dominant hypothesis is the hydroconsolidation, which explains the fragipan formation as reorganization of clay size particles in soil matrix, so they connect coarse grains and reorganize pore space. In this study comparative analysis of soils with fragipans developed in contrasting conditions was done. Different techniques of analysis were applied but pore space was studied by methods of analysis in undisturbed samples in 2D (micromorphology) and 3D (Computed Tomography). The study of the fragipan revealed the access to soil memory and it was applied for the paleoenvironmental reconstruction.

Two area of investigation were chosen, in Russia and Mexico. The Russian soil is located at the Karelia region, in humid climate and with snow cover from November until April. The area of investigation is characterized by relatively young landscape developed on glacial till of approximate age of 13ka. Another object of study is fragipan type tepetate located in Tlaxcala State, Mexico. The actual conditions are characterized the humid climate and rain season from May until October. It is located the high of 2600 m above sea level. The tepetate was found in soil-sedimentary sequence and is located above a paleosol dated to 33 ka.

The soil memory contained at the fragipans was compared to the soil memory of complete soil profiles. It allowed to access to the sequence of soil forming process. In case of Karelia the fragipan was formed after clay illuviation which probably occurred at the Holocene Optimum. After that, the climate has changed to a colder one and the fragipan was formed at the transition zone between eluvial and illuvial parts of the profile and has restricted further clay illuviation. The porosity of fragipan is between 12.5 and 15 %, it consists mostly of textural pores, while pores of other types are almost absent. The presence of fragipan has provoked water stagnation and formation of iron

nodules at the E horizon. Actual processes of biogenic and cryoturbation did not disturb the compacted horizon. In case of Tlaxcala the fragipan was formed from a pedosediment saturated by water and posteriorly it was transformed to an *argic* horizon where clay coatings have favored additional compaction of fragipan. Fragipan porosity is about 27% and it consists mostly of textural pores and of remains of pores-channels filled by illuviated clay. At the overlying horizon iron nodules were formed, like in case of Karelia. The formation of iron nodules in Tlaxcala sequence most likely happened at the Late Pleistocene, MIS 2. After that the profile was buried and posterior soil development in arid climate of Holocene did not affect the fragipan. However, its presence affected the landscape development: the agricultural activity of last 3000 years provoked a net of gullies at the area of study and the studied profile is under risk of disappearance. Summarizing, this investigation has concluded that in contrasting climatic conditions of Karelia and Tlaxcala different soil forming processes led to fragipan formation, which is a case of isomorphism. Also, it was concluded that the soil memory of fragipans contains important information about landscape evolution, and it was applied in this study.

Introducción

Fragipán es un término de las clasificaciones internacionales del suelo WRB (IUSS Working Group WRB, 2015) y Soil Taxonomy (Soil Survey Staff, 2014), que se refiere a un horizonte subsuperficial natural no cementado pero endurecido de tal manera que el agua y las raíses de las plantas lo atraviesan únicamente por las grietas poligonales que separan los bloques estructurales. Este horizonte, estudiado por décadas, hasta el día de hoy sigue siendo de interés científico, tanto por su proceso de formación como por la complejidad del manejo del suelo en las áreas donde está presente y también por su significado paleoambiental. A pesar de que el término "fragipán" y los estudios sobre este tema nacieron en los Estados Unidos de América (EUA) y Europa, el fragipán se encuentra también en otras partes del mundo, entre las cuales están Canadá, Nueva Zelanda (FAO, 1974; Witty y Knox, 1989), Inglaterra, Brasil (Witty y Knox, 1989), Indonesia (Suharta y Prasetyo, 2009), México (Krasilnikov, 2016) e Irán (Eghbal et al., 2012).

Los fragipanes se encuentran sobre todo en los suelos desarrollados en loess, pero también en las morrenas o depósitos coluviales o aluviales de las terrazas fluviales y lacustres. Se encuentran en una variedad de clases texturales posibles: la mayoría se ha encontrado en clase franco, pero puede ser más limoso o arcilloso, o hasta arenoso. El fragipán típicamente se encuentra en posiciones elevadas del paisaje y con drenaje desarrollado, con más frecuencia en las regiones con el régimen de humedad Udic. La presencia tan amplia de los fragipanes a nivel mundial en diversos suelos provoca dificultades para explicar cómo se ha desarrollado y cuál es su papel en el funcionamiento y evolución del suelo.

A través de los años, la hipótesis de su formación evolucionó desde cementación por sílice (Steinhardt y Franzmeier 1979; Karathanasis, 1989; Tremocoldi et al., 1994; Norfleet y Karathanasis,1996; Duncan y Franzmeier, 1999), compactación por la combinación de ciclos de humedad y secado (Attou y Brua, 1998; Miller et al., 1971a,b), compactación por la presión alta de un glaciar (Lindbo y Veneman 1993; Miller et al., 1993), hasta la propuesta de que en un ambiente periglacial se combinan factores físicos y químicos y ocurre un proceso identificado como hidroconsolidación (Bryant 1989; Assalay et al., 1998; Weisenborn y Schaetzl, 2005). En este proceso se supone que arcilla acumulada en el horizonte se reorganiza y crea puentes entre los granos de minerales resultando en una reorganización del espacio poroso, lo cual es la hipótesis dominante en últimos años.

En el año 2013 se publicó unartículo sobre los fragipanes en EUA (Bockheim y Hartemink) donde mostraron en un mapa la distribución de todos los suelos estudiados con el horizonte fragipán. En este mapa, la frontera norte del área de distribución coincide con el límite de expansión máxima de la Glaciación de Wisconsin, mientras la frontera del oeste coincide con el límite de la distribución actual de los bosques. A la base de la hipótesis de la formación en los ambientes periglaciales, Van Vliet-Lanoë y Langohr (1981) han propuesto la formación del fragipán a través del permafrost, que también sigue siendo actual para los fragipanes formados en loess durante la Glaciación de Würm (análogo de la Glaciación de Wisconsin en Europa) y que se encuentran en Bélgica y Francia. Se encontró la similitud entre la estructura poligonal del fragipán y las grietas del permafrost. Además, ellos observaron que la expansión de los fragipanes tiene límites y que la frontera superior del fragipán como un horizonte coincide muy bien con el límite abrupto del permafrost.

En Rusia existen suelos similares en los cuales se reportan horizontes fragipanes, así como la misma combinación de los factores con los cuales se formaron algunos de los fragipanes en Estados Unidos o en Europa. No obstante, apenas hay solo una publicación donde se menciona la presencia de horizontes fragipanes en suelos de Rusia (Krasilnikov y Gerasimova, 2004). Por lo tanto, todavía no hay estudios que verifiquen los procesos de formación de los fragipanes en Rusia. El fragipán en Rusia se encuentra en el estado de Karelia, en la zona que se ha liberado de la Glaciación de Valday (análogo de la Glaciación de Wisconsin en Rusia). En particular, el suelo que contiene fragipán se ha formado en la morrena de aproximadamente 13 ka de edad (Svendsen et al., 2004), lo que implica el desarrollo del suelo dentro del Holoceno.

Al mismo tiempo hay fragipanes en otras regiones que pertenecen a zonas con clima Tropical y Subtropical, donde no ha habido glaciación, cuyos sedimentos se formaron por el volcanismo durante el Cuaternario. Los procesos de formación de dichas capas se estudian independientemente de las hipótesis de estudios de fragipanes de zonas afectadas por glaciación. Por ejemplo, en México hay una clase de fragipán que se llama tepetate tipo fragpan. El término “tepetate” se usaba anteriormente para cualquier suelo o capa endurecida, en la actualidad se refiere a una capa endurecida formada en material piroclástico. Hay diferentes tipos de tepetates y uno de estos es tepetate tipo fragipán. En un territorio de 660,000 km^2 de la República Mexicana se reporta la presencia de tepetates de diferentes tipos (Flores et al., 1991). Varios autores relacionan el

endurecimiento de los tepetates con diferentes formas de sílice (Campos y Dubroeucq, 1990; Dubroeucq 1992; Hidalgo et al., 1992; Miehlich 1992; Quantin 1992; Poetsch y Arinkas, 1997; Poetsch, 2004), sin embargo, mencionan que no es la única razón de su endurecimiento y proponen la combinación de sílice y minerales arcillosos. Por ejemplo, en el trabajo nombrado "La cementación de los tepetates: estudio de la silificación" de Hidalgo et al. Se dice: "los principales resultados indican que la presencia de sílice es evidente y aun cuando la silificación podría ser un proceso reciente queda por precisar la contribución secundaria de la pedogénesis y la localización de la sílice que contribuye al endurecimiento. […] Finalmente concluyó que la sílice no era la única causa del endurecimiento de los tepetates." Con referencia a este artículo entre otros, el Dr. Prat y coautores (2015) explican el origen de los tepetates como geológico, con una posterior fase pedogenética. También hay autores que suponen que durante los periodos de actividad volcánica se depositan materiales piroclásticos que se desplazan pendiente abajo con fuertes eventos de lluvias, en forma de flujos laháricos, y se depositan en las posiciones intermedias del glacis incorporando materiales edáficos re-depositados (Solleiro-Rebolledo et al., 2003; Díaz-Ortega et al., 2010).

La presencia de la arcilla iluviada en los tepetates tipo fragipán indica su participación en el desarrollo del suelo y formación por procesos pedogenéticos. Eso implica la posibilidad de estudios de la memoria edáfica (Targulian y Goryachkin, 2004) en los tepetates y su aplicación para los estudios de diferentes épocas. La abundancia de cutanes de iluviación permite considerar que los tepetates normalmente se encuentran en los Luvisoles, como la mayoría de los fragipanes. La importancia del proceso de consolidación de los minerales arcillosos iluviados ha sido el objeto de estudio en laminas delgadas de los tepetates (Oleschko et al.,1992; Acevedo-Sandoval et al., 2004). La abundancia de los cutanes de iluviación permite clasificar los tepetates tipo fragipán como horizontes Btx (Gutiérrez-Castorena et al., 2007). Sin embargo, el Dr. Prat con referencia a este estudio doctoral de los tepetates de Tlaxcala (comunicación personal, 2021) no está de acuerdo en nombrar a un horizonte con illuviación de arcilla como un Bt sino como una toba u horizonte C. Esta opinión está en desacuerdo con los principios básicos de la génesis de suelo y el papel de los cutanes de illuviación en edafología establecido en 1960 por Brewer y desarrollado posteriormente.

Un grupo de tepetates muy estudiado por la comunidad científica son los que se localizan en el Valle de México y Tlaxcala, y justo en esos lugares predomina el tepetate tipo fragipán (Etchevers et al., 2006), y se observa con abundancia en diversas secuencias pedosedimentarias de diferentes edades. Una de esas secuencias en el estado de Tlaxcala, en la barranca Tlalpan (Santiago de Tlalpan), ha sido conocida desde los setentas (Heine y Schönhals, 1973), posteriormente fue estudiada en noventas por Miehlich (1991) y Hessman (1992) y luego por M. Haulon bajo supervisión del Dr. G. Werner en los años 2002-2005. En su trabajo, Haulon menciona que el endurecimiento de los tepetates no se puede explicar solo por la cementación con sílice, sino también por la iluviación de la arcilla (Haulon et al., 2007). La capa superior de la secuencia contiene un horizonte de tepetate que yace sobre un paleosuelo de la edad de 33 ka (Sedov et al., 2009). Encima del tepetate mencionado hay otros suelos, y la secuencia completa que se estudió tiene más de dos metros de profundidad. Sedov et al. ha estudiado la memoria edáfica de los paleosuelos de la secuencia, sin embargo, no quedó estudiado el fragipán como una fuente de información paleoambiental.

La amplia distribución de los fragipanes en el mundo y gran variedad de hipótesis que explican su formación por diferentes procesos revela la importancia de un estudio comparativo de los fragipanes en los sitios contrastantes de Karelia y Tlaxcala para aportar al conocimiento sobre el desarrollo de este horizonte y su presencia en diferentes sitios. La memoria edáfica que contiene el perfil del suelo con fragipán en Rusia es importante para el conocimiento de procesos de formación de suelo y evolución del paisaje en Karelia durante el Holoceno. El estudio completo de la secuencia pedosedimentaria en Tlaxcala es importante fuente de información sobre la evolución del paisaje y cambios climáticos del pasado en el territorio del México Central, donde hay poca información sobre el periodo de la transición del Pleistoceno Tardío al Holoceno. En particular, un apoyo importante para tal estudio comparativo de los horizontes compactados no cementados sería el estudio de las muestras inalteradas, donde se pueda observar y analizar el espacio poroso, que forma una parte importante de la memoria edáfica. Es confuso la falta de información sobre el espacio poroso de los fragipanes, cuya organización de la matriz se ha estudiado muy poco a pesar de su importancia. Mientras tanto, la mayoría de los estudios del fragipán se basa en muestras alteradas y tratadas para análisis físicos y químicos.

Hipótesis: el fragipán tiene un papel en el desarrollo del perfil del suelo y tiene memoria edáfica que permite hacer la reconstrucción del ambiente pasado.

Por lo tanto, se proponen los siguientes objetivos de este estudio:

Objetivo general: estudiar la morfogénesis de los fragipanes, así como su papel en el desarrollo del perfil que los contiene y su relación con las condiciones ambientales del presente y del pasado.

Objetivos particulares:

- Investigar en 2D y 3D la organización de la matriz del fragipán y su porosidad en la muestra inalterada para definir las etapas de su formación.
- Investigar cómo se incorpora el fragipán en el desarrollo de un perfil eluvio-iluvial de suelo tipo Retisol.
- Estudiar las etapas de formación de la secuencia tephro-paleopedológica de Tlaxcala usando el tepetate tipo fragipán como una parte de memoria.

Metodología

Para abordar este tema se aplicaron los siguientes métodos, cuya descripción detallada se encuentra en los capítulos de los resultados. En este capítulo se presenta la justificación de uso de cada método y se define su contribución anticipada al desarrollo del modelo pedogenético y paleoecológico de formación de los fragipanes estudiados

Trabajo de campo

Descripción en el campo (capítulos 3.1, 3.2, 3.3, Anexo 1)

- Para hacer la descripción completa de los perfiles estudiados y definir los tipos de suelo generales de acuerdo con la clasificación internacional WRB (IUSS Working Group WRB system, 2015) y toma de muestras (Karelia y Tlaxcala). El principio básico de la investigación programada consiste en el estudio detallado que abarca no solamente los horizontes de fragipán, pero también otros horizontes pedogenéticos (recientes y antiguos) y estratos sedimentarios que acompañan a los fragipanes en los perfiles estudiados. Eso con el fin de entender cómo el desarrollo del fragipán está relacionado con los procesos pedogenéticos que generan el cuerpo edáfico completo y sus horizontes.

Análisis con georadar (GPR) y reflectómetro de dominio del tiempo (TDR) (Capitulo 3.3)

- Para poder analizar con el método no invasivo la extensión lateral del horizonte fragipán en la cobertura edáfica a la distancia de 52m del perfil de estudio en Karelia.

Técnicas de análisis en la muestra no alterada

La porosidad como uno de los rasgos morfológicos que se ha estudiado implica la necesidad de estudio de las muestras inalteradas. El método más común siempre fue el análisis micromorfológico de la lámina delgada en 2D, sin embargo, este método tiene límites (capitulo 3.2). Últimamente se ha desarrollado el uso de la Tomografía Computacional en los estudios 3D del suelo. La importancia del estudio de la porosidad en 3D y su memoria se refleja en el incremento drástico de la cantidad de estudios publicados en los últimos 5 años.

Análisis micromorfológico (capítulos 3.1, 3.2, 3.3, Anexo 1)

- Para diferenciar los rasgos edáficos a diferentes escalas y hacer un estudio en 2D del espacio poroso que permitió estudiar la secuencia de los procesos pedogenéticos ocurridos. Se han hecho en detalle las observaciones micromorfológicas en cada horizonte de los dos perfiles de estudio (Karelia y Tlaxcala).

Tomografía Computacional (capítulos 3.1, 3.2, Anexo 1)

- Para analizar en detalle los poros en 3D y poder complementar los datos obtenidos en 2D (Karelia y Tlaxcala). Los análisis cuantitativos en 3D se han aplicado para la comparación más detallada de la porosidad en los fragipanes y los horizontes más cercanos, en particular: horizontes EBx, Btx y Bt en Karelia, y 3EBtx y 3BCtx en Tlaxcala.

Técnicas de análisis en la muestra alterada

Difracción de Rayos X (capítulo 3.3)

- Para conocer la composición mineralógica del perfil de estudio en Karelia y a base de esto analizar los procesos de formación del perfil completo y el papel de los minerales esmectíticos en la compactación del fragipán.

Análisis granulométrico (capítulo 3.3, Anexo 1)

- Para poder definir las etapas sedimentarias por los diferentes patrones de distribución de la fracción gruesa en los horizontes de los perfiles en Tlaxcala y Karelia y analizar los cambios texturales derivados por los procesos de formación del suelo.

Fluorescencia de Rayos X (Anexo 1)

- Para conocer la distribución de los elementos mayores (Fe, Ca, K) y traza (Ti) a lo largo del perfil de suelo en Tlaxcala y definir fases de intemperismo activas por falta de minerales que se remueven fácilmente (K, Ca) y que se conservan prácticamente sin cambio en su concentración (Fe, Ti) y, a través de la pedogénesis, poder relacionarlos con los cambios climáticos del pasado.

Parámetros magnéticos χlf y χld (Anexo 1)

- Para determinar las fases activas de la pedogénesis a través de la concentración relativa de los minerales ferromagnéticos (χlf) y el contenido de las partículas superparamagnéticas (χld) relacionadas con la pedogénesis.

Bioindicadores (Anexo 1)

- Para determinar fitolitos y otros bioindicadores que pueden dar información específica de la cubierta vegetal antigua y así contribuir a la reconstrucción de los ambientes en las cuales se han formado.

Resultados

La tesis se presenta en base a los artículos que se encuentran en la parte de los resultados. Hay tres artículos publicados (capítulos 3.1-3.3) y uno sometido a la revista y que actualmente está en proceso de revisión (revisión mayor) (Anexo 1).

Morphogenesis and quantification of the pore space in a tephra-palaeosol sequence in Tlaxcala, central Mexico

Pogosyan L., Gastelum A., Prado B., Marquez J., Abrosimov K., Romanenko K., Sedov S. 2019 Morphogenesis and quantification of the pore space in a tephra-palaeosol sequence in Tlaxcala, central Mexico. Soil Research 57, 559-565.

Este artículo describe los aspectos de la porosidad estudiada en las muestras inalteradas y revela las fases de desarrollo del espacio poroso en los tepetates tipo fragipán en Tlaxcala.

How is the fragipán incorporated in the pore space architecture of a boreal Retisol?

Pogosyan L., Abrosimov K., Romanenko K., Marquez J., Sedov S. 2019 How is the fragipán incorporated in the pore space architecture of a boreal Retisol? Soil Research 57, 566-574.

Este artículo describe los aspectos de porosidad de horizonte frágico en el suelo estudiado en Rusia, haciendo el análisis en las muestras inalteradas y comparando la porosidad en todo el perfil del suelo.

Pedogenesis of a Retisol with fragipán in Karelia in the context of the Holocene landscape evolution

Pogosyan, L., Sedov, S., Pi-Puig, T., Ryazantsev, P., Rodionov, A., Yudina, A.V., Krasilnikov, P., 2018. Pedogenesis of a Retisol with fragipán in Karelia in the context of the Holocene landscape evolution.Baltica, 31 (2), 134-145

Este artículo propone un modelo de desarrollo de perfil de suelo durante el Holoceno, dividiendo las etapas de formación más contrastantes, que se definieron a la base de diferentes métodos de estudio.

Anexo 1 Evidence for stages of landscape evolution in Central Mexico during the Late Quaternary 1 from paleosol-pedosediment sequences

Sycheva, S.A., Pogosyan, L., Sedov, S., Golyeva, A.A., Barceinas Cruz, H., Abrosimov, K.N., Romanenko, K.A., Solleiro Rebolledo, E., 2021 1.1 Stages of soil formation and erosion in the Central Mexican Plateau in the Late Pleistocene and Holocene. Quaternary Research. *Revisión mayor.*

Este artículo propone un modelo de desarrollo del paisaje en México Central durante el Pleistoceno Tardío y el Holoceno, basado en las propiedades de los horizontes *frágicos.* El trabajo incluye una síntesis de estudio geomorfológico de múltiples perfiles de la barranca hecho por coautores del artículo, y la estudiante contribuyó en esta publicación con la parte de estudio analítico detallado del perfil Tlalpan analizado durante su doctorado.

Comentario: en la versión de la tesis enviada al Jurado en junio de 2021 este artículo estuvo incluido como un archivo pdf generado por la revista Quaternary Research al momento de subir el manuscrito. El artículo fue revisado y se encuentra en la etapa de corrección siguiendo los comentarios de los dos editores, dos árbitros y de los miembros del Jurado. Sin embargo, algunos de los comentarios están relacionados con las correlaciones de la parte del estudio geomorfológico y las figuras, lo cual actualmente está en elaboración con los coautores. Los comentarios con referencia al perfil Tlalpan que fue el objeto de estudio de la tesis doctoral ya están corregidos. En la versión de la tesis de agosto de 2021 en al Anexo 1 está el texto corregido del artículo.

CSIRO PUBLISHING
Soil Research
https://doi.org/10.1071/SR18185

Morphogenesis and quantification of the pore space in a tephra-palaeosol sequence in Tlaxcala, central Mexico

L. Pogosyan[A,E], *A. Gastelum*[B], *B. Prado*[C], *J. Marquez*[B], *K. Abrosimov*[D], *K. Romanenko*[D], *and S. Sedov*[C]

[A]Posgrado en Ciencias de la Tierra, Instituto de Geología, Universidad Nacional Autónoma de México, Ciudad Universitaria, 04510, Mexico City, Mexico.
[B]Instituto de Ciencias Aplicadas y Tecnología, Universidad Nacional Autónoma de México, Circuito Exterior S/N, Ciudad Universitaria, 04510, Mexico City, Mexico.
[C]Instituto de Geología, Universidad Nacional Autónoma de México, Ciudad Universitaria, 04510, Mexico City, Mexico.
[D]V.V. Dokuchaev Soil Science Institute, 119017 Moscow, Russia.
[E]Corresponding author. Email: lilit-tos@yandex.ru

Abstract. Tepetates are indurated subsoil horizons developed in tephra-derived materials in various parts of the Trans-Mexican Volcanic Belt. The term 'tepetate' includes fragipans, duripans, pedosediments and saprolites, derived from vitric rhyolitic tuff, Pleistocene volcanic ashes or pyroclastic flows. All soils with tepetates are at high risk of erosion and so they have been intensively studied for decades. The tepetates are common in Tlaxcala State of central Mexico, being formed under Ustic Isomesic soil climate. The aim of this investigation was to characterise the pore space of fragipan-type tepetates and the role of clay components in their formation. We studied porosity of tepetate from a tephra-palaeosol sequence in the north of Tlaxcala State, in undisturbed soil samples. Observations of pore space were made in 2D and 3D by analysing microscope images of thin sections and cross-sectional images from a computed tomography scanner. In the thin sections we also identified and described clay illuvial pedofeatures. Micromorphological observations showed two main pore types. Small rounded pores had a homogeneous distribution and were probably formed before the clay illuviation process that took place in a palaeosol formed on the tepetate material. The distribution pattern of the small pores in the studied tepetate was similar to that in the fragic horizon, which was probably formed by a hydro-consolidation process. Large crack-pores were formed during the palaeosol formation. Later these large pores were filled by illuvial clay coatings and so we conclude that each tepetate was part of the set of Bt horizons in the palaeosols of Luvisol type.

Additional keywords: 3D computer tomography, clay illuviation, fragipan.

Received 30 June 2018, accepted 26 March 2019, published online 28 May 2019

Introduction

Soils with indurated horizons, known as tepetate, present the most vulnerable component of the central Mexican soil mantle, with high risk of erosion and badland formation that has motivated intensive study of these horizons over recent decades. The term tepetate is derived from Nahuatl (Aztec language) meaning 'stone bed' (Williams 1972; Gama-Castro *et al*. 2007) and does not belong to any formal modern soil classification. Nowadays the most common meaning of this term is a sub-surface hardened horizon developed in the tephra deposits of central Mexican volcanic highlands (Zebrowski 1992), either exposed on the surface after erosion of the overlying soil, or as part of the soil profile at variable depth (Etchevers *et al*. 2003). Tepetates occupy an area of 30 700 km^2 and cover ~27% of the Trans-Mexican Volcanic Belt (Peña and Zebrowski 1991). In Tlaxcala State, tepetates are very common and cover 2175 km^2, of which 598 km^2 are exposed to the surface and represent ~15% of the state's surface (Werner 1988). As a result, tepetates in this area have been more extensively studied than anywhere else in Mexico.

Tepetates correspond to fragic and duric diagnostic horizons of WRB (IUSS Working Group WRB 2015) – fragipans and duripans of Soil Taxonomy (Soil Survey Staff 2014). Their presence accelerates erosion because these layers hamper infiltration and promote surface runoff and lateral water flow. Normally tepetates can be found in gully landscapes as a result of anthropogenic activity (Quantin and Zebrowski 1995) (Fig. 1). Tepetates are usually located in the lower part of the profiles of Luvisols, Cambisols, Vertisols and other mature soils forming their BC and C horizons. Proposals for detailed classification of tepetates were presented by Dubroeucq *et al*. (1989). The hardening depends on different factors such as the nature of the original material or deposition conditions. According to Miehlich (1992), tepetates in Tlaxcala State are

Fig. 1. Tepetate horizons (red arrows) in tephra-palaeosol sequence of the Tlalpan gulley, Tlaxcala State, Mexico.

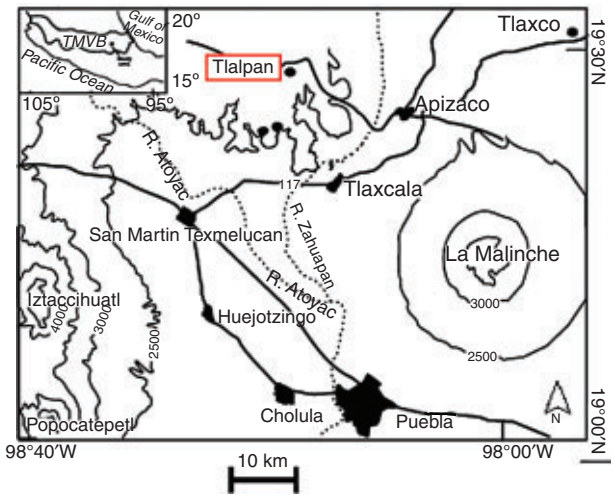

Fig. 2. Map of study area of Tlalpan showing a disposition of the tephra-palaeosol sequence (according to Sedov *et al*. 2009). TMVB, Trans-Mexican Volcanic Belt.

consolidated by amorphous silica cementation, the silica being a product of volcanic ash weathering. Until now the hypothesis of cementation with amorphous silica has been the most accepted explanation for tepetate induration (Campos and Dubroeucq 1990; Dubroeucq 1992; Quantin 1992; Poetsch 2004). An alternative hypothesis explains formation of at least part of tepetate with compaction during pedosediment deposition by lahars or mudflows (Díaz-Ortega *et al*. 2011; Sedov 2015).

The tepetates involved in our study show the properties of fragic horizon or fragipan as defined in both international soil classifications mentioned above (Soil Survey Staff 2014; IUSS Working Group WRB 2015). Although they are very hard and compact when dry, they easily slake when placed in water. It is improbable that materials cemented with silica could have such properties. Usually silica cementation causes irreversible hardening, observed in the duric horizon or duripan (Flach *et al*. 1992) – also known as silcretes in the geological literature (Thiry 1992). Fragipan development is related to the compaction and pore space reduction due to specific clay particle distribution. There are different modern theories for its formation, explaining compaction by a combination of physical processes. One of them, for example, is the 'Bryant hydro-consolidation' hypothesis, which involves a collapse of soil structure when it is 'loaded and wet', and this collapse happens because of clay bonding (clay-bridging) agents (Assallay *et al*. 1998). In addition to *in situ* clay reorganisation, clay translocation due to illuvial processes could also contribute to the compaction and reduction of pore space in tepetate. As mentioned above, tepetate frequently occurs within Luvisol profiles. Sedov *et al*. (2009) found that most palaeosols within the Tlaxcala tephra-palaeosol sequence show evidence of clay illuviation. Oleschko *et al*. (1992) and Sedov *et al*. (2009) described a large variety of the clay illuvial pedofeatures in central Mexican tepetate. We suppose that illuviation processes reduce pore space by filling it with translocated clay and thus contribute to the induration of these horizons.

The purpose of our morphological study was to assess reorganisation of pore space in fragipan-type tepetates compared with non-tepetate horizons of the same profile and to verify if this reorganisation is connected with clay precipitation in the pore space.

Materials and methods

Study area

The study area is located in the Tlaxcala block, which is part of the Trans-Mexican Volcanic Belt in central Mexico (Fig. 2). The Tlaxcala block was uplifted in the early Miocene (Mooser 1975). The block is bounded to the west by the Sierra Nevada and to the east by Malinche volcano. The research was conducted in the Tlalpan gulley (19°28′N; 98°18.6′W). The modern climate of the study area corresponds to a subhumid-temperate, with a mean annual temperature of 13°C and annual rainfall of 600–700 mm (García 1988) providing Ustic soil moisture and Mesic soil temperature regimes. Natural vegetation cover was, centuries ago, mixed oak forest, now largely substituted with agricultural lands. Since tepetates are very common in this region it is intensively studied by soil scientists. Geologically, this area was formed by Pleistocene volcanic deposits that cover Pliocene diatomites with underlying lacustrine sediments (Sedov *et al*. 2009). The studied profile comprised the uppermost part of the section exposed in the Tlalpan gulley, where Hessmann (1992) described a complete tephra-palaeosol sequence including seven tepetate layers and buried Cambisols and Luvisols between them. The description was later refined by Sedov *et al*. (2009). According to the predominant colour of soil and tepetate material, the whole sequence was separated into three main units: Grey, Brown and Red Units (Sedov *et al*. 2009). In the oldest, the Red Unit, the Matuyama–Brunhes geomagnetic reversal was detected, setting a reliable chronological marker at the bottom of the sequence (Soler-Arechalde *et al*. 2015). Below the Red Unit there were basaltic lava flows.

In this study we focused only on the Grey Unit (Fig. 3), which is uppermost in the sequence. The studied section is located 300 m to the east of the key-exposure Tlalpan, studied and dated by Sedov *et al*. (2009), and just 100 m to the south-west of the profile investigated micromorphologically by Poetsch (2004). In this paper, we use indexes of palaeosols

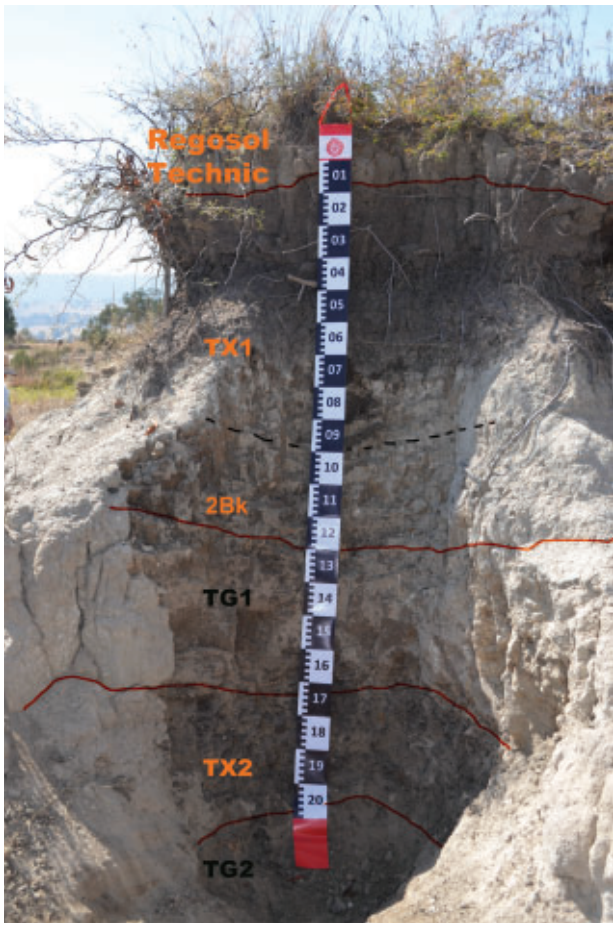

Fig. 3. Tlaxcala tephra-palaeosol sequence, the Grey Unit.

proposed by Sedov *et al*. (2009), whereas for tepetate horizons of the Grey Unit we propose specific indexes TG1 and TG2, which mark tepetates related to palaeosols TX1 and TX2 respectively.

From top downward, the Grey Unit consists of the modern Regosol Technic, which overlays the first palaeosol (TX1), first grey tepetate (TG1), second palaeosol (TX2) and second grey tepetate (TG2). In the bottom of TX1 there is a 2Bk horizon that is in contact with TG1 (Fig. 3).

The Regosol Technic has greyish colouration and contains artefacts: ceramic shards, burned stones and obsidian flakes. The TX1 palaeosol is dark grey coloured at the A horizon and has two B horizons with blocky structure. The lowest, 2Bk horizon, contains no carbonates in groundmass and does not react with HCl; however, a few hard calcitic concretions of 2 cm in diameter are observed there. The TG1 horizon has columnar structure, where columnar blocks are separated by large fissures. The lowest palaeosol of the Grey Unit (TX2) is a Vertisol, which overlies the TG2 horizon, of 33 595 ^{14}C year BP (Sedov *et al.* 2009). Below the TG2 tepetate lies the first tepetate unit.

Methods

One section of the Grey Unit of Tlaxcala tephra-palaeosol sequence (2.6 m depth) was described in the field and sampled for different morphological observations. Since tepetates naturally have columnar structure, it was easy to collect undisturbed samples by extracting the columnar blocks along the fissures. The profile was excavated in the isolated hill because in other places this unit was mostly eroded (Fig. 3).

The profile includes modern soil, represented by an Ah horizon and underlying palaeosols, interlayered with tepetate horizons. In the lower part of the first palaeosol there is a 2Bk horizon which rests on the first tepetate horizon. Under this tepetate (TG1) there is a vertic palaeosol (TX2) overlying a second tepetate (TG2). Under this second tepetate there is an older tepetate layer of brown colour (Fig. 3).

For micromorphological description of macro- and meso-pores we prepared thin sections for each horizon. Thin sections (30 µm thick) were prepared using undisturbed soil samples preserving the original vertical orientation. The samples were impregnated at room temperature with the resin Cristal MC-40, studied under a petrographic microscope and described following the terminology of Bullock *et al*. (1985).

The computed tomography (CT) analysis is described below:

High resolution CT

(1) Sample preparation: for each horizon, one sample of equal size (2 cm) and shape was collected; one from the 2Bk horizon and the second from the tepetate TG1 horizon. They were hermetically packed in plastic containers to protect them from drying.

(2) Scanning and 3D reconstruction of images: scanning was done on a 3D scanner Bruker SkyScan 1172 with 3.15 µm pix^{-1} resolution and 100-kV acceleration tension of the X-ray tube. This resolution allows detection of water conducting pores ~10 µm and solid particles of such size. Reconstruction of tomography images was done in the Bruker SkyScan 'NRecon' software (Bruker 2018*a*).

(3) Data analysis was conducted with the Bruker SkyScan 'CTan' software (Bruker 2018*b*). The minimum object (pore) size for meaningful analysis was set to 6.3 µm pix^{-1} to comply with the Nyquist sampling limit of our scanner resolution of 3.15 µm pix^{-1} (the Nyquist criterion requires sampling of half the size of the feature of interest or, given a sampling resolution, the minimum size of the feature is fixed as twice the sample spacing). CTan performed a volume reconstruction from the stack of images and then the software applied the standard method of Otsu's thresholding to binarise the volume, providing a 3D array with pore structures. CTan obtained the following descriptors from the volume of interest: number of pores, porosity, bounding box, volume of solid phase and amount of contacts between solid phases of pore walls. Porosity is the volume of all pores divided by the total volume, a closed pore is defined as a connected set of void voxels fully surrounded in 3D by solid voxels, and an open pore has some void voxels connecting one of the volume walls. The size distribution of pores and solid phase components were derived, also in percent of volume. The size range could be adjusted to filter very small or very large pores, but the automatic option of 'all pore sizes' was employed.

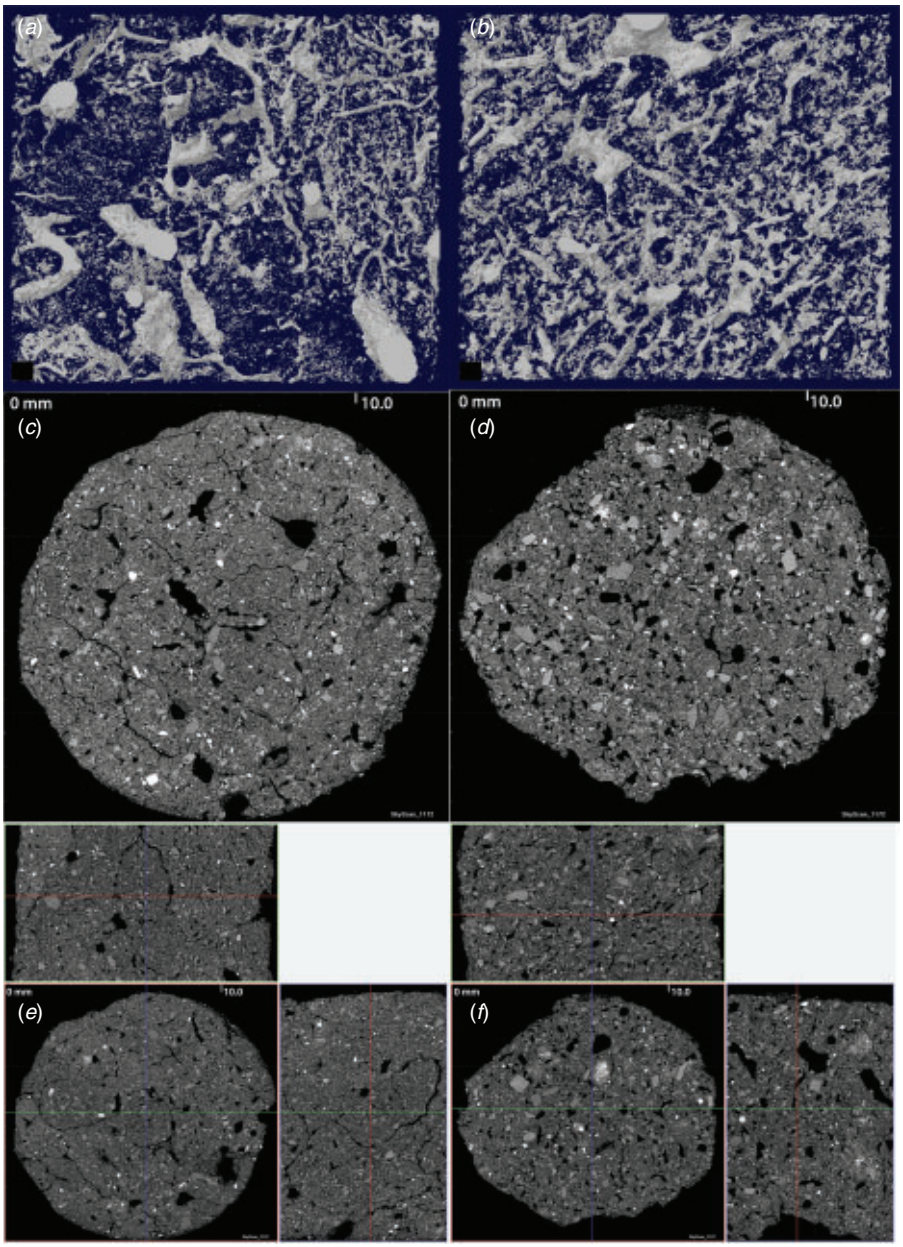

Fig. 4. The pore space from 3D CT in 6.3 μm pix^{-1} resolution. (*a*) Part of the volume model of pore space of 2Bk horizon, size 1 cm × 0.8 cm × 0.03 cm. (*b*) Part of the volume model of pore space of 2Bk horizon, size 1 cm × 0.8 cm × 0.03 cm. (*c*) Slice picture with scale, horizontal CT image of 2Bk horizon; solid phase, different shades of grey; mineral grains, white; pores, black. (*d*) Slice picture with scale, horizontal CT image of TG1 horizon; solid phase, different shades of grey; mineral grains, white; pores, black. (*e*) Vertical and horizontal images of 2Bk sample; solid phase, different shades of grey; mineral grains, white; pores, black. (*f*) Vertical and horizontal images of TG1 sample; solid phase, different shades of grey; mineral grains, white; pores, black.

Axial tomographic images were generated in the Brucker SkyScan 'DataViewer' program from the original acquisitions (generated by the scanner as coronal slice images, with respect to the volume sample). The software 'CTvox' produced a volume model for further analysis and 'DataViewer' allowed its interactive visualisation (Fig. 4).

Low resolution CT

From the whole profile, samples of volume 37 cm^3 of the tepetate horizons and overlying soil horizons were imaged using the CT-scanner Nikon Metrology XT H 225 with a 225-kV reflection target. The scan resolution in this case was 57 μm pix^{-1}. The pores in the volume were labelled and segmented

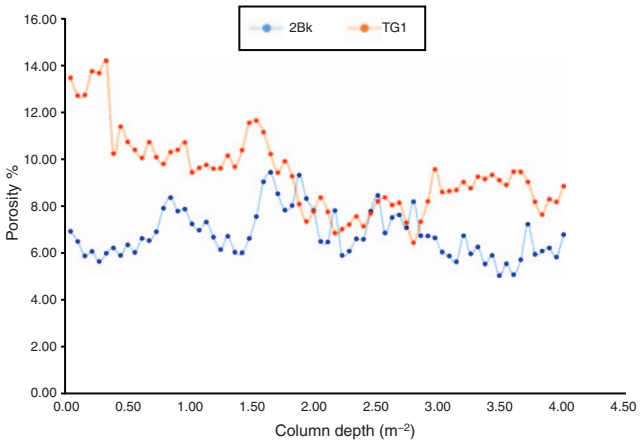

Fig. 5. The 2D porosity in 2Bk and TG1 horizons by CT in 57 µm pix^{-1} resolution slice.

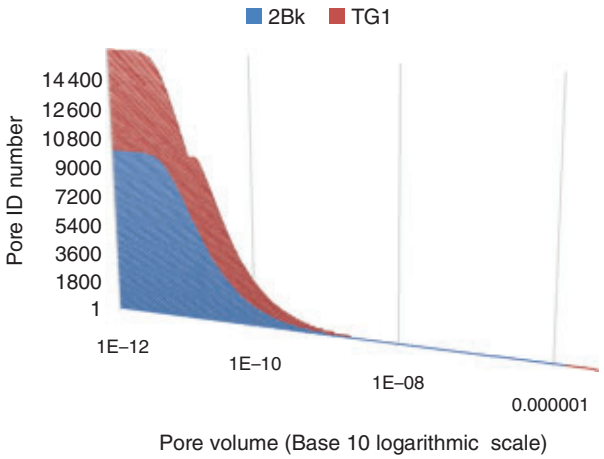

Fig. 6. Pore volume distribution in 2Bk and TG1 horizons by CT in 57 µm pix^{-1} resolution.

using the module fuzzy – c – means clustering method of the program SMAS (Gastelum-Strozzi 2018). The porosity percentage with respect to the depth of the samples is shown in Fig. 5 and the frequency of different pore volume sizes for each sample in Fig. 6.

Results

Morphological observations of thin sections under a petrographic microscope

The thin sections showed strong evidence of pedogenic processes. Clay illuviation pedofeatures were detected in the palaeosol B horizons and tepetates (Fig. 7).

Modern Regosol Technic

The A horizon – had a fine granular structure, abundant pores and most of the material had been affected by biogenic activity.

First palaeosol TX1

2A – poorly developed granular structure, compact with lower porosity and higher frequency of cracks, it had a grey humus pigmentation.

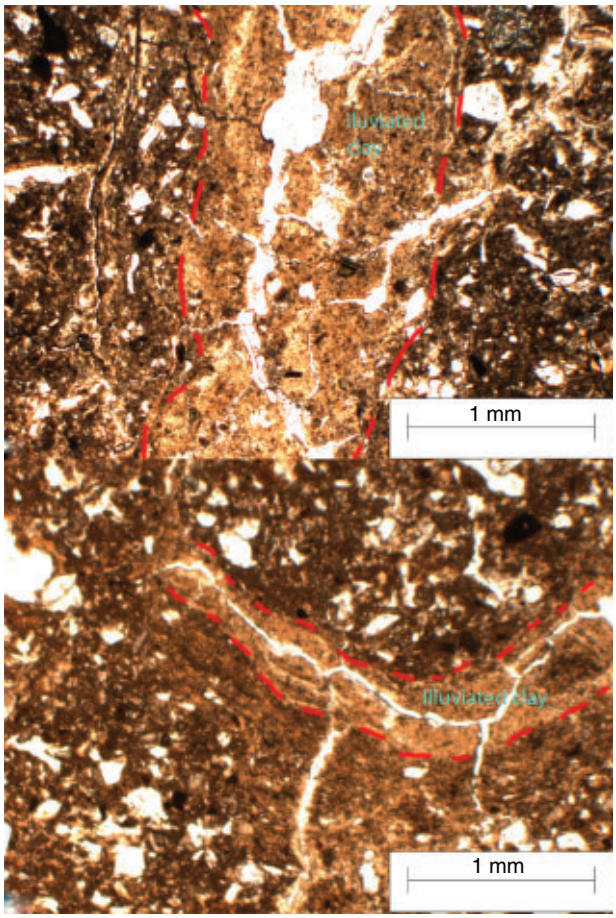

Fig. 7. Micromorphological photographs of clay coatings of TG1 horizon. The red line indicates original walls of pore cracks. The original pore space was reduced after the clay illuviation.

2B – blocky structure and few deformed illuvial clay coatings.

2Bk – very few and deformed illuvial clay coatings.

First grey tepetate TG1

In this sample, clay coatings were frequent and well developed. It had very few pores and they were mostly filled with well-preserved illuvial clay.

Second palaeosol TX2

Vertic palaeosol had a 3 ABi horizon that showed strong evidence of clay illuviation processes before formation of vertic palaeosol. Clay coatings in this case were deformed by vertic cracks and slickensides and partly incorporated into the groundmass.

Second grey tepetate TG2

TG2 had no vertic attributes, but illuvial clay coatings and infillings occupied more pore space than in TG1. In this horizon there were almost no open pores and illuvial clay pedofeatures were very well preserved.

In thin sections, observed by petrographic microscope, more than 80% of the original space of large pores was filled with illuvial clay in the course of palaeo-pedogenesis (Fig. 7*a*, *b*). It is important to mention that these data have low sensitivity because of the thickness of the thin sections (30 μm).

Quantification and morphological description of the pore space based on 3D CT images

The high resolution CT showed the pore space in 2Bk, represented by several pore types (Fig. 4). Large pores were formed by plant roots or animals. The largest pore was 1–1.5 mm in diameter (mean diameter in horizontal images), which occupied the major part of the porosity volume. About 50% volume of the sample was occupied by small closed pores (15–50 μm) inside the aggregates. The minor part of sample pore space comprised crack interaggregate pores, clearly detected by 3D scanning. No pore types had exact vertical orientation. The distribution of small rounded pores in the studied sample was not uniform; there were several areas of high and low individual pore concentration.

In the TG1 horizon, the pore space was represented by interaggregate and intergrain packing pores and there were many small pores homogeneously distributed in all samples. Also a large number of channel pores of different size and deformation grade were detected. Connectivity of pore space was very low, and the tendency to preferential horizontal orientation of pores was tracked. To this end, thin sections (30 μm thick) were prepared using undisturbed soil samples, preserving the original vertical orientation. Total porosity in the 2Bk horizon was 23.9%, and 27.3% in the TG1 horizon.

The CT results with low resolution showed that porosity varied slightly with depth from 14% at the top to ~7% at the bottom in all samples (Fig. 5). Regarding the total number of pores, in the volume studied, the amount of pores varies from 10 000 to ~16 500. The largest pore in the samples had a volume of 2.2 cm^3 and the smallest had a volume of 1.5×10^{-4} cm^3. The results of morphological thin section observations showed that the 2Bk horizon had more large crack-pores and the TG1 horizon had more small pores (Fig. 6).

Discussion

Both micromorphological observations in the undisturbed samples, at the two different scales, showed the polygenetic origin of all main horizons of the profile. The distribution of illuvial clay coatings and organisation of pore space showed that the tepetate TG1 and related palaeosol TX1 experienced different soil forming processes. Most significantly, the clay illuviation process played a crucial role during one of the early stages of tepetate formation. The abundance of well-preserved clay coatings seen in the thin sections means that, during a certain period of palaeo-pedogenesis, the tepetate horizons occupied the position of a Bt horizon of the buried soil (probably the TX1) which developed on the past land surface. The illuviation was so intensive that the illuvial clay coatings filled the major part of the pore space of large crack-pores. As a result, the modern large crack-pores in the tepetate horizon were not well connected. We suggest that this is an additional reason for the high compactness of today's tepetate.

There were two main pore types found in the tepetate horizons: large crack-pores and small rounded pores uniformly distributed in all tepetates. Some of those small pores, detected by high resolution CT, were likely pores of volcanic glass and not directly connected with tepetate formation. However, a similar size distribution was observed at low CT resolution, where the smallest detected pores were larger than volcanic glass grains. We assume that these small rounded pores were formed during the consolidation process, before the formation of pore cracks followed by infilling with illuvial clay. At the later stage, new pores were formed as cracks; however, they were later partly filled by clay illuviation. In the case of vertic palaeosol, the formation of illuvial clay coatings in the 3ABi horizon probably happened at the same time as in the TG2 horizon. The 2Bk horizon was perhaps a lower part of the B horizon during the formation of upper palaeosol. The formation of calcitic concretions in the B horizon occurred much later. Radiocarbon dating indicated that this is related to recent pedogenesis (Sedov *et al*. 2009).

Conclusions

Analysis of porosity space in undisturbed samples allowed us to infer stages of pore space development in the horizons of the sequence. We conclude that during the development of all tepetates of the studied profile they were part of a Bt horizon with accumulation of illuvial clay in the pores, probably after the compaction processes. The vertic palaeosol developed after the stage of clay illuviation into tepetate Grey 2, so clay coatings in the 3ABi horizon were deformed by shrink–swell phenomena. The vertic process did not affect the lower part of the profile, which made possible the conservation of clay illuvial pedofeatures in the layer tepetate Grey 2 until now. The 2Bk horizon was originally an upper part of the illuvial horizon, because it had fewer clay coatings than the tepetate Grey 1. The morphological analysis of thin sections enabled us to assess the reorganisation of pore space compared to non-tepetate horizons of the same profile and to verify if this reorganisation was related to clay accumulation in pore space. Clay accumulation in pores of ancient illuvial horizons is an important factor of tepetate formation and reduction of their pore space. The 3D CT analysis showed that there were two main pore types in tepetates, corresponding to the different stages: small rounded pores were formed earlier than large pore cracks.

Conflicts of interest

The authors declare no conflicts of interest.

Acknowledgements

Lilit Pogosyan gratefully acknowledges CONACyT for her PhD scholarship (51849333-2). Field research was supported by the project PAPIIT IN106616 'Paleoecology, biotic transformation and cultural development during the late Pleistocene and beginning of the Holocene: paleopedological perspective'. The high resolution computed tomography analysis was done with the help of equipment of 'Functions and properties of soils and soil cover' from the shared-use centre of the Dokuchaev Soil Science Institute. The authors thank Jaime Diaz for his help in preparation of soil thin sections. We also thank two anonymous reviewers for their helpful comments that allowed us to improve the paper.

References

Assallay AM, Jefferson I, Rogers CDF, Smalley IJ (1998) Fragipan formation in loess soils: development of the Bryant hydroconsolidation hypothesis. *Geoderma* **83**, 1–16. doi:10.1016/S0016-7061(97)00135-3

Bruker (2018*a*) Micro-CT software support. Available at https://www.bruker.com/service/support-upgrades/software-downloads/micro-ct.html [verified 4 April 2019]

Bruker (2018*b*) Micro-CT software. Available at https://www.bruker.com/products/microtomography/micro-ct-software.html [verified 4 April 2019]

Bullock P, Fedoroff N, Jongerius A, Stoops G, Tursina T, Babel U (1985) 'Handbook for soil thin section description.' (Waine Research Publications: Wolverhampton, UK)

Campos A, Dubroeucq D (1990) Formación de tepetates en suelos provenientes de las alteraciones de materiales volcánico. *Terra (Helsinki, Finland)* **8**(2), 137–141.

Díaz-Ortega J, Solleiro-Rebolledo E, Sedov S (2011) Spatial arrangement of soil mantle in Glacis de Buenavista, Mexico as a product and record of landscape evolution. *Geomorphology* **135**, 248–261. doi:10.1016/j.geomorph.2011.02.012

Dubroeucq D (1992) Los tepetates de la región de Xalapa, Veracruz (México): un endurecimiento de origen pedológico. *Terra (Helsinki, Finland)* **10**, 233–240.

Dubroeucq D, Quantin P, Zebrowski C (1989) Los tepetates de origen volcánico en México. Esquema preliminar de clasificación. *Terra (Helsinki, Finland)* **7**, 3–12.

Etchevers JD, Hidalgo C, Prat C, Quantin P (2003) Tepetates of Mexico. In 'Encyclopedia of Soil Science'. (Ed. R Lal) pp. 1745–1748. (Marcel Dekker: New York, USA)

Flach KW, Nettleton WD, Chadwick OA (1992) The criteria of Duripans in the U.S. soil taxonomy and the contribution of micromorphology to characterize silica indurated soils. *Terra (Helsinki, Finland)* **10**, 34–45.

Gama-Castro J, Solleiro-Rebolledo E, Flores-Román D, Sedov S, Cabadas-Báez H, Díaz-Ortega J (2007) Los tepetates y su dinámica sobre la degradación y riesgo ambiental: el caso del Glacis de Buenavista, Morelos. *Boletín de la Sociedad Geológica Mexicana* **59**(1), 133–145. doi:10.18268/BSGM2007v59n1a11

García E (1988) 'Modificaciones al sistema de clasificación climática de Köppen: México.' (Instituto de Geografía, Universidad Nacional Autónoma de México)

Gastelum-Strozzi A (2018) SMAS: Soil morphological analysis software. Available at http://www.biocomlab.com/apps/SMAS.html [verified 14 May 2019]

Hessmann R (1992) 'Untersuchungen verhärteter Vulkanascheböden (Tepetate) in den Becken von Mexico und Tlaxcala (Mexico).'(Giessen, Bericht für die Kommission der Europäischen Gemeinschaft: Paris)

IUSS Working Group WRB 2015. World Reference Base for Soil Resources 2014, update 2015 International soil classification system for naming soils and creating legends for soil maps. World Soil Resources Reports No. 106. (FAO: Rome)

Miehlich G (1992) Formation and properties of tepetate in the Central highlands of Mexico. *Terra (Helsinki, Finland)* **10**, 137–144.

Mooser F (1975) Historia geológica de la cuenca de México, in Memoria de las obras del sistema de drenaje profundo del Distrito Federal México *Departamento del Distrito Federal* **1**, 7–38.

Oleschko K, Zebrowski C, Quantin P, Fedoroff N (1992) Patrones micromorfológicos de organización de arcillas en tepetates (México). *Terra (Helsinki, Finland)* **10**, 183–191.

Peña HD and Zebrowski C (1991) Los suelos volcánicos endurecidos en América Latina In 'Memoria Primer Simposio Internacional, Suelos Volcánicos Endurecidos (uso y manejo de tepetates)' pp. 151–155. (Colegio de Posgraduados, Montecillo, Edo. de México). [In Spanish]

Poetsch T (2004) Forms and dynamics of silica gel in a tuff-dominated soil complex: Results of micromorphological studies in the central highlands of Mexico. *Revista Mexicana de Ciencias Geológicas* **21**, 195–201.

Quantin P (1992) L'induration des matériaux volcaniques pyroclastiques en America Latine: processus geologiques et pedologiques. *Terra (Helsinki, Finland)* **10**, 24–33.

Quantin P, Zebrowski C (1995) Impact de l'homme sur l'érosion des sols à "tepetate" de la région de Mexico. In 'Environnement humain de l'érosion'. (Eds G De Noni, E Roose, J Nouvelot, Y Veyret) pp. 104–110. (IRD: Bondy, France)

Sedov S (2015) Tepetate in central Mexican volcanic highlands: a relict pedosediment formed in Late Pleistocene paleolandscape? *Erlanger Geographische Arbeiten Band* **42**, 267–280.

Sedov S, Solleiro-Rebolledo E, Terhorst B, Solé J, Flores-Delgadillo ML, Werner G, Poetsch T (2009) The Tlaxcala basin paleosol sequence: a multiscale proxy of middle to late Quaternary environmental change in central Mexico. *Revista Mexicana de Ciencias Geológicas* **26**(2), 448–465.

Soil Survey Staff 2014. 'Keys to soil taxonomy.' 12th edn. (USDA-Natural Resources Conservation Service: Washington, DC)

Soler-Arechalde AM, Goguitchaichvili A, Carrancho Á, Sedov S, Caballero-Miranda CI, Ortega B, Solis B, Contreras JJM, Urrutia-Fucugauchi J, Bautista F (2015) A detailed paleomagnetic and rock-magnetic investigation of the Matuyama-Brunhes geomagnetic reversal recorded in the tephra-paleosol sequence of Tlaxcala (Central Mexico). *Frontiers in Earth Science* **3**, 11. doi:10.3389/feart.2015.00011

Thiry M (1992) Pedogenic silicifications: structures, micromorphology, mineralogy and their interpretation. *Terra (Helsinki, Finland)* **10**, 46–59.

Werner G (1988) 'Die böden des staates Tlaxcala im Zentralen Hochland vom Mexiko.' (Das Mexiko Projekt der Deutschen Forschungsgemeinschaft 20: Stuttgart, Germany)

Williams BJ (1972) Tepetate in the valley of Mexico. *Annals of the Association of American Geographers* **62**(4), 618–626. doi:10.1111/j.1467-8306.1972.tb00890.x

Zebrowski C (1992) Los suelos volcánicos endurecidos en America Latina. *Terra (Helsinki, Finland)* **10**, 15–23.

Handling Editor: Karin Müller

CSIRO PUBLISHING
Soil Research, 2019, **57**, 566–574
https://doi.org/10.1071/SR18239

How is the fragipan incorporated in the pore space architecture of a boreal Retisol?

L. Pogosyan[A,E], *K. Abrosimov*[B], *K. Romanenko*[B], *J. Marquez*[C], *and S. Sedov*[D]

[A]Posgrado en Ciencias de la Tierra, Instituto de Geología, Universidad Nacional Autónoma de México, Ciudad Universitaria, 04510, Mexico City, Mexico.
[B]V.V. Dokuchaev Soil Science Institute, 119017, Moscow, Russia.
[C]Instituto de Ciencias Aplicadas y Tecnología, Universidad Nacional Autónoma de México, Circuito Exterior S/N, Ciudad Universitaria, 04510, Mexico City, Mexico.
[D]Instituto de Geología, Universidad Nacional Autónoma de México, Ciudad Universitaria, 04510, Mexico City, Mexico.
[E]Corresponding author. Email: lilit-tos@yandex.ru

Abstract. A fragipan is a diagnostic subsurface soil, not a cemented horizon, which is characterised by high density, and so restricts root penetration and water percolation. Although fragic horizons are considered to be pedogenic, the exact genesis of this phenomenon is not well understood. Quantitative study of pore space characteristics in a profile with a fragipan could help in understanding its origin and its pedogenic links to the other diagnostic horizons. Micromorphological and morphometric study of the porous network in soil thin sections and computed tomography in an Albic Fragic Retisol (Cutanic), formed in glacial till of Valday (Wurm) Glaciation in the South Karelia region in the north of Russia, showed a differentiation of pores by shape and distribution for each soil horizon controlled by the type of soil-forming processes. In particular we detected a difference in pore space organisation in the fragic EBx compared with other horizons. The pore space in the EBx was mainly represented by closed micropores, spread homogenously in the soil horizon body, independent of fissure and packing pores. Thus we propose that the pore system in this horizon was heterochronous, with micropores formed at the time of structural collapse and the fissures and other pores formed later.

Additional keywords: Holocene pedogenesis, soil computed tomography, pore space descriptors.

Received 15 August 2018, accepted 26 June 2019, published online 13 August 2019

Introduction

A fragipan is a subsurface soil horizon that restricts the penetration of roots and water; it has a specific coarse prismatic blocky structure and high bulk density. This horizon is considered to be a product of pedogenesis and is defined as diagnostic horizon in both WRB (fragic horizon) and Soil Taxonomy classifications (Soil Survey Staff 2014; IUSS Working Group WRB 2015). The genesis of this soil layer remains unclear. In the first studies of fragipans it was supposed that they were cemented by silica (Marbut, 1935; Karathanasis 1989), but this hypothesis is not in accordance with the current fragipan definition that the air dry fragments have to slake when they are submerged in water (Soil Survey Staff 2014; IUSS Working Group WRB 2015). Many authors now explain fragipan formation as a reorganisation of the soil matrix due to combination of some physical and chemical processes (Bryant 1989; Bockheim and Hartemink 2013); clay is thought to be responsible for compaction by linking the coarser particles (Assallay *et al*. 1998). This leads to a list of likely environmental conditions under which soil with a fragipan can occur (Bockheim and Hartemink 2013).

Soils with fragipans are widely distributed in the world because of the wide range of soil-forming factors that promote their formation or permit their conservation if they were formed previously (Van Vliet and Langohr 1981; Ciolkosz *et al*. 1995). The most common soils in which fragipans occur are those with a texture differentiation in the profile, like Luvisols. In most cases they are formed in loess or low-lime tills parent material of loam, silt loam or silt clay loam textures (Bockheim and Hartemink 2013). They normally occur in forested areas, probably because the suitable soil moisture regime for their formation is Udic. Fragipans can be found on watersheds or gentle slopes. One important factor is soil drainage: some authors propose that drainage class may affect the depth of fragipan formation (Ciolkosz and Thurman 1992) or give a formation hypothesis based on drainage level, explaining that the depth of the upper boundary of the fragipan horizon depends on wetness. Fragipans occur closer to the surface with increasing wetness (Van Vliet and Langohr 1981).

The features of fragipans are strongly connected with configuration of pore space because of their collapsed

construction and low permeability. A piece of fragipan according to its definition must slake in water, and so we assume that water can penetrate the soil horizon matrix and that the cementing agent is not silica. However, despite many studies on fragipans there is little information concerning their pore structure.

Falsone and Bonifacio (2009) measured pore volume in a soil with fragipan using a Hg porosimeter. They showed the connection between clay content and pore size, and a greater presence of fine pores, in a fragipan compared with other horizons. However, most studies of porosity use classical soil physics methods that do not provide information about real pore configuration. Morphological investigation of the porous network in all horizons of a profile with a fragipan is an important complement to understanding the genesis of this phenomenon in a framework of soil-forming processes. To reach this goal we made a morphometric description of thin sections throughout the soil profile. Because the studied soil profile showed clear differentiation of soil structure because of soil formation processes, we wanted to quantify various parameters that could describe the structural differences between horizons and compare this with a qualitative description.

Because most pores in fragipans are micropores, we applied a micro computed tomography (CT) analysis to investigate real pore connections, forms and shapes, and further to infer how these characteristics depend on pedogenic processes.

Materials and methods

Study area

The investigated soil profile is located in the southern part of Karelia (Northern Russia) (Fig. 1). This zone is characterised by earlier spring and later autumn than the rest of Karelia. The mean annual temperature is 2°C. The mean temperature in February is –10°C, that in July +16°C. There are 150 days with temperatures above +5°C, and only 40 days have temperature above +15°C. The sum of active temperatures (above +10°C) reaches 1400°C. Precipitation ranges within 550–600 mm, with 400 mm as summer rainfall, hence the moistening coefficient (precipitation/evaporation) exceeds 1. Soils are covered with snow during November–April and remain frozen for at least 4 months. The snow cover is 40–70 cm high (Morozova 1991). Summarising, the investigated area is characterised by an Udic soil moisture regime and by a Cryic Interfrost soil temperature regime according to USDA maps of soil properties.

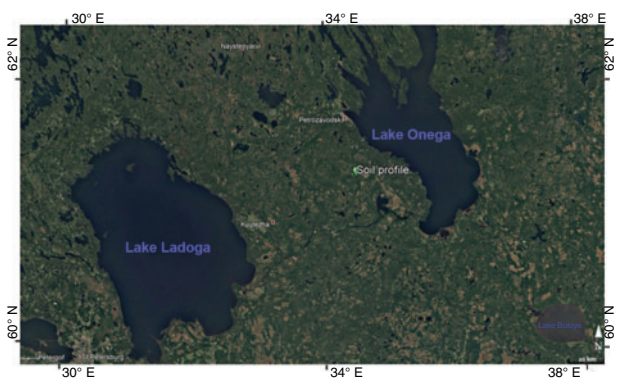

Fig. 1. Location of the studied soil profile (based on Field Workshop Guidebook of the International Conference 2004).

Denudation-tectonic hilly and hilly-ridged moderately swampy landscapes with spruce forests prevail in the region. The maximum altitude is 210 m, and elevation range is 60–100 m. The ridge consists of dome-like hills, and descends towards Onega Lake in a series of terraces.

Geologically, the territory is characterised as Western-Onega uplifted massif due to tectonic activity in the zone of a Lower-Proterozoic syncline that existed at the contact of the Fenno-Scandian shield and the Russian platform. The massif was uplifted in the Mesozoic and affected by the Quaternary glaciations. Rock outcrops are found only on the shore of Onega Lake. The crystalline basement is directly covered by the Luga moraine of the Valday glaciation; it is represented mostly by sands and sandy or clay loams containing abundant gravel and boulders.

In South Karelia (34.50921°E, 61.33186°N, 110 m asl) we studied the soil profile of an Albic Fragic Retisol (Cutanic) (Fig. 2), developed in the glacial till of Valday (Wurm) Glaciation on the flat watershed land surface under an aspen–spruce forest. Data on lateral extension and heterogeneity of fragipan, particle size distribution, mineralogical composition and micromorphological indicators of pedogenic processes were recently published by Pogosyan *et al*. (2018). The soil was first described, specifying the physical and chemical data, and classified according to the World Reference Base (IUSS Working Group WRB 2015). In general our taxonomic attribution agrees with that made for the excursion of the International Conference on Soil Classification (Field Workshop Guidebook of the International Conference 2004) made according to the previous version of WRB.

We relied on the following morphological observations and laboratory data (the latter provided by the Field Workshop Guidebook of the International Conference 2004) to define the exact position of the studied soil within WRB classification:

(1) Morphological examination of the profile shows a distinct albic horizon. Bleached tongues occupy more than 10% of the total area within the contact zone.
(2) Morphological evidence to qualify the soil as fragic is the high-density non-cemented horizon located at 35 cm below the surface.
(3) Concerning the Cutanic qualifier, the pedofeatures related to clay illuviation (clay coatings and infillings) are common and diverse.

In the studied profile, pH values in water suspension are low (5.1 in the Ah horizon and 5.9 in the BC horizon respectively), and soil organic carbon content is 6.0 $g \cdot kg^{-1}$ in the Ah horizon and decreases to 1.4 $g \cdot kg^{-1}$ in the BC horizon. The FAO Textural Class for this soil is Silty Loam with an increase of clay content in the argic part of the profile, which supports the proposed classification.

Undisturbed samples for CT and for preparation of thin sections were collected from genetic horizons of the soil profile.

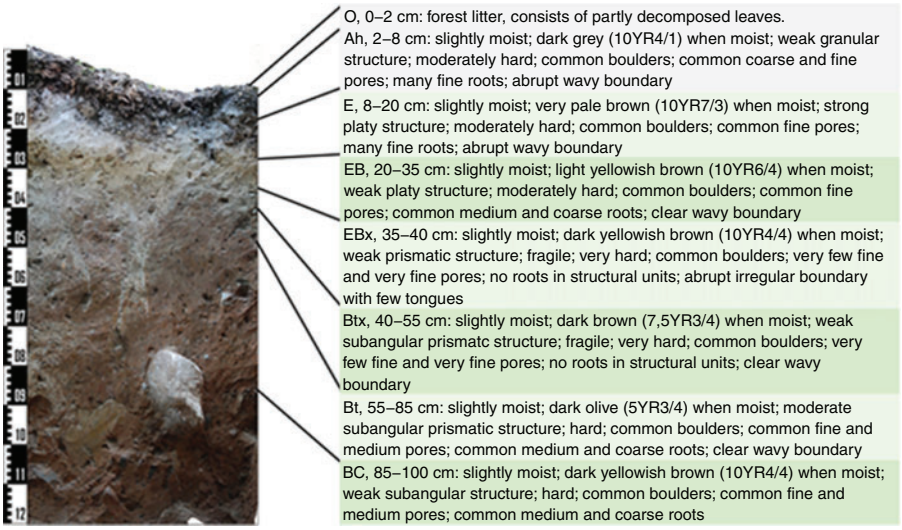

Fig. 2. The studied soil profile of an Albic Fragic Retisol (Cutanic).

Soil thin sections

Thin sections (30 μm thick) were prepared from undisturbed soil samples impregnated at room temperature with the Poliformas resin PP Cristal. These were prepared, studied under a petrographic microscope and described following the terminology of Bullock *et al*. (1985). We especially focused on the microscopic indicators of the pedogenic processes which have major influence on pore space, i.e. biogenic and cryogenic aggregation and clay illuviation.

Each thin section was scanned with a high resolution of 12 800 dpi. The resulting image was analysed with ImagePro Plus program version 7.0. Scanned colour images were binarised and the amount of pores with mean diameter >100 μm was calculated. Pores of smaller size were not counted to avoid errors, because small mineral grains looked like pores in the thin section and because part of these minor pores inclined in relation to the section surface were invisible. After sorting pores by size, each thin section was analysed under the petrographic microscope to exclude mineral grains >100 μm in mean diameter. Relying on earlier works that combined CT with observations of thin sections, we selected the following parameters:

- Porosity, Z, is estimated by the sum of area all pores in a soil thin section A and the total area of analysed soil thin-section A_t using the equation:

$$Z = \frac{\sum A}{A_t} \times 100\% \quad (1)$$

- Roundness, R, estimated from perimeter P and area A for each pore using equation:

$$R = \frac{P^2}{4\pi A} \quad (2)$$

This parameter is included in the ImagePro Plus software measurements, but is also known as a longitudinal index (I_a; Prado *et al*. 2009) and takes a minimum value of 1 for a perfectly round pore and increases for longer pores or of irregular profile. Following the classification proposed by Ringrose-Voase (1996), three categories of pore shapes were defined: (1) tubular pores, $R \leq 5$; (2) fissure pores, $5 < R \leq 10$; and (3) packing pores, $R > 10$.

- The shape factor (F) is obtained from R (Eqn 2) and isometry (D/L), where D is width and L is length (Karsanina *et al*. 2015; Skvortsova *et al*. 2017). The equation is:

$$F = \left(\frac{4\pi A}{P^2} + \frac{D}{L}\right) \Big/ 2 \quad (3)$$

The first element of Eqn 3 refers to so-called object roundness, and the second element characterises pore isometry. The F has values of 0–1 and has several advantages over more commonly used definitions of roundness. For example, it allows distinguishing between round and fissure-like pores, as well as a broad range of other possible shapes (Karsanina *et al*. 2015). Based on the classification five categories of pore shapes were defined: (1) fissure-like, with $0 < F \leq 0.2$: (2) elongated dissected, $0.2 < F \leq 0.4$; (3) isometric dissected, $0.4 < F \leq 0.6$; (4) isometric slightly dissected, $0.6 < F \leq 0.8$; and (5) round, $0.8 < F \leq 1.0$.

Computed tomography

The inner structure was studied using CT imaging, because it was not possible to study pores of mean diameter <100 μm in soil thin sections. So three horizons – EBx, Btx and Bt – were analysed by CT scanner with resolution of 6.26 μm.

To carry out the study, cylindrical soil samples diameter of 2 cm and height of 6 cm were packed in polypropylene holders. Polypropylene has low attenuation for X-rays and so does not affect the scanning results.

The samples were scanned with a μCT Bruker SkyScan 1172 with energy level of 100 kV and resolution 3.15 μm/pix. Image reconstruction was performed in the specialised Bruker SkyScan 'NRecon' software (Bruker 2018*a*).

To prepare images for analysis, they were segmented to separate pores from solid phase. Before performing 3D analysis, resolution was reduced to 6.3 μm/pix to remove noise and scanning artefacts from images. The 3D analysis was performed in Bruker SkyScan 'CTan' software (Bruker 2018*b*). The software allowed us to obtain the following information:

- total volume of the sample, and coefficients such as open and closed pore space, and total solid phase for each object
- amount of pores and solid particles
- surface area of pore space and solid phase both total and individual for each object
- size distribution of pores and solid particles. Size of an object is defined by Hildebrand and Ruegsegger (1997) as the diameter of the largest sphere inscribed in the object.

Porosity was calculated after the procedure of binarisation to separate space of pores as black voxels and solid phase as white voxels. Open porosity was calculated as the ratio between volume of pores that touched the border of volume of interest and the volume of interest multiplied by 100%. Closed porosity was defined as the ratio between volume of pores that did not touch the border of the volume of interest and volume of the solid phase.

A pseudo-colour image presented pores of different volume: yellow pores were 100–1499 voxels and red were ≥1500 voxels. Pores of <100 voxels were removed with the 3D despeckle tool of Bruker CTAn software.

Results

The field description as well as thin-section observations showed sharp differences in soil structure and pore space organisation among the soil genetic horizons throughout the profile. Below we provide their general micromorphological characteristics with special emphasis on pore and aggregate configuration (Figs 3–5).

Ah – dark coloured due to organic pigment, contained decomposed plant debris, with isometric dissected pores, and rounded forms of microaggregates (Figs 3, 5).

E – pale colour and consisted predominantly of bleached coarse mineral material; abundant fissures predominantly sub-horizontal which gave rise to platy and lenticular aggregates, pores were elongated cracks, or rounded micropores inside platy aggregates or isometric mesopores slightly dissected (Figs 3, 5).

EB – predominantly pale but with some brownish microareas and few isolated thin clay coatings. Pores were isometric micropores or dendroid, as well as sub-horizontal fissures which produced platy aggregation (Figs 3, 5).

EBx – darker colour of soil horizon material than in E and EB horizons, high-density horizon with a structure of prismatic blocks of ~10 cm in diameter separated by vertical cracks, contained few isolated thin clay coatings inside of blocks. In a thin section of the block material there were no pores >100 mm in diameter. Smaller pores were few and rounded (Figs 4, 5).

Btx – contains more brown fine material in the groundmass and has prismatic blocky structure of ~10 cm in diameter with high density, pores were few, elongated and slightly dissected. Under the microscope we observed both bleached areas enriched in coarse material and brown areas containing fine clay components and ferruginous pigment; in the latter clay coatings (partly deformed) were present (Fig. 4).

Bt – poorly developed lumpy structure. Pores were elongated cracks of diverse orientation. There were abundant clay coatings and infillings, which were laminated, and with strong interference colours. These illuvial pedofeatures had uniform morphology and filled major parts of the pore space in the horizon (Figs 4, 5).

BC – poorly developed clod structure, pores were slightly dissected elongated or isometric mesopores (Figs 4, 5). Quantification of porosity in soil thin sections for pores >100 μm showed great differences in profile distribution (Fig. 6). The upper part of the soil profile, including Ah, E and EB horizons had higher porosity of 20–26%. This parameter sharply decreased in the EBx horizon, in which pores of this size were absent. In the underlying Btx horizon, porosity increased up to almost 3%. In the lowest part of soil profile, porosity further rose to almost 9%.

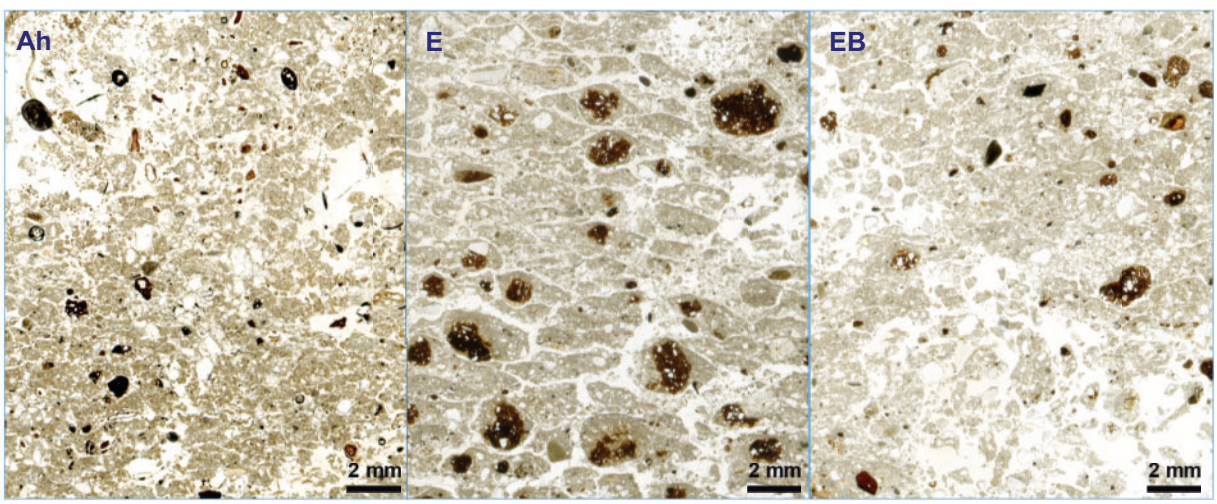

Fig. 3. Scanned images of soil thin sections: Ah, biogenic aggregation; E, platy structure; and EB, weak platy structure.

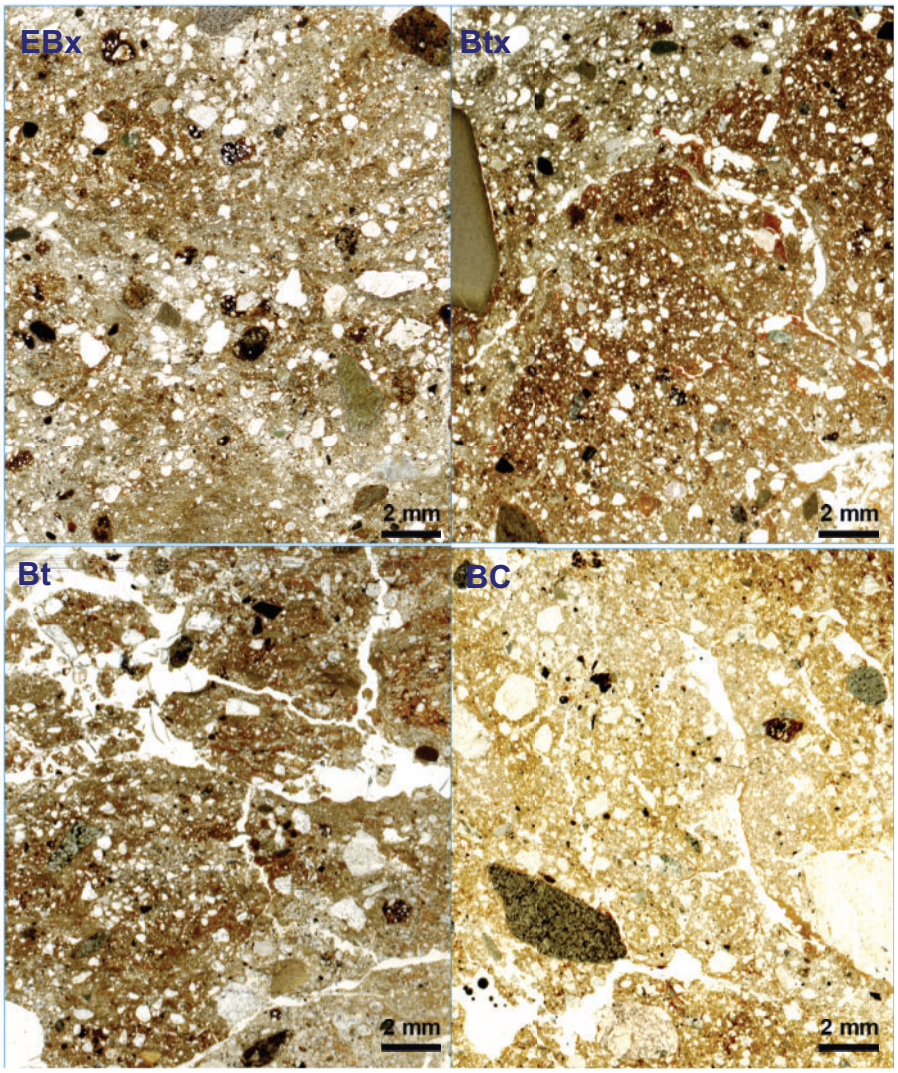

Fig. 4. Scanned images of soil thin sections: EBx, compact composition; Btx, compact composition with some fissure cracks; Bt, fissure pores with clay illuviation; and BC, compact composition with some fissure cracks.

At the same time *R* showed that in each soil horizon there were tubular, fissure and packing pores (Fig. 7). Their percentage did not vary much within the profile. In every soil horizon, tubular pores prevailed over other pore types and always accounted for >35% of total space of pores >100 µm. The percentages of fissure and packing pores were almost equal for each horizon. Only in the BC horizon were packing pores not as prominent.

The *F* showed a clear differentiation of pore shapes in the soil thin sections. The BC horizon had the highest variability in pore shapes, and also a higher amount of pores close to circular shape, compared with other horizons (Fig. 8). The most frequent in all of the soil profile were pores of elongated dissected and isometric dissected shapes.

The CT analysis showed that total porosity (Table 1) changed from 15.23% in the EBx horizon to 7.91% in the Bt, and correspondingly the open porosity decreased from 10.72% to 2.63%. Although total porosity of the EBx horizon was nearly twice that in the Bt horizon (Table 1), there were no pores >100 µm in thin sections, thus most of the pore space in the EBx horizon was micropores and mesopores (Fig. 9). Closed porosity maintained almost the same value, but the organisation of closed pores was quite different among analysed horizons. In the EBx horizon, micropores were uniformly spread in the soil matrix and their positions were not connected to a large crack pore (Fig. 9). In the underlying Btx and Bt horizons, the distribution of small pores was heterogeneous, with some areas of higher and lower pore density observed – these areas depended on the network of larger interaggregate pore cracks. Micropores were mostly located in the inner part of aggregates or orientated and located close to fissure and packing pores and followed in their directions.

Discussion

The field morphological description and micromorphological study allowed us to infer a list of main soil-forming processes in

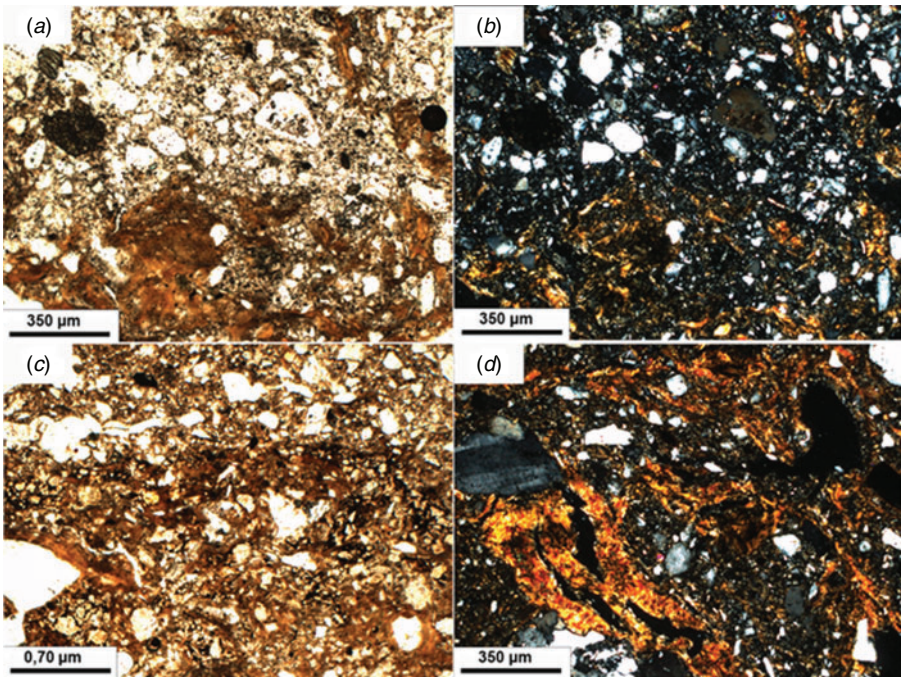

Fig. 5. Micromorphology of the Retisol genetic horizons: (*a*) bleached coarse material, deformed clay coating, EBx horizon, PPL; (*b*) same as for *a* and note strong interference colours of the clay coating fragments, N+; (*c*) porphyric coarse/fine related distribution, clay coatings and iron mottles, BC horizon, PPL; and (*d*) thick laminated clay coating with strong interference colours; Bt horizon, N+. PPL, plane polarised light; N+, crossed polarisers.

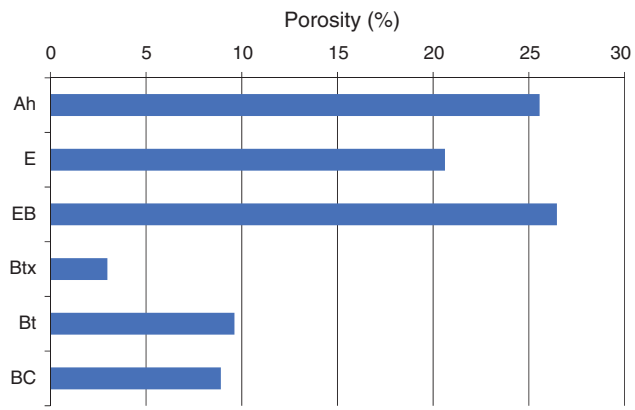

Fig. 6. The 2D porosity of soil horizons measured in thin sections.

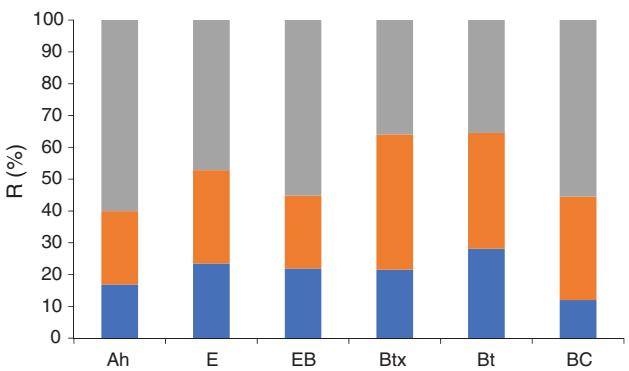

Fig. 7. Roundness (*R*) of pores of mean diameter >100 µm in soil thin sections: grey, tubular pores, $R < 5$; orange, fissure pores, $5 < R < 10$; and blue, packing pores, $R > 10$.

the studied profile of the Fragic Retisol. In the Ah horizon, dark pigmentation of groundmass and the shape of aggregates indicated processes of humus accumulation and zooturbation. The E and EB horizons showed bleaching and clay depletion but also had clear attributes of cryogenic processes: platy aggregation, due to ice lenses developing during the course of annual freezing. Ice lensing was related to the moisture regime and mainly occurred in horizons with relatively high moisture content. Presence of the argic horizon with low permeability and waterlogging above it, in seasonally frozen soils, supports the formation of ice lenses in the eluvial horizon and was long ago shown by direct observation (Kachinsky 1927). In the studied soil profile, the fragipan was overlying the argic part of the profile and also restricted water percolation. This provokes retention of water in the uppermost horizons and explains the cryogenic aggregation in the E and EB horizons. Additional moisture for ice lensing was provided by the upward water migration to the freezing front. The aggregation processes – biogenic and cryogenic – produce abundant micropores and now prevent compaction of upper horizons and fragipan formation.

The EBx horizon showed no frost cracking, so the partly bleached albic material seemed undisturbed and there were no pores >100 µm in the soil thin section. In the underlying Btx horizon, compact composition was disturbed by a poorly developed prismatic blocky structure. A combination of

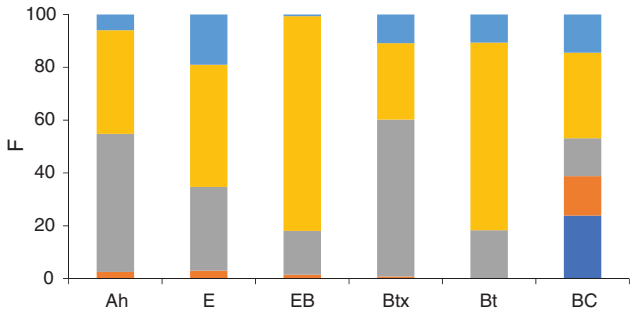

Fig. 8. The shape factor (F) of pores of mean diameter >100 μm in soil thin sections: dark blue, fissure-like, $0 < F < 0.2$; 2); yellow, elongated dissected, $0.2 < F < 0.4$; grey, isometric dissected, $0.4 < F < 0.6$; orange, isometric slightly dissected $0.6 < F < 0.8$; 5); and light blue, round, $0.8 < F < 1$.

Table 1. Porosity types of soil samples determined by computed tomography

	Total porosity (%)	Open porosity (%)	Closed porosity (%)
EBx	15.23	10.72	5.05
Btx	12.41	7.41	5.40
Bt	7.91	2.63	5.43

bleached and brown microzones indicated that this was a transition zone between the albic and argic layers of the profile. The Bt horizon was characterised by morphologically well-defined clay illuviation processes, that slowly decreased in the BC horizon where illuvial coatings were few. We connect the origin of fissure pores and cracks with enrichment of clay fraction in these horizons with abundance of smectites in the clay fraction because the smectite content sharply increased below the EBx horizon (as shown by Pogosyan *et al*. 2018). Because smectites are the clay minerals most susceptible to chemical alteration, their full destruction due to acid weathering is thought to take place in the upper part of Retisol profiles (Targulian *et al*. 1974). We think this process is at least partly responsible for clay and smectite depletion of the upper bleached horizons during formation of the texture differentiated E–Bt profile and before fragipan consolidation (Pogosyan *et al*. 2018). Being expansible minerals, smectites provoke shrink–swelling processes that give rise to desiccation cracks. This cracking can be caused by seasonal changes in soil moisture, particularly by the already mentioned upward migration of water towards the freezing front in the beginning of each freeze–thaw cycle (for explanation of this process see Lu *et al*. 2016). In his classic monograph on geocryology, Kudryavtsev et al. (1978) states that moisture migrates from the unfrozen zone to the freezing front and could cause water depletion and shrinking of the unfrozen layer that in turn could produce vertical desiccation cracks. We conclude that the fragipan formed in the part of the profile unaffected by cryogenic cracking and zooturbation (active in the upper horizons) and not in the argic part of the profile, enriched in smectites, because they provoke fracturing and limit compaction due to shrink–swelling processes.

The proposed scenario explains differentiation of the pore system in the studied eluvial–illuvial profile of the Retisol (including fragipan) mostly by recent physical and biological soil processes. However, we should also consider the alternative model that links the development of European clay illuvial (lessivé) soils, as well as fragipan horizons with the past pedological and cryogenic phenomena during the periglacial paleoenvironments of the terminal Pleistocene (Van Vliet and Langohr 1981; Van Vliet-Lanoë *et al*. 1992). The authors of this model claim that fragipan properties, including specific porosity, could be best explained by their formation due to permafrost aggradation (Van Vliet and Langohr 1981). Clay translocation, gleysation and formation of eluvial E and illuvial Bt horizons is supposed to occur because of snow and ice melting during the warmer Bølling and Allerød stages of the Late Glacial (Van Vliet-Lanoë *et al*. 1992). We propose, however, that certain constraints for application of this hypothesis to the studied Karelian Retisol are set by age of the parent material. The latter is a till formed in the course of deglaciation of this region during 13–14 ka BP – that roughly corresponds to Bølling–Allerød. This means that the land surface and parent rock development were still in process during the period when, according to Van Vliet-Lanoë *et al*. (1992), clay illuviation and E–Bt profile development should already have taken place. Further research is needed to solve this contradiction.

Another scenario involving the relict origin of the fragipan supposes its development during the cold phase in the Subboreal period of the Holocene, after development of the Retisol profile in the Atlantic optimum (Pogosyan *et al*. 2018).

The histogram of the porosity parameter (Fig. 6) supports morphological observations. The higher porosity in the upper part of the profile was determined by bioturbation, for example due to roots and soil fauna. In the albic horizon, the biological processes sharply decreased; however, frost cracking still produced macroporosity. The lower part of soil profile with argic properties did not suffer any turbations, so these horizons did not change their grade of compactness. A certain amount of fissures could be produced there, due to desiccation cracking induced by illuvial clay accumulation. The specific conditions developed in the EBx horizon which was already below the upper zone of biogenic and cryogenic macropore formation, but still within the albic part of the profile depleted of clay. Under these conditions, a minimum of macropores caused high compaction. The macropores of the EBx could be locked in the soil mass at the beginning of the fragipan formation, in a hydroconsolidation process, before desiccation of the moist mass. The EBx horizon, because of its high density, served as a protection from penetrating roots for the underlying part of the profile.

The low presence of packing pores in the BC horizon could be explained by less developed pedogenic structure in this soil horizon and, at the same time, strong glacial compaction at the stage of sedimentation (Fig. 4, 5). All horizons with well-developed structure had a higher percentage of pores per unit area.

The porosity calculated by CT image analysis expressed the important difference in pore formation of these soil horizons. Although the closed porosity did not change significantly, the organisation of micropore space changed depending on processes of horizon formation. The homogeneous distribution of thin closed pores means that the unique large pore cracks were formed after fragipan consolidation and after formation of micropores, because the large pores cut the rest of

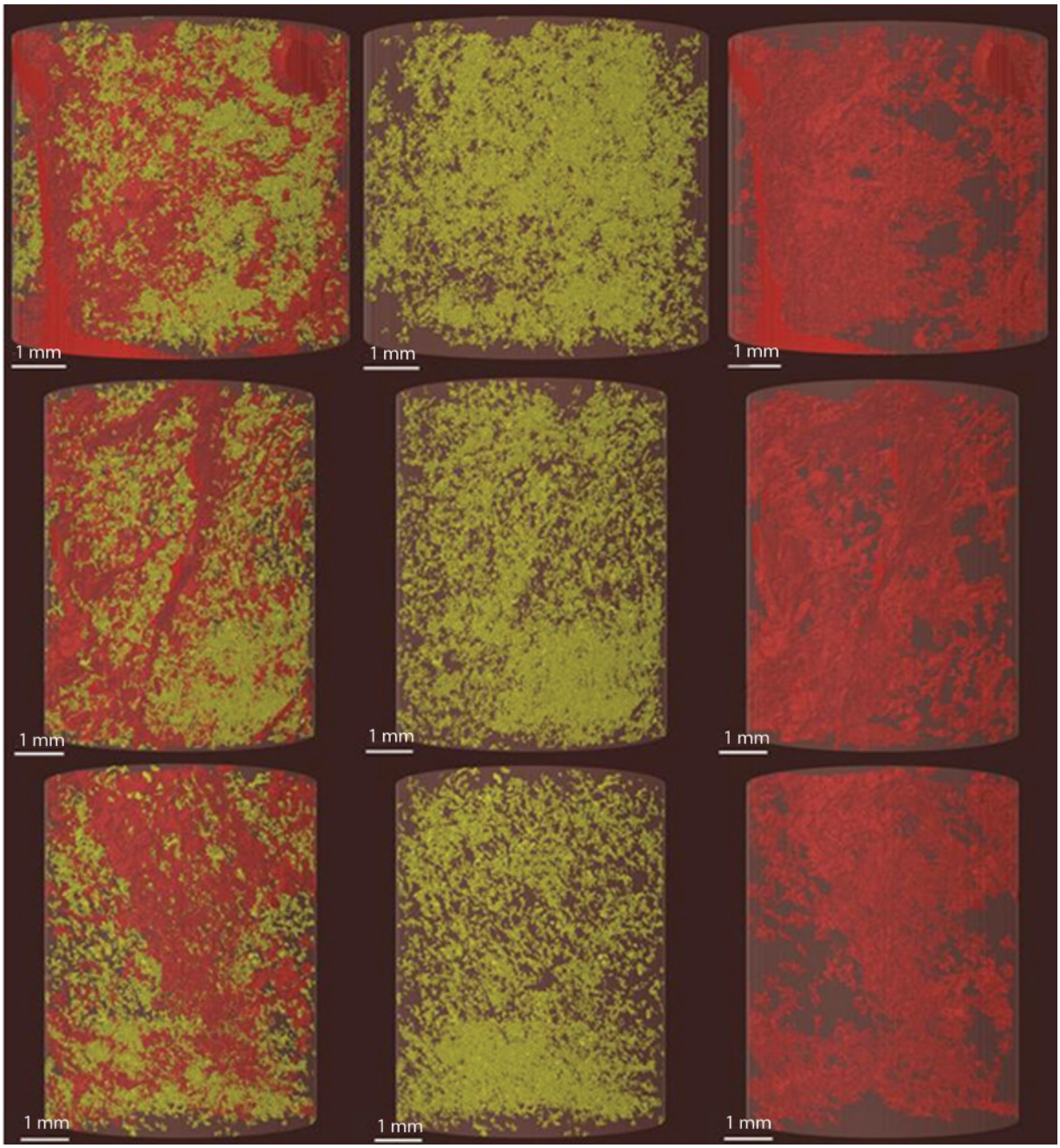

Fig. 9. Pore space from CT. Coloured image presents pores of different volumes: yellow pores are 100–1499 voxels and red are ≥1500 voxels.

the pore space and the distribution of small pores did not depend on large pore position. The pattern of the distribution of thin pores in Btx and Bt horizons was related to interaggregate pores, their distribution fitted the position of large pores and followed their inclination and direction, thus it is likely that the different types of pores developed together.

Conclusions

In this study we related the pore space characteristics to soil formation processes. In our case, the fragic EBx horizon had a quite different pore space compared to the other studied horizons. First, because of the high compactness, micromorphological observations showed no pores >100 μm in this horizon. Even though a single fissure pore was detected in this horizon by CT, the pore space there was formed mainly by unconnected micropores, which were distributed homogenously. So, we consider that micropore formation happened previously during the time of compaction, and the single fissure pore detected in a 3D image of the horizon was formed later. In contrast, the formation of micropores in the Btx and Bt horizons was connected to formation of

fissure and packing pores, which probably originated simultaneously.

It is important to note that the soil porosity of the upper horizons was higher than in the fragic part or in underlying horizons. Pore shape observations showed that macropore development was provoked by specific processes in each horizon: frost cracking in the albic part of the soil profile and biogenic turbation in the Ah horizon specifically. The high density of the fragic horizon does not allow penetration of roots or water percolation into the fragipan. This could be explained by the absence in the EBx horizon of both biogenic turbation, which was most active in the Ah horizon, and lenticular aggregation due to ice lensing that developed in the E and EB horizons.

Conflicts of interest

The authors declare no conflicts of interest.

Acknowledgements

The research was aided by use of equipment of 'Functions and properties of soils and soil cover' and a shared use of facilities at the Dokuchaev Soil Science Institute. The field research was supported by the project 0221–2017–0047 financed by the Russian Academy of Sciences. Collaboration with Pavel Krasilnikov (Institute of Biology, Karelian Research Centre RAS) was most important for selection of the site, field description, classification and pedogenic interpretation of the studied profile. The authors would like to acknowledge the contribution of Elena B. Skvortsova (Dokuchaev Soil Science Institute) in helpful suggestions and Jaime Diaz (Institute of Geology of the UNAM) for the help with preparing soil thin sections.

References

Assallay AM, Jefferson I, Rogers CDF, Smalley IJ (1998) Fragipan formation in loess soils: development of the Bryant hydroconsolidation hypothesis. *Geoderma* **83**, 1–16. doi:10.1016/S0016-7061(97)00135-3

Bockheim JG, Hartemink AE (2013) Soils with fragipans in the USA. *Catena* **104**, 233–242. doi:10.1016/j.catena.2012.11.014

Bruker (2018*a*) Micro-CT software support. Available at https://www.bruker.com/service/support-upgrades/software-downloads/micro-ct.html [verified 9 July 2019].

Bruker (2018*b*) Micro-CT software. Available at https://www.bruker.com/products/microtomography/micro-ct-software.html [verified 9 July 2019].

Bryant RB (1989) Physical processes of fragipan formation. In'Fragipans: their occurrence, classification and genesis'. (Eds NE Smeck, EJ Ciolkosz) pp. 141–150. (SSSA: Madison, WI, USA)

Bullock P, Fedoroff N, Jongerius A, Stoops G, Tursina T, Babel U (1985) 'Handbook for soil thin section description.' (Waine Research Publications: Wolverhampton, UK)

Ciolkosz EJ, Thurman NC (1992) 'Pennsylvania State University soil characterization laboratory database.' (Agronomy Department, Pennsylvania State University: University Park, PA)

Ciolkosz EJ, Waltman WJ, Thurman NC (1995) Fragipans in Pennsylvania soils. *Soil Survey Horizons* **36**, 5–20. doi:10.2136/sh1995.1.0005

Falsone G, Bonifacio E (2009) Pore-size distribution and particle arrangement in fragipan and nonfragipan horizons. *Journal of Plant Nutrition and Soil Science* **172**, 696–703. doi:10.1002/jpln.200800066

Fedorets NG, Morozova RM, Bahmet ON, Gerasimova MI, Krasilnikov PV. (2004) 'Field Workshop Guidebook of the International Conference (August 3–8, 2004, Petrozavodsk, Karelia, Russia).' (Petrozavodsk).

Hildebrand T, Ruegsegger P (1997) A new method for the model independent assessment of thickness in three dimensional images. *Journal of Microscopy* **185**, 67–75. doi:10.1046/j.1365-2818.1997.1340694.x

IUSS Working Group WRB 2015. World Reference Base for Soil Resources 2014, update 2015 International soil classification system for naming soils and creating legends for soil maps. World Soil Resources Reports No. 106. FAO, Rome.

Kachinsky NA (1927) 'Freezing, de-freezing and moisture content in soil in the winter season in the forest and in the field areas.' (Association of Research Institutes of Physics and Mathematics Department, Moscow State University: Moscow) [in Russian]

Karathanasis AD (1989) Solution chemistry of fragipans—thermodynamic approach to understanding fragipan formation. In'Fragipans: their occurrence, classification and genesis'. (Eds NE Smeck, EJ Ciolkosz) pp. 113–139. (SSSA: Madison, WI, USA)

Karsanina MV, Gerke KM, Skvortsova EB, Mallants D (2015) Universal spatial correlation functions for describing and reconstructing soil microstructure. *PLoS One* **10**(5), e0126515. doi:10.1371/journal.pone.0126515

Kudryavtsev VA, Dostovalov BN, Romanovsky NN, Kondratieva KA, Melamed VG (1978) 'General permafrost science.' 2nd edn. (Moscow University Editions: Moscow). [In Russian]

Lu Y, Liu S, Weng L, Wang L, Li Z, Xu L (2016) Fractal analysis of cracking in a clayey soil under freeze–thaw cycles *Engineering Geology* **208**, 93–99. doi:10.1016/j.enggeo.2016.04.023

Marbut CF (1935) 'Atlas of American Agriculture. Part III, Soils of the United States.' (USDA, Bureau of Chemisty and Soils: Washington, DC)

Morozova RM (1991) 'Forest soils of Karelia.' (Nauka Publ.: Leningrad) [In Russian]

Pogosyan L, Sedov S, Pi-Puig T, Ryazantsev P, Rodionov A, Yudina AV, Krasilnikov P (2018) Pedogenesis of a Retisol with fragipan in Karelia in the context of the Holocene landscape evolution. *Baltica* **31**(2), 134–145. doi:10.5200/baltica.2018.31.13

Prado B, Duwig C, Márquez J, Delmas P, Morales P, Etchevers JD (2009) Image processing-based study of soil porosity and its effect on water movement through Andosol intact columns. *Agricultural Water Management* **96**(10), 1377–1386. doi:10.1016/j.agwat.2009.04.012

Ringrose-Voase AJ (1996) Measurement of soil macropore geometry by image analysis of sections through impregnated soil. *Plant and Soil* **183**, 27–47. doi:10.1007/BF02185563

Skvortsova EB, Rozhkov VA, Yudina AV, Vasil'eva NA (2017) The diversity of the morphometric profiles of the pore space in soddy-Podzolic and gray forest soils of East European Plain. *Byulleten Pochvennogo instituta im. V.V. Dokuchaeva* **87**, 73–85.

Soil Survey Staff 2014. Keys to Soil Taxonomy, 12th edn. USDA-Natural Resources Conservation Service. (Washington, DC)

Targulian VO, Sokolova TA, Birina AG, Kulikov AV, Tselishcheva LK (1974) 'Arrangement, composition and genesis of sod-palepodzolic soil derived from mantle loams'. Analytical investigation, 10th International Congress in Soil Science. (Moscow).

Van Vliet B, Langohr R (1981) Correlation between fragipans and permafrost with special reference to silty Weichselian deposits in Belgium and northern France. *Catena* **8**, 137–154. doi:10.1016/0341-8162(81)90002-3

Van Vliet-Lanoë B, Fagnart JP, Langohr R, Munaut A (1992) Importance de la succession des phases écologique anciennes et actuelles dans la différentiation des sols lessivés de la couverture loessique d'Europe occidentale: argumentation stratigraphique et archéologique. *Science du Sol* **30**, 75–93.

Handling Editor: Patrice Delmas

since 1961

Baltica

BALTICA Volume 31 Number 2 December 2018: 134–145
https://doi.org/10.5200/baltica.2018.31.13

Pedogenesis of a Retisol with fragipan in Karelia in the context of the Holocene landscape evolution

Lilit Pogosyan, Sergey Sedov, Teresa Pi-Puig, Pavel Ryazantsev, Aleksander Rodionov, Anna V. Yudina, Pavel Krasilnikov

Pogosyan, L., Sedov, S., Pi-Puig, T., Ryazantsev, P., Rodionov, A., Yudina, A.V., Krasilnikov, P. 2018. Pedogenesis of a Retisol with fragipan in Karelia in the context of the Holocene landscape evolution. *Baltica, 31 (2)*, 134–145. Vilnius. ISSN 0067-3064.
Manuscript submitted 6 October 2018 / Accepted 24 November 2018 / Published online 10 December 2018

Abstract Fragipan is a compacted but non-cemented subsurface horizon, considered as a pedogenic horizon, but the mechanism of its formation is not well understood. The main hydro-consolidation hypothesis involves a collapse of soil structure when it is loaded and wet, resulting a reorganisation of pore space. Soils with fragipan never have been marked in Russian soil maps. In the South Karelia, located in Eastern Fennoscandia (34.50921 E and 61.33186 N, 110 m asl) we studied a soil profile of Albic Fragic Retisol (Cutanic), developed in the glacial till of Last Glaciation with flat subhorizontal topography under an aspen-spruce forest. The aim of this study was to demonstrate how the fragic horizon was formed in the Retisol located in South Karelia. Observations were made in each soil horizon using micromorphological method, particle size analysis and the study of mineralogical composition of clay fraction by X-ray diffraction. The analysis of the morphological description combined with the laboratory data have led us to the conclusion that the consolidation of the fragipan occurred after the textural differentiation of the profile, following the Atlantic Optimum, and does not depend on the presence of swelling clay minerals. The well-developed argic horizon was probably formed around 6000 years ago, under climatic conditions more favourable for clay illuviation than in present time. Fragipan is supposed to be developed during the Sub-Boreal cooling.

Keywords *• soil genesis • illuviation clay • Holocene soil*

✉ *Lilit Pogosyan* (*lilit-tos@yandex.ru*), *Sergey Sedov* (*serg_sedov@yahoo.com*), *Teresa Pi-Puig* (*tpuig@geologia.unam.mx*), *Instituto de Geología UNAM & LANGEM, Ciudad Universitaria, 04510, Cd. de México; Pavel Ryazantsev* (*chthonian@yandex.ru*), *Department of Multidisciplinary Scientific Research, Karelian Research Centre RAS, Petrozavodsk, Russia; Aleksander Rodionov* (*fabian4695@gmail.com*), *Institute of Geology, Karelian Research Centre RAS, Petrozavodsk, Russia; Anna V. Yudina* (*anna.v.yudina@gmail.com*), *V.V. Dokuchaev Soil Science Institute, Moscow, Russia; Pavel Krasilnikov* (*pavel.krasilnikov@gmail.com*), *Institute of Biology, Karelian Research Centre RAS, Petrozavodsk, Russia*

INTRODUCTION

Soils are sensitive to the environmental conditions. In North-Western Europe the soils were developing since deglaciation in the terminal Pleistocene and throughout the Holocene and suffered periods of contrasting climate and environmental changes. The records of those changes are present in the pollen assemblages from the peat sequences and lacustrine sediments accumulated in the landscape depressions (Yelina, Filimonova 2007; Dolukhanov *et al.* 2009). Some upland soils developed under good drainage conditions have evidences of different stages of soil formation for this period in their profiles. The relicts of Late Pleistocene sedimentary and cryogenic processes were registered e.g. in the loess soils of the East European Plain (Makeev 2009) and in the slope soils of Central Europe as periglacial cover beds (Kleber, Terhorst 2013). Variable well preserved evidences of different climatic phases of the Holocene were detected in the soils of Eastern Europe, especially within forest-steppe zone (Alexandrovskiy 1983, 2000). Most of these soil records were obtained from the soils of the European regions outside the limits

of the Last Glaciation. Soils developed in the circum-Baltic region within the Valday (Weichselian) glaciation area also have complex profile developed in response to landscape evolution (Nikonov *et al.* 2005; Rusakov *et al.* 2007) and thus contain rich "soil memory" (see Targulian, Goryachkin, 2004).

A common and informative element of the European mid-latitude soil profiles is the fragic horizon, often interpreted as a relict feature (Habecker *et al.* 1990; Ciolkoszet *et al.* 1995; Payton 1992, 1993a, 1993b; van Vliet, Langohr 1981). Fragic horizon (IUSS Working Group WRB 2014), also known as fragipan (Keys to Soil Taxonomy 2014), is a compacted but non-cemented subsurface soil horizon which restricts the penetration of roots and water; it has a specific coarse prismatic blocky structure and high bulk density. Even though the fragipan is considered to be a pedogenic horizon, its genesis is not well understood yet. A review of fragipan studies in the USA (Bockheim, Hartemink 2013) presents a broad list of possible hypotheses for its formation. Originally fragipans were supposed to be irreversible-cemented by silica (Winters 1942), but even at that time some scientists tended to explain its formation rather by strong compaction (Nikiforoff 1948). The cementation hypothesis does not fit into the current definition of fragipan: the air dried fragments have to slake when they are submerged in water (WRB 2014; Keys to Soil Taxonomy 2014).

There are several alternative explanations of the fragipan formation through reorganization of soil matrix due to combination of some physical and/or chemical processes (Bryant 1989; Bockheim, Hartemink 2013). Many authors considered that this structural collapse takes place as a result of frost heave in the presence of permafrost under periglacial conditions (Fitzpatrick 1956; Gallardo *et al.* 1988). This theory cannot explain the fragipan formation in tropical regions, where the glaciation has never been registered during the soil formation time.

The main "Bryant hydro-consolidation" hypothesis, involves a collapse of soil structure when it is "loaded and wet", and in this case clay is believed to be responsible for compaction by linking coarser particles (Assalay *et al.* 1998). This hypothesis is confirmed in recent studies (Szymanski *et al.* 2012; Nikorych *et al.* 2014; Falsone *et al.* 2017) and can be applied for areas that were not affected by glacial or periglatial conditions during the consolidation.

The fragipans have been mapped primarily in the USA and Europe but have never been registered in soil maps of Russia. For this reason it is important to investigate its genesis when in was firstly noted in Karelia, in the northern part of European Russia. There are numerous publications about the deglaciation in Karelia with many data about the age of exposed sediments (Saarnisto, Saarinen 2001; Svendsen *et al.* 2004). The study site is located within the area of Luga deglaciation stage of the Valday (Weichselian) glaciation. The parent material was exposed to the surface around 13–14.2 ha (Svendsen *et al.* 2004). The particular interest of this study is the fragipan that was not previously studied directly in the zone of Valday glaciation. This soil profile was previously presented on the field tour of International Conference of Soil Classification (Field Workshop Guidebook of the International Conference, 2004), where specialists of both international (WRB and Soil Taxonomy) and Russian soil classification teams have defined this soil as Aquic Fraglossudalfs (or Aquic Fragic Glossic Udic Alfisols) (Galbraith 2004) according to Soil Taxonomy (2003).

The main goal of this study was to understand how the fragic horizon appeared in the Retisol profile in Karelia that was formed during the Holocene, and what kind of processes is responsible for its formation. We further try to relate the Retisol and fragipan formation with the Holocene regional landscape history.

MATERIAL AND METHODS

The soil profile is located in the southern part of the Republic of Karelia in North-Eastern Russia (34.50921 E and 61.33186 N, 110 m asl). In this area (Fig. 1), the period with temperatures higher than 5°C is 140–160 days long, and there are more than 100 days a year with the temperature higher than 10°C. The mean annual temperature is 2°C and annual precipitation is 600 mm. According to the Soil Taxonomy, this soil is characterized by the Udic soil moisture regime and Cryic Interfrost soil temperature regime.

The soil profile was classified as an Albic Fragic Retisol (Cutanic) (IUSS Working Group WRB 2014), and it is developed in the glacial till of Last Glaciation on the sub-horizontal watershed surface under an aspen-spruce forest. Detailed morphological description of the soil profile was followed by sampling following the genetic horizons: bulk samples for physical and mineralogical characteristics as well as blocks with undisturbed structure for thin sections were collected. For the morphological and mineralogical analyses the following methods were employed:

Geophysical methods

The ground penetrating radar (GPR) and time domain reflectometry (TDR) were used on the initial stage of research to detect spatial behavior of soil horizons and in particular to check the lateral extension of the fragipan in a soil cover. In this study, OKO-2

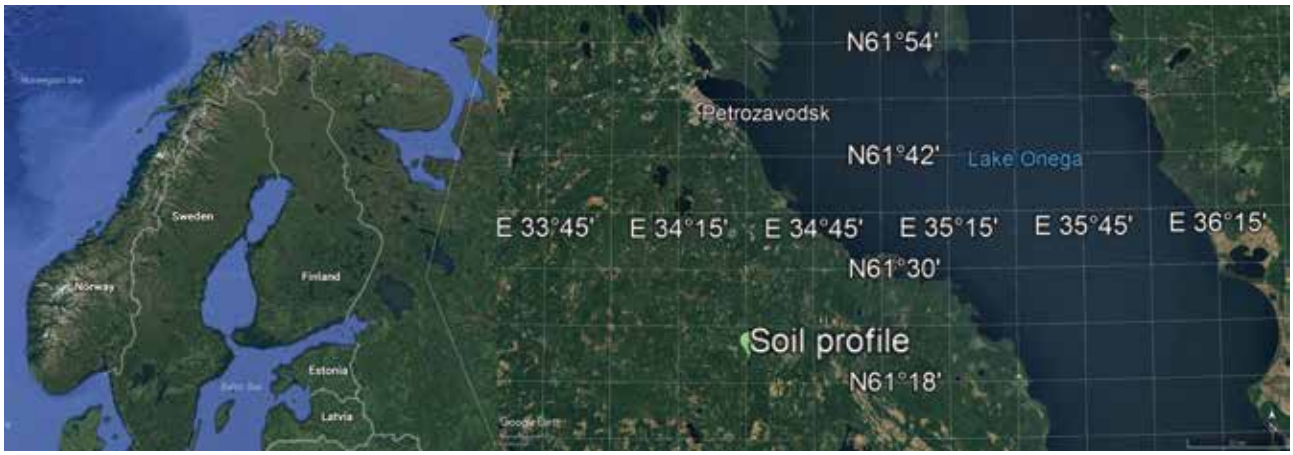

Fig. 1 A schematic map of the study area

GPR with an antenna unit with a central frequency of 1700 MHz (Logis-Geotech, Russia) was used, permitting sounding down to 1 meter depth with a vertical resolution of at least ±3 cm. Measurements were taken from individual profiles with a scanning step of 5 cm. TDR observations were performed by the TDR 200 measurement system with CS635-L probe (Campbell Scientific, USA). Measurements were taken each 5 cm across the cross-section, with ε and σ readings recorded simultaneously. After the reference data for interpretation have been gathered on the main soil pit (*lfc*), for the detailed study by GPR we realized running from *lfc* to the additional soil pit *lfv* on the distance of 52 m with the same soil and at the same geomorphological position, to track the spatial distribution of fragipan.

Particle size analysis

Laser analyser Microtrac Bluewave (Microtrac, USA) was used to determine the particle size distribution in soil samples. The speed of circulation was 50% of the maximum. Calculation of results was made with the following parameters. Particles were described as absorbing (absorption coefficient – 1) and of irregular shape, refractive index of distilled water – 1.33. Equipment software takes into account the fact that refractive index of absorbing particles does not significantly affect the results. Selected parameters are in agreement with early studies (Sochan *et al.* 2014). Samples were previously prepared by horn type ultrasonic disruptor (Stepped Solid Horn 1/2'', Digital Sonifier S-250D, Branson Ultrasonics, USA). The output of ultrasonic power was calibrated calorimetrically by the generally accepted method (North 1976). Ultrasonic dispersion energy was 450 J · ml-1. Then the sample aliquot (few ml) was placed directly to sample dispersion controller unit of analyser and processed. The upper limits of fractions were established based on Schoeneberger *et al.* (2012). Thus, the upper limit for the clay fraction is 0.002 mm, for silt 0.05 mm and for sand 2.0 mm.

Mineralogical composition of clay fraction by X-ray diffraction (XRD)

Clay size fraction (<2 μm) was separated by sedimentation in distilled water according to Stoke's law using the most unaggressive method (Moore, Reynolds 1997).

From the <2 μm fractions, air-dried oriented samples of clay saturated with Mg were obtained by pipetting some drops of the suspensions onto a glass slide, which was then dried at 30°C for a few hours (Moore, Reynolds 1997). Ethylenglycol solvation of the slides was achieved by exposing them to ethylenglycol vapor at 70°C for 24 hours.

Measurements were made using an EMPYREAN XRD diffractometer operating with an accelerating voltage of 45kV and a filament current of 40 mA, using CuKα radiation, nickel filter and PIXcel 3D detector. All samples were measured with a step size of 0.04° (2θ) and 40 s of scan step time.

Clay sample was examined by XRD in the air-dried form (AD), saturated with ethylenglycol (EG) and after heating (550°C). The preparations were measured over a 2θ angle range of 2–70° (air-dried) and 2–30º (glycolated and heated) at a speed of 1°(2θ)/min.

Clay species were estimated in semiquantitative form, from oriented preparations using simple peak weighting factors. For area estimation we used Fityk (Wojdyr 2010), a program for data processing and nonlinear curve fitting, simple background subtraction and easy placement of peaks and changing of peak parameters.

Micromorphological analysis

The micromorphology of soil horizons was studied in thin sections (30 μm thick) prepared from un-

disturbed soil samples impregnated at room temperature with the resin Cristal MC-40 using a standard procedure (e.g., FitzPatrick 1984). Micromorphological observations were performed under petrographic microscope OLIMPUS and the descriptions followed the terminology of Bullock *et al.* (1986) and Stoops (2003). The preparation of soil thin sections has been compounded by the presence on numerous rock fragment of different size class, so it was difficult to take the undisturbed sample.

RESULTS

The investigated Retisol profile (Fig. 2) was 1 m depth and contained abundant boulders from the top down to the bottom. Some of them had slightly rounded elongated shape; they were oriented vertically in a pit. The rock fragments on the bottom of the soil pit had a flat slightly rounded shape and were oriented horizontally. This soil had a clear texture differentiation, an argic horizon and albeluvic tonguing. The details of soil description are listed in Table 1. In the field description we marked the fragipan in EBx and Btx horizons, located between EB and Bt horizon. In the 'fragic' part of the profile there were some well-defined differences in the structure and composition of soil material, and also in the distribution of Fe-Mn nodules.

At the first stage of the geophysical studies, the reference interpretation model was obtained from the *lfc* soil pit. After sounding by GPR and TDR, the resultant data were compared to the established ho-

Fig. 2 The studied soil profile

Table 1 Main morphological properties of the soil profile. Codes according to Guidelines for soil description (FAO 2006)

Horizons	Depth cm	Boundary	Munsell colour (wet)	Structure	Coatings	Concentrations	Rock fragments	Roots
		D_T		G_T_S	A_K	A_K_S_Sh_H_N_C	A_S_Sh	A_D
O	0–2	A_W	–	–	–	–	C_BL_S	M_ F
Ah	2–8	A_W	10YR4/1	WE_GR_VF	N	N	C_BL_S	M_ F
E	8–20	C_W	10YR7/3	ST_PL_ME	N	F_C_F_R_H_FM_BR	C_BL_S	C_MC
EB	20–35	C_W	10YR6/4	WE_PL_ME	N	V_C_F_R_H_FM_BR	C_BL_S	C_MC
EBx	35–40	A_I	10YR4/4	WE_PR→PL_ CO→ME	N	N	C_BL_S	N
Btx	40–55	C_W	7,5YR3/4	WE_PS_FI	C_ST	N	C_BL_S	N
Bt	50–85	G_W	5YR3/4	MO_SB_FI	M_C	F_S_V_I_S_FM_BL	C_BL_S	V _ C
BC	85–100	–	10YR4/4	WE_SB_FI	F_C	F_S_V_I_S_FM_BL	C_BL_F	N

Horizon boundary: (D) distinctness: A = abrupt, C = clear, G = gradual; (T) topography: S = smooth, W = wavy, I = Irregular.

Structure: (G) grade: WE = weak, MO = moderate, ST = strong; (T) type: SB = subangular blocky, PR = prismatic, PS = subangular prismatic, GR = granular, PL = platy; (S) size class: VF = very fine/thin, FI = fine/thin, ME = medium.

Coatings: (A) abundance: N = none, F = few, C = common, M = many; (K) kind: C = clay, ST = silt coatings.

Concentrations: (A) abundance: N = none, V = very few; F = few; (K) kind: C = concretion, S = soft segregation; (S) size class: F = Fine; (Sh) shape class: R = rounded (spherical), I = irregular; (H) hardness: H = hard, S = soft; (N) nature: FM = iron-manganese; (C) colour: BR = brown, BL = black.

Rock fragments: (A) abundance: C = common; (S) size class: BL = boulders and large boulders; (Sh) shape class: F = flat, S = subrounded.

Roots: (A) abundance: N = none, V – very few, C = common, M = many; (D) diameter: F = fine, MC = medium and coarse.

rizon interfaces (Fig. 3A). The comparisons clearly showed that all the structural elements of the soil pit were manifested in the electrical properties. The plot for σ represented with a high degree of probability the conductivity (i.e. soil mineralization). It demonstrated that the conductivity changed from 3.6 · 10-4 to 10.1 · 10-4 S/m and increased with depth, and that specific step change regions were observed at -35 – -40 and -75 – -85 depths, corresponding to the EB(x) and BC horizons. The plot for ε showed that this parameter is less variable, the range of values being 2.5–5.2, and the sharpest transition occurred at the -20 depth (Ah–E boundary) where the value shift of one conditional unit was observed.

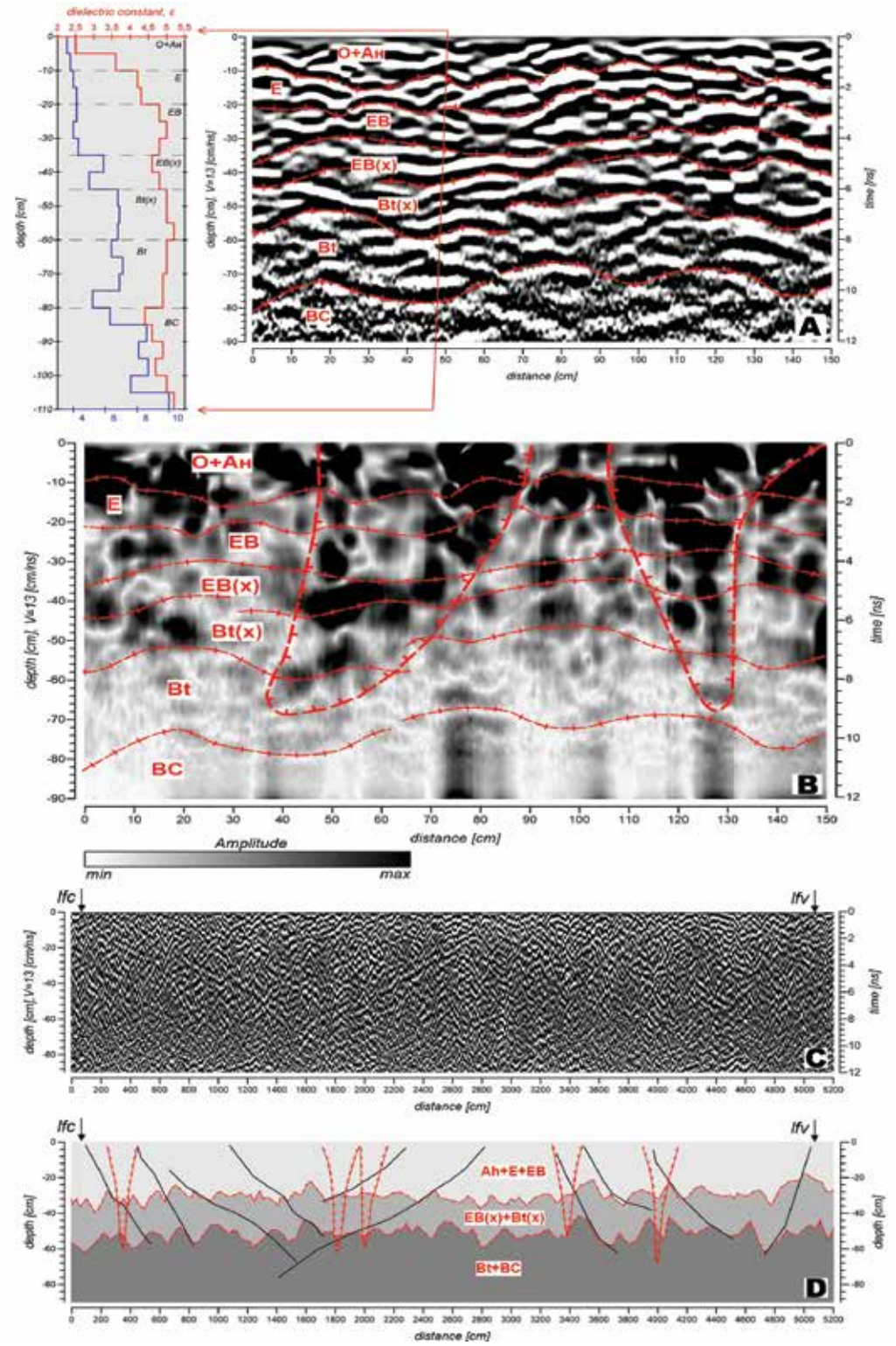

Fig. 3 Geophysical investigations: A – in *lfc* soil pit: left – TDR plot, right – GPR profile; B – amplitude profile, running from *lfc* to *lfv*; C – GPR profile; D – the interpretation model

Moving over to radargram analysis we recorded that in addition to the above mentioned boundaries it contained numerous extra reflections generated by internal variation of the composition, presence of boulders, roots, etc. The greatest contrast was observed at the Ah–E, EB–EB(x), Bt(x)–Bt boundaries, securing their reliable mapping throughout the study area.

Based on the available GPR profile with mapped soil boundaries (Fig. 3A) we obtained an amplitude profile (Fig. 3B). The structural boundaries were not visualized by the amplitude profile, but it clearly showed two areas with high reflection intensity (40–80 and 110–140 points), which could be interpreted as areas of precipitation seepage from the surface to the underlying horizons. This fact was corroborated by σ measurements by TDR data. Normally, the average conductivity is $\sigma = 6 \cdot 10\text{-}4$ S/m, whereas in the infiltration area it increases to $25 \cdot 10\text{-}4$ S/m. In addition to moisture migration areas, local maximums in the amplitude profile might indicate high stoniness of all horizons.

After reference data for interpretation have been gathered, a detailed study of the GPR profile running from lfc to lfv soil pit became possible (Fig. 3C). Relying on the established criteria, we developed the interpretation model and located the Ah + EB + E – EB(x) + Bt(x) and EB(x) + Bt(x) – Bt + BC boundaries, between which the studied fragipan horizon was situated (Fig. 3D). It was traced all along the GPR profile, showing a relatively steady thickness of ca. 15 cm. The boundaries were tortuous, suggesting there are numerous streaks with a vertical span of around 10 cm from overlying to underlying horizons. Also, a number of above-mentioned large infiltration areas were observed along the GPR profile. An interesting finding in the radargram was subtabular reflecting boundaries with different incidence directions (black lines in Fig. 3D). These boundaries do not correspond to specific soil horizons, but most probably represent some structural characteristics or, possibly, a bedding deformation of the entire surveyed formation.

The micromorphological observations demonstrated the indicators of various pedogenetic processes that took place in the studied soil profile (Fig. 4).

The Ah horizon was rich in roots and detritic organic material of different stages of decomposition (Fig. 4A). It had a complex microstructure with a combination of granular and isometric crumby aggregates. Dark organic pigment with heterogeneous distribution caused combination of dark-coloured and light-coloured micro-zones.

In the E (Fig. 4B) horizon we observed well-developed platy structure formed by a dense net of sub-horizontal fissures. Bleached loosely packed coarse sand and silt grains were dominant in the soil material. The structural aggregates demonstrated clear micro-zonality of the spatial distribution of different size fractions: prevailing bleached coarse grains were located in the lower part of platy units and close to the pores whereas fine material (silt with admixture of clay) was concentrated in the central and upper parts (Fig. 4B). This structure and micro-zonality resembled the "banded fabric" described by Van Vliet-Lanoë (2010). Furthermore, Fe-Mn nodules were widespread in the groundmass with rounded shapes and sharp boundaries (Fig. 4B).

All these properties were presented in the EB horizon (Fig. 4C), but the platy aggregates in this horizon were thinner, the Fe-Mn nodules were smaller although still having similar rounded shape.

The EBx horizon (Fig. 4D) showed strong differences with the overlying horizon. At the micromorphological scale, it demonstrated very compact homogeneous structure with no signs of platy aggregates. At the same time, it still had concentrations of bleached uncoated sand and silt material which showed signs of grain size micro-zonation: lenses of finer silty material alternate with the concentrations of sand grains. There were few brownish clayey areas in which sometimes illuvial clay coatings were observed. The latter however were deformed, fragmented and not related to the pores. The Fe-Mn nodules in this horizon were few; they were smaller, had irregular shape and diffuse boundaries.

The Btx horizon (Fig. 4E) was also a very compact horizon. It still had some concentrations of bleached coarse material; however brown clayey areas were dominant. Clay coatings were more frequent and less deformed than in the EBx horizon. There were some Fe-Mn nodules, with irregular shape and diffuse boundaries.

In the underlying Bt horizon the groundmass was enriched in clay and had brown colour. Large Fe-Mn mottles of irregular shape were frequent (Fig. 4G). Clay coatings filled a large part of available pore space (Fig. 4F). The larger ones were laminated and had strong interference colours (Fig. 4F). Few illuvial pedofeatures were deformed, fragmented and incorporated in ground mass that was a result of turbation processes.

The BC horizon (Fig. 4H) again had quite compact structure, coarse grains of various sizes were immersed in the clayey groundmass (porphyric c/f related distribution). Clay coatings and Fe-Mn mottles were small and few. We observed rock fragment containing clay coatings much larger than in the pores; we concluded that this feature was derived from parent material.

The texture analysis results are presented in the Table 2. All the horizons fell into the silt loam texture class. We paid major attention to the profile distribution of the sand sub-fraction contents as indicators of

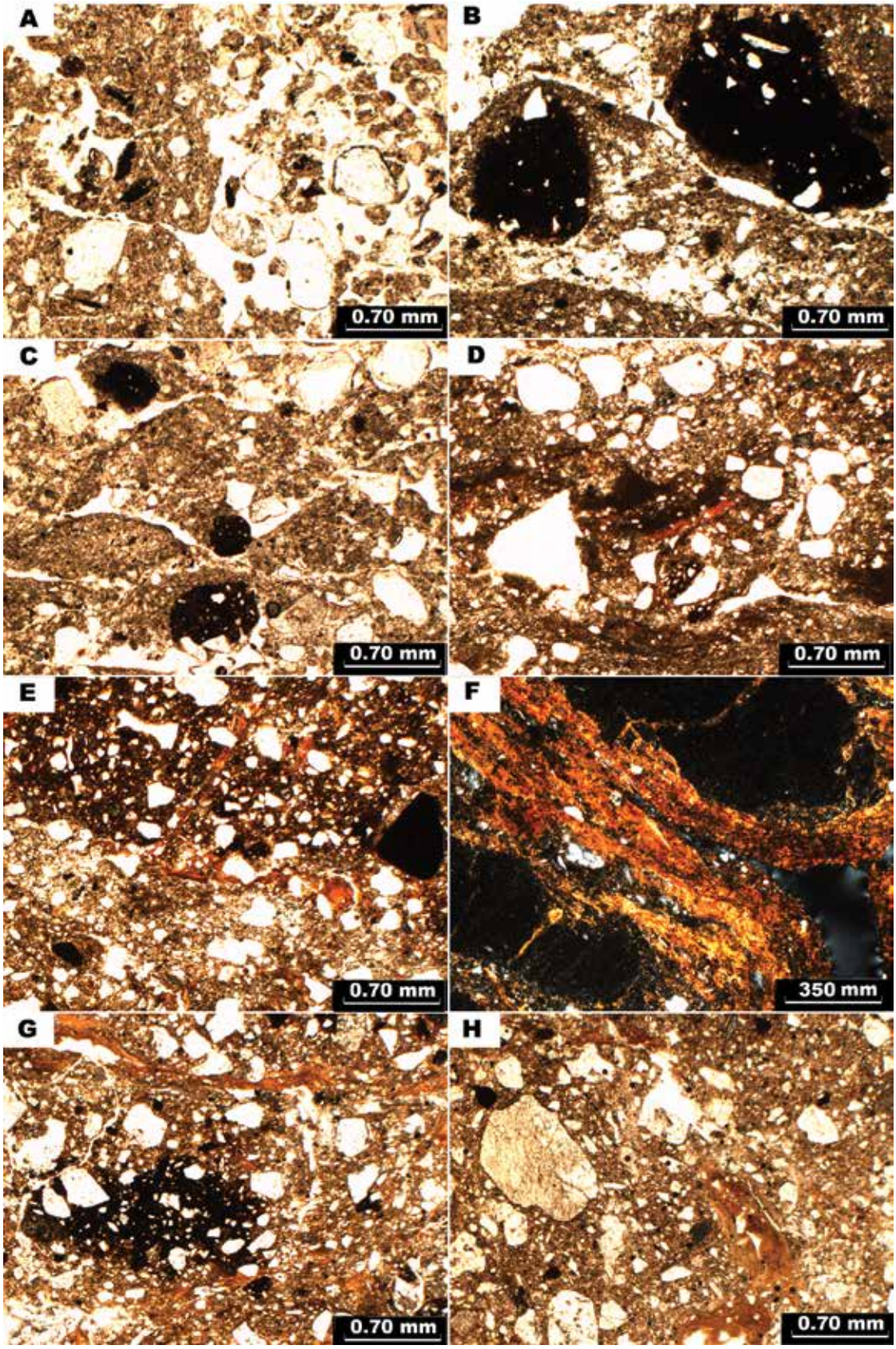

Fig. 4 Micromorphology of the Retisol genetic horizons; PPL – plane polarized light, N+ – crossed polarizers. A – coprogenic granular aggregates, fragmented plant residues; A horizon, PPL. B – platy structure, Fe-Mn nodules, banded fabric; E horizon, PPL. C – thin platy aggregates, small Fe-Mn nodules; EB horizon, PPL. D – compact structure, thin deformed clay coating, EBx horizon, PPL. E – neighbouring bleached and brown clayey microzones; Btx horizon, PPL. F – thick laminated clay coating with strong interference colours; Bt horizon, N+. G – illuvial clay coatings, ferruginous mottle; Bt horizon, PPL. H – porphyric c/f related distribution, thin clay coating; BC horizon, PPL

the lithological discontinuity. Nevertheless, there was almost no variation in subdivisions of sand fraction in each compared layer directly superimposed on the other. We further applied one of the criteria proposed by the WRB (IUSS Working Group 2014): as far as the soil is poor in coarse sand fraction; we calculated profile variations of the medium to fine sand ratio. The difference between the values of this coefficient in the neighbouring horizons reached maximum 15%, whereas the value not less than 25% is required as a reliable indicator of lithic discontinuity. The silt content was slightly higher in the upper part of the profile, and tended to decrease slowly in the argic horizon. The highest value was found in the E horizon, and the lowest was in the Bt horizon. The distribution of the clay material was much more differentiated: it was around 9% in the upper part of the profile and reached 15% at the bottom. The main change was detected in the transition from the EBx horizon to the Btx horizon.

The results of micromorphological and textural analysis were strongly connected with clay mineral composition. The clay minerals composition was complex in the studied soil (Fig. 5). The clay mineralogy of the profiles was composed by illite, chlorite, vermiculite, mixed layered and in lower amount by smectite and kaolinite. Smectite was confirmed by a strong (001) diffraction peak at about 14Å in air-dried condition that shifted to about 17Å in ethylene glycol treated samples and collapsed to 10Å after heating

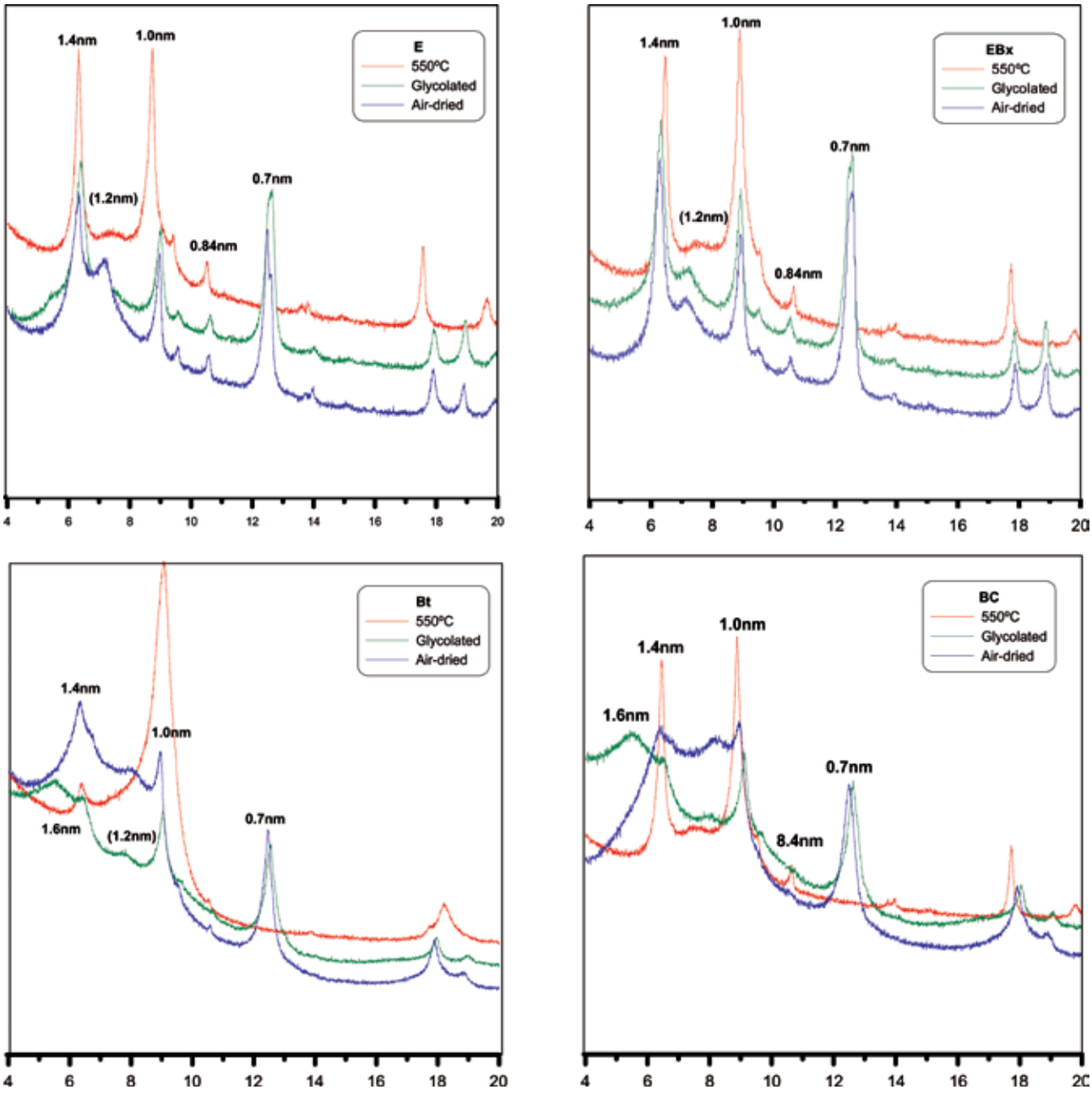

Fig. 5 X-ray diffraction patterns of clay fractions

Table 2 Particle size distribution of the soil profile and variation of the medium to fine sand ratio in horizons directly superimposed on the other

Horizons	Coarse Sand	Medium Sand	Fine Sand	Silt	Clay	Medium Sand/ Fine Sand
Volume, %						
Ah	1	17	7	56	9	15
E	2	17	6	57	9	3
EB	1	18	6	55	10	14
EBx	1	17	7	55	10	5
Btx	1	17	7	53	14	5
Bt	1	19	8	49	13	5
BC	1	16	7	52	15	

at 550°C. Vermiculite was not affected by ethylenglycol treatment and collapsed to 10 Å after heating while illite and chlorite profiles were unaffected by ethylenglycol solvation and heating. The discrimination between kaolinite and chlorite was complex due to the presence of the different peaks of other clay minerals and several heating experiments had to be carried out. By heating to 550ºC kaolinite becomes amorphous and its diffraction pattern disappears. In few samples kaolinite was identified in high resolution XRD measurements, because this mineral has the 002 peak at 24.9º and chlorites have their 004 reflection at 25.1º.

The presence of shoulders on ~14Å peak in most of the samples indicated the presence of illite-smectite mixed layer (I/S), which was determined in quantitative form after decomposing the spectra (air-dried and ethylenglycol treated samples) using profile fitting techniques.

Some of clay minerals were present in each soil horizon, for example chlorite, vermiculite and illite. The others occurred only in a specific part of the profile. The mixed layer minerals occurred almost in each horizon, except for the BC. The strongest differentiation was observed for smectites. These clay minerals were abundant only in the lower part of the profile, starting from the Btx horizon whereas in the upper eluvial part they were present as minor components.

DISCUSSION

We tried to reconstruct the formation of the Retisol during Holocene since the soil was formed after the deglaciation that happened in this area around 13–14.2 ha.

The typical soils of the Karelian region are Podzols (Classification and diagnostics of soils of the USSR 1987; Russian Soil Classification System 2001) due to the abundance of sandy deposits in this part of the country. The studied soil profile was formed in loamy glacial sediments and thus has an argic horizon at the depth of more than 50 cm and strong textural contrast: clay depletion together with strong bleaching in the upper horizons and clay increase in the medium and lower parts of the profile. The lateral continuity of this type of horizons was confirmed by the GPR profile measurements.

The verification of the litological uniformity versus discontinuity was one of the research tasks. As described above we applied the criterion proposed by WRB (IUSS Working Group WRB 2014): profile variations of the medium to fine sand ratio. As shown in Table 2 the differences between the neighboring horizons never exceed 15% whereas the shift of 25% is proposed as an indicator of discontinuity. These results fit well into macro- and micromorphological observations: in all the horizons we found a variety of coarse particles (from stones to silt) of similar sizes, shapes and mineralogical composition. Presence of stones in all horizons as a prominent feature was also detected by geophysical methods.

A notorious change related to the coarse material consists in the increase of silt fraction in the upper horizons. Frequently this tendency in the profiles of the Pleistocene periglacial area of Europe is explained by the input of eolian dust (e.g. Kleber, Terhorst 2013). We think that the alternative (or complementary) explanation of silt increase due to cryogenic fragmentation of coarser – sand and gravel – particles should be also considered, as proposed by Sedov and Shoba (1996). The process of physical breakdown of coarse mineral grains affected by freeze-thaw cycles is widely known and well documented experimentally; this process is known to produce silt-size particles (Konischev, Rogov 1994). It was shown that this breakdown could be accelerated when frost action is combined with the acid chemical weathering in the upper horizons of boreal forest soils (Leporsky *et al.* 1990). Taking into account this previous research and considerable resource of coarse particles in the studied profile we suppose that cryogenic fragmentation should be responsible at least partly for the silt accumulation in the upper horizons. Anyway if addition of eolian dust had taken place it could provide only minor admixture and did not result in the formation of a specific upper stratum and major lithological discontinuity – as shown by grain size and morphological criteria.

As far as no signs of a major lithological discontinuity have been detected, we suppose that differences in particle size distribution were generated predominantly by pedogenic processes. High clay content in the lower part of the profile is explained by clay illuviation, evidenced by the clay coatings observed

in the thin sections especially abundant in the Bt horizon. Another mechanism of clay differentiation could be related to acid weathering of unstable clay minerals. Strong differentiation of clay mineral assemblages within the profile with strong decrease in the smectites, the most weatherable components, in the upper soil horizons proves this assumption (Targulian *et al.* 1974, Tonkonogov *et al.* 1987).

What combination of soil forming factors could be responsible for such strong clay migration process? Since we know that this soil was formed during the Holocene, we revised published data about paleoecological records for Karelia for this period.

During the Holocene, the climate conditions in Karelia were changing, and in some periods were different from the actual conditions. Thus, around 6000 years ago, the vegetation in this area was characterized by such trees like *Quercus, Tilia, Ulmus*, that are common in broad-leaved forests (Sandgren *et al.* 2004; Yelina, Filimonova 2007). The southern taiga zone was at that time up to 66˚ of North Latitude, so the studied soil developed under warmer temperature regime and had less acidity due to the composition of litter. The texture differentiation most likely took place at that time, so we could associate the formation of strong clay coatings with the Atlantic period of the Holocene. During the succeeding period around 3000–3500 years ago this area suffered relative fall of the temperature and was covered by boreal (north taiga) pine and spruce forests (Yelina, Filimonova 2007; Dolukhanov *et al.* 2009).

The consolidation took place in the lower part of the EB horizon and the upper part of the Bt horizon, that is confirmed by the interpretation of GPR observations. The micromorphological analysis has shown that compaction occurred in the material which already had features of eluvial (bleached microzones) and illuvial (deformed clay coatings) processes, typical for the transitional horizons of a Luvisol profile. At the same time a frost-induced feature – grainsize microzonation – developed in EBx. We suppose that the formation of the fragic horizon happened after the texture differentiation, probably during the Sub-Boreal period.

The upper E and EB horizon have well-developed platy structure that was formed because of recent ice lensing during seasonal freezing. The current seasonal cryogenic aggregation and the bioturbation are destroying the consolidated part and involve it into the modern soil formation. We also attribute the stagnic (surface redox) processes which produce rounded Fe–Mn nodules in the E and EB horizons to the modern active soil forming processes as well. The material of the albeluvic tongues has the same properties as the entire E horizon, but is more compact.

Fragipan horizon, although being partly inherited feature, has an important influence on the present day soil processes and regimes. Geophysical investigations showed strong spatial differentiation of soil hydrological characteristics associated with fragipan structure. Along glossic features there are directions of preferential water flow, demonstrated by higher water content in the radargram and amplitude profile of geophysics observations. Taking into account that the major part of fragipan has low permeability and that according to the GPR profile it is laterally continuous, we suppose that it is a major factor of water logging and stagnic processes in the overlying E and EB horizons.

Recent investigations connect the fragipan formation with high concentration of swelling clay minerals (Szymanski *et al.* 2012; Nikorych *et al.* 2014). In the case of Karelian fragipan, there are no smectite clay minerals in the EBx horizon; they appear only in the lower horizons. This feature also correlates with a texture class analysis, because the argic horizon is enriched with clay minerals if compared to the textural composition of the albic horizon. The smectites are the most unstable component of clay minerals complex (Targulian *et al.* 1974). Probably, their accumulation in the lower part of the profile happens because of the preferential mobilization by the illuviation processes and/or because those minerals were selectively destroyed in the upper part of the profile with more aggressive weathering conditions.

CONCLUSIONS

We consider that in the studied soil profile the fragipan, the high density soil horizon, the features of eluvial, gleyic and turbation processes are less intensive than in overlying and underlying soil horizons as it was developed in the transitional zone of Albic Retisol profile. We also suppose that the compaction process has occurred in a Sub-Boreal period after a previous illuviation took place during the Atlantic optimum. The consolidation of fragipan is not connected with swelling clay minerals in the case of Karelia Retisol profile.

ACKNOWLEDGEMENTS

The field research was supported by the project 0221-2017-0047 financed by the Russian Academy of Sciences. The authors thank to Jaime Diaz (Institute of Geology of the UNAM) for the help with soil thin section preparation and the organizers of the INQUA Peribaltic Conference 2018 for the possibility to present the studied soil profile during the field excursion. The authors express they sincere thanks for

two anonymous reviewers for critical comments and valuable remarks.

REFERENCES

Alexandrovskiy, A.L. 1983. Evolyutsiya pochv Vostochno-Evropeiskoi ravniny v golotsene [The Holocene Evolution of Soils in the East European Plain]. Nauka, Moscow, 150 pp. [In Russian].

Alexandrovskiy, A.L. 2000. Holocene development of soils in response to environmental changes: the Novosvobodnaya archaeological site, North Caucasus. *Catena 41(1–3)*, 237–248.

Arnold, R.W. (ed.) 2001. *Russian Soil Classification System*. Oykumena, Smolensk, 214 pp.

Assalay, A.M., Rogers, C.D.F., Smalley, I.J., Jefferson, I.F. 1998. Fragipan formation in loess soils: development of the Bryant hydroconsolidation hypothesis. *Geoderma 83*, 1–16.

Bockheim, J.G., Hartemink, A.E. 2013. Soils with fragipans in the USA. *Catena 104*, 233–242.

Bryant, R.B. 1989. Physical processes of fragipan formation. In: Smeck, N.E., Ciolkosz, E.J. (eds.). *Fragipans: Their Occurrence, Classification and Genesis*. SSSA Special Publications 24, SSSA, Madison, Wisconsin, 141–150.

Bullock, P., Fedoroff, N., Jongerius, A., Stoops, G., Tursina, T., Babel, U. 1985. *Handbook for soil thin section description*. Waine Research Publications, Wolverhampton, United Kingdom,152 pp.

Ciolkosz, E.J., Waltman, W.J., Thurman, N.C. 1995. Fragipans in Pennsylvania soils. *Soil Survey Horizons 36*, 5–20.

Dolukhanov, P.M., Subetto, D.A., Arslanov, Kh.A., Davydova, N.N., Zaitseva, G.I., Djinoridze, E.N., Kuznetsov, D.D., Ludikova, A.V., Sapelko, T.V., Savelieva, L.A. 2009. The Baltic Sea and Ladoga Lake transgressions and early human migrations in North-western Russia. *Quaternary International 203 (1–2),* 33–51.

Egorov, V.V., Fridland, V.M., Ivanova, E.N., Rozov, N.N., Nosin, V.A., Friev, T.A. 1987. *Classification and diagnostics of soils of the USSR*. A.A. Balkema Publ., Rotterdam, The Netherlands, 288 pp.

Falsone, G., Stanchi, S., Bonifacio, E. 2017. Simulating the effects of wet and dry on aggregate dynamics in argillic fragipan horizon. *Geoderma 305 (1)*, 407–416.

FAO. Guidelines for soil description. 2006. Food and Agriculture Organization of the United Nations, 4th edition, Rome, 77 pp.

Fitzpatrick, E.A. 1956. An indurated soil horizon formed by permafrost. *Jornal of Soil Science 7*, 248–257.

Galbraith, J. 2nd Conference for Soil Classification – Aug. 2–8, 2004 Petrozavodsk, Karelia 31(Russia) Additional Field Tour Notes Concerning Soil Taxonomy Classification (unpublished).

Gallardo, J., Alvarez, A., Cala, V. 1988. Horizontes de fragipan de tipo "ison" formados por permafrost en la Sierra de Guadarrama. *Estudios geologicos 44*, 83–91.

Gerasimova, M.I. (ed.) 2004. *Field Workshop Guidebook of the International Conference* (August 3–8, 2004, Petrozavodsk, Karelia, Russia). Petrozavodsk, 34 pp.

Habecker, M.A., McSweeney, K., Madison, F.W. 1990. Identification and genesis of fragipans in Ochrepts of north central Wisconsin. *Soil Science Society of America Journal 54*, 139–146.

World Reference Base for Soil Resources 2014: IUSS Working Group WRB, International soil classification system for naming soils and creating legends for soil maps, World Soil Resources Reports No. 106, FAO, Rome.

Kleber, A., Terhorst, B. 2013. *Mid-Latitude Slope Deposits (Cover Beds)*. Developments in Sedimentology 66, Elsevier, Amsterdam, 320 pp.

Konishchev, V.N., Rogov, V.V. 1994. Metody kriolitologicheskih issledovanij [Methods of cryolithological studies]. MGU Publ., Moscow, 135 pp. [In Russian].

Leporskiy, O.R., Sedov, S.N., Shoba, S.A., Bgantsov ,V.N. 1990. Role of freezing in comminution of primary minerals of podzolic soils. *Pochvovedeniye 6,* 107–111.

Moore, D., Reynolds, R.C.Jr. 1997. *X-Ray Diffraction and the Identification and Analysis of Clay Minerals*. 2nd ed., Oxford University Press, Oxford, New York, 378 pp.

Nikiforoff, C.C., Humbert, R.P., Cady, J.G. 1948. The hardpan in certain soils of the coastal plain. *Soil Science 65*, 135–154.

Nikonov, A.A., Rusakov, A.V., Korkka, M.A., Spiridonova, E.A. 2005. The finding of early Holocene Relict soil on the southern coast of the Gulf of Finland and its paleogeographic implications. *Doklady Academii Nauk 403 (5),* 794–798.

Nikorych, V., Szymański, W., Polchyna, S., Skiba, M. 2014. Genesis and evolution of the fragipan in Albeluvisols in the Precarpathians in Ukraine. *Catena 119*, 154–165.

North, P. F. 1976. Towards an absolute measurement of soil structural stability using ultrasound. *European Journal of Soil Science 27 (4),* 451–459.

Payton, R.W. 1992. Fragipan formation in argillic brown earths (Fragiudalfs) of the Milfield Plain, north-east England. I. Evidence for a periglacial stage of development. *Journal of Soil Science 43*, 621–644.

Payton, R.W. 1993a. Fragipan formation in argillic brown earths (Fragiudalfs) of the Milfield Plain, north-east England. II. Post Devensian developmental processes and the origin of fragipan consistence. *Journal of Soil Science 44*, 703–723.

Payton, R.W., 1993b. Fragipan formation in argillic brown earths (Fragiudalfs) of the Milfield Plain, north-east England. III. Micromorphological, SEM and EDXRA studies of fragipan degradation and the development of glossic features. *Journal of Soil Science 44*, 725–739.

Rusakov, A.V., Korkka, M.A., Kerzum, P.P., Simakova, A.N. 2007. Paleosols in the moraine-mantle loam sequence of northeastern Europe: the memory of pedogenesis rates and evolution of the environment during OIS3. *Catena 71 (3),* 456–466.

Saarnisto, M., Saarinen, T., 2001. Deglaciation chronology of the Scandinavian Ice Sheet from the Lake Onega Basin to the Salpausselka End Moraines. *Global and Planetary Change 31*, 387–405.

Sandgren, P., Subetto, D.A., Berglund, B.E., Davydova, N.N., Savelieva, L.A., 2004. Mid-Holocene Littorina Sea transgressions based on stratigraphic studies in coastal lakes of NW Russia. *GFF 126 (4, December)*, 363–380.

Schoeneberger, P.J., Wysocki, D.A., Benham, E.C. 2012. *Soil Survey Staff*. Field Book for Describing and Sampling Soils. Version 3.0. Natural Resources Conservation Service. National Soil Survey Center, Lincoln, NE.

Sedov, S.N., Shoba, S.A. 1996. Methods of investigating a mineral skeleton of soils: assessment of possibilities and application to solving soil-genetic problems. *Eurasian Soil Science 29 (10)*, 1081–1089.

Sochan, A., Polakowski, C., Łagód, G. 2014. Impact of optical indices on particle size distribution of activated sludge measured by laser diffraction method. *Ecological Chemistry and Engineering 21 (1)*, 137–145.

Soil Survey Staff, 2003. Keys to Soil Taxonomy, 9th edn., USDA-Natural Resources Conservation Service, Washington, DC.

Soil Survey Staff, 2014. Keys to Soil Taxonomy, 12th edn., USDA-Natural Resources Conservation Service, Washington, DC.

Stoops, G. 2003. *Guidelines for Analysis and Description of Soil and Regolith Thin Sections*. Soil Science Society of America, Madison, Wisconsin USA.

Svendsen, J.I., Alexanderson, H., Astakhov, V.I., Demidov, I., Dowdeswell, J.A., Funder, S., Gataullin, V., Henriksen, M., Hjort, C., Houmark-Nielsen, M., Hubberten, H.W., Ingolfsson, O., Jakobsson, M., Kjaer, K., Larsen, E., Lokrantz, H., Lunkka, J.P., Lysa, A., Mangerud, J., Matiouchkov, A., Murray, A., Möller, P., Niessen, F., Nikolskaya, O., Polyak, L., Saarnisto, M., Siegert, C., Siegert, M.J., Spielhagen, R.F., Stein, R. 2004. Late quaternary ice sheet history of northern Eurasia. *Quaternary Science Reviews 23 (11–13)*, 1229–1271.

Szymanski, W., Skiba, M., Skiba, S. 2012. Origin of reversible cementation and brittleness of the fragipan horizon in Albeluvisols of the Carpathian foothills, Poland. *Catena 99*, 66–74.

Targulian, V.O., Goryachkin, S.V. 2004. Soil memory: Types of record, carriers, hierarchy and diversity. *Revista Mexicana de Ciencias Geológicas 21*, 1–8.

Targulian, V.O., Sokolova, T.A., Birina, A.G., Kulikov, A.V., Tselishcheva, L.K. 1974. *Arrangement, composition and genesis of sod-palepodzolic soil derived from mantle loams*. Analytical investigation, 10th International Congress in Soil Science, 107 pp.

Tonkonogov, V.D., Gradusov, B.P., Rubilina, N.Y.E., Targulian, V.O., Chizhikova N.P. 1987. Differentiation of the mineral and chemical composition in sod-podzolic and podzolic soils. *Soviet Soil Science 19 (4),* 23–35.

Van Vliet, B., Langohr, R. 1981. Correlation between fragipans and permafrost with special reference to silty Weichselian deposits in Belgium and northern France. *Catena 8*, 137–154.

Van Vliet-Lanoë, B., 2010. Frost Action. In: Stoops, G., Marcelino, V., Mees F. (eds.). *Interpretation of Micromorphological Features of Soils and Regoliths*. Elsevier, Amsterdam, 81–108.

Winters, E. 1942. Silica hardpan development in the Red and Yellow Podzolic region. *Soil Science Society of America Proceedings 7*, 437–440.

Wojdyr, M., 2010. Fityk: a general-purpose peak fitting program. *Journal of Applied Crystallography 43,* 1126–1128.

Yelina, G.A., Filimonova, L.V. 2007. Late Glacial and Holocene vegetation and climate at the Eastern Fennoscandia and problems of mapping. In: *Actual problems of geobotany. III All-Russian school-conference, lections*. Karelian Research Centre of RAS, Petrozavodsk,117–143.

Discusión

Según la clasificación internacional de la WRB (IUSS Working Group WRB, 2015) “El horizonte frágico (del latín frangere, romper) es un horizonte subsuperficial natural no cementado con agregación y un patrón de porosidad tal que las raíces y el agua de percolación sólo penetran el suelo a lo largo de caras interpedales y vetas.” Como se ha mencionado en la introducción, hay una variedad de hipótesis que se han aplicado para explicar su génesis (Bockheim and Hartemink, 2013). Una de las más comunes en Europa se refiere a las condiciones periglaciales (Fitzpatrick, 1956; Van Vliet y Langohr, 1981), sin embargo, esta no puede explicar la génesis de estos horizontes en otras condiciones climáticas. Sin embargo, la hipótesis de hidroconsolidación (Rogers et al., 1994; Smalley and Markovic, 2014; Smalley et al., 2016) parece ser la más adecuada para poder unir los casos en condiciones contrastantes, y nuestros resultados de estudio de la porosidad apoyan a esta explicación. En este trabajo se han analizado los dos muy diferentes casos, en ninguno hubo presencia de condiciones periglaciales durante la formación y desarrollo de los perfiles analizados. Consideramos que en diferentes condiciones el proceso de hidroconsolidación puede ser iniciado por causas diferentes que implican un humedecimiento de material y su posterior proceso de desecación con reorganización del espacio poroso, de lo cual consiste la hidroconsolidación en sí como lo ha explicado Bryant en 1989. Al mismo tiempo, los tepetates de tipo fragipán conocidos en México por décadas están llenos de rasgos pedogenéticos (como se ha demostrado por estudios micromorfológicos de las Dras Oleschko, Hidalgo y Gutierrez-Castorena y en este mismo trabajo); y cumplen con los requisitos de la lista de WRB para ser nombrados fragipan. Por ejemplo, Zebrowski en 1992 escribió lo siguiente: “La clasificación de este último [tepetate] debe considerar su carácter de dureza más o menos reversible (se debe utilizar el término de “fragipan” solamente para los horizontes que se disgregan en el agua) y la naturaleza del cemento.” Como se ha demostrado en el Capitulo 3.1 de la tesis, los tepetates de este estudio han pasado esta prueba que divide entre si los fragipanes y duripanes.

Porosidad – memoria edáfica de formación de los fragipanes en diferentes zonas climáticas. Estudio de porosidad en las muestras inalteradas.

La porosidad forma parte la memoria edáfica. Una parte de ello son los poros alrededor de los agregados, y otra, los poros que están dentro de los agregados y se llaman texturales. Hay poros que atraviesan varios agregados (como los canales biogénicos). Los poros texturales se consideran

como relativamente estables y no cambian durante el desarrollo del suelo (Chandrasekhar et al., 2019). Se forman al momento inicial de la pedogénesis y su distribución es característica de la matriz del horizonte. Observando los poros texturales, estudiamos en la porosidad la grabación del momento "cero" de la evolución del suelo. En su mayoría, el tamaño de estos poros es de unos micrómetros. Pero los poros más grandes (≥5µm), que corresponden al desarrollo de los procesos pedogenéticos que transforman el material parental y forman los agregados específicos del suelo, a lo largo de la evolución de dichos procesos están dispuestos a cambiar su forma (Leij et al., 2002; Bormann y Klaassen, 2008; Chandrasekhar et al., 2019; de Oliveira et al., 2021), tamaño, orientación, conectividad e, inclusive, algunos hasta pueden dejar de ser "poros" por haberse llenado de algún material. Esta parte de la memoria edáfica es una evidencia de los procesos que han ocurrido dentro del suelo y forman la memoria de tipo palimpsesto (Targulian y Goryachkin, 2004). Así por ejemplo, podemos observar los cutanes de iluviación intactos, como registro de un poro antiguo que ahora no existe o está tapado y no funciona de la misma manera que antes. Si durante el desarrollo del suelo con iluviación de arcilla el ambiente ha cambiado y se empezaron a formarse los agregados de forma de cuña de un Vertisol, los poros nuevos en las superficies de los slickensides van a atravesar los cutanes de iluviación y esto será otro ejemplo de este tipo de la memoria edáfica del espacio poroso.

En el caso de los fragipanes, los poros texturales forman la mayor parte de la porosidad (Falsone y Bonifacio 2009). Esto se pudo comprobar a partir del estudio en 2D y 3D realizado en los fragipanes de Karelia y Tlaxcala (capítulos 3.1, 3.2). En los dos casos, se han encontrado los poros texturales, distribuidos de manera homogénea en la matriz del horizonte. Sin embargo, en el caso del fragipán de Karelia que se compactó durante el desarrollo del suelo, los poros texturales también son de origen pedogenético. En el suelo de Karelia se ha presentado la ausencia de los poros estructurales en la lámina delgada del fragipán, y su porosidad solamente se ha podido estudiar por medio de microtomografía computacional (capitulo 3.2). Se ha observado que hubo una variedad de poros estructurales en los otros horizontes del perfil, que se han formado por los procesos biogénicos (horizonte Ah) y criogénicos (horizonte E) en la parte superior, y poros-grietas formados más abajo en los horizontes Bt y BC. En el caso de Tlaxcala (capítulo 3.1) se ha encontrado que la presencia de poros texturales es mayor en el horizonte fragipán, mientras que el horizonte superior, que se asume como el producto del mismo evento de sedimentación (Anexo 1) tiene más poros grandes. Es importante, que la porosidad total del horizonte *frágico* fue más alta

que en el horizonte subyacente Bt en Karelia y el horizonte 3EBtx superior en Tlaxcala. La mayor diferencia de los dos casos es que en el fragipán de Tlaxcala se han encontrado los poros, rellenados de arcilla iluviada, posteriormente a la compactación primaria de la matriz y distribución de los poros texturales, que implica la pedogénesis activa. Por otro lado, en el horizonte fragipán en el suelo de Karelia parece no haber ocurrido ninguna alteración posterior a la compactación a pesar de haberse posicionado en medio del Retisol y de que la compactación haya ocurrido como parte del proceso del desarrollo del suelo.

Fragipán – desarrollo y conservación dentro de un perfil de suelo formado por procesos de eluviación-iluviación.

Fragipán se reconoce como un horizonte subsuperficial EB, BE o, más común, B. De acuerdo a la clasificación WRB (IUSS Working Group WRB, 2015), la parte superior y caras de los bloques estructurales tienen las características *álbicas* o de horizonte eluvial, o cumplen con los requisitos de *lenguas albelúvicas*, también en esta zona se puede observar los procesos *stágnicos*. La hipótesis de formación por el proceso de hidroconsolidación supone una saturación con agua para que el horizonte se compacte durante el proceso de secado. Es probable que la formación del fragipán esta favorecida por la presencia de una capa poco permeable, como un horizonte Bt. En Karelia, el fragipán se formó encima de un horizonte Bt, en un perfil de suelo ya desarrollado previamente y con diferencia textural (capítulos 3.2 y 3.3). También sabemos que este suelo se formó durante el Holoceno, lo que implica que la hipótesis de Van Vliet-Lanoë y Langohr del desarrollo tanto del fragipán como del horizonte eluvial e iluvial durante el glacial tardío en el ambiente periglacial (1981) no es aplicable en este caso. En Karelia, por su apariencia y rasgos morfológicos, el fragipán se aproxima más a un horizonte EB con fuertes rasgos de eluviación. Además, se ha documentado la ausencia de los componentes esmécticos en la parte eluviada del perfil. Esto no coincide con los resultados de estudio de los fragipanes en Cárpatos (Nikorych et al. 2014) donde el fragipán corresponde a un horizonte iluvial tipo Bt y como agente principal de la consolidación se asumieron las arcillas expandibles. Por otro lado, en la clasificación de la WRB (IUSS Working Group WRB, 2015) se considera una mayor contribución de caolinita en la mineralogía de arcillas del fragipán.

En Tlaxcala la formación del fragipán es un episodio referenciado al Pleistoceno Tardío (Anexo 1). A diferencia de Karelia, el fragipán en Tlaxcala se formó a partir de un pedosedimento y su

compactación primaria probablemente pasó brevemente después de la sedimentación de un material saturado de agua y que incluía material redepositado del suelo anterior erosionado. Esta secuencia de la formación se asemeja a la hipótesis publicada anteriormente por y Solleiro-Rebolledo et al., (2003) y Díaz-Ortega et al. (2010). De esto surge la otra diferencia entre los casos de Karelia y Tlaxcala: en Tlaxcala la iluviación ocurrió después de la compactación primaria del fragipán (capitulo 3.1), lo que provocó la acumulación de cutanes de arcilla en los poros-grietas y su compactación secundaria, mientras que en Karelia el horizonte Bt ya existía antes de la formación del fragipán. Este resultado, la formación del mismo horizonte fragipán provocado por diferentes procesos en diferentes condiciones, demuestra el isomorfismo a nivel de un horizonte diagnostico (Targulian y Goryachkin, 2004).

Los cutanes de iluviación y su papel en los tepetates tipo fragipán anteriormente ya se han estudiado en detalle en 1992 por Oleschko (1992), Hessmann (1992), Hidalgo (1992, 1995), Gutiérrez-Castorena et al., (2007). En este estudio los resultados publicados en el capítulo 3.1 y en Anexo 1 demuestran dos etapas de compactación. En la segunda fase de compactación de los tepetates es sumamente importante la fase pedogenética (iluviación de arcilla). En el caso de la tesis doctoral de la Dra. Hidalgo (1995), ella especifica que el origen de los tepetates no se debe solamente a pedogénesis, sino que lo más importante es la compactación original, lo que provocó la acumulación de arcillas en los poros. Sin embargo, a diferencia de los trabajos anteriores, el tepetate 3BCt(x) se considera formado de un pedosedimento, lo cual se basa, por ejemplo, en los datos de análisis de bioindicadores (Anexo 1) que demuestran (a) presencia de fitolitos, mientras que en los tepetates 5BCt(x) y 6BCt(x) no los hay; (b) una disminución gradual hacia arriba de cantidad de fitolitos comparando con el paleosuelo anterior. En otras palabras, el tepetate 3BC(t)x tiene los fitolitos arrastrados del suelo anterior al momento de traslado del material. Considerando las propiedades morfológicas idénticas de los tres tepetates estudiados, se concluye que tienen un origen similar, y la poca presencia de los fitolitos en los horizontes 5 y 6BCt(x) se debe a que el traslado (erosión) ha ocurrido con mayor frecuencia y no se han acumulado suficientes fitolitos. La razón de transportación de los materiales y formación de los pedosedimentos puede ser derivada a los flujos volcánicos tipo lahar.

Los estudios de la secuencia en Tlaxcala que se presentan en Anexo 1 también han revelado información de los paleosuelos, entre los cuales se encuentran los tepetates. Por ejemplo, el análisis

de la fracción de arcilla en los paleosuelos de la Unidad Gris de Tlaxcala, estudiados por Sedov et al. (2009), mostró caolinita y halloysita en difractogamas, sin embargo, los estudios tomográficos (Anexo 1) demuestran claramente presencia de los slikensides en estos paleosuelos. Anteriormente Heidari et al. (2008) han enlistado en su trabajo una lista de evidencias de desarrollo de los Vertisoles en suelos con ausencia de minerales esmectiticos o su poca presencia, incluyendo un ejemplo de El Salvador.

En el caso de Karelia el horizonte *frágico* se ha formado dentro de un perfil tipo Luvisol, que se desarrolló durante el óptimo del Holoceno. Sin embargo, posterior a esta compactación, no se ve la evidencia de la perturbación de la estructura masiva del horizonte. Se concluye que el fragipán, como un horizonte poco permeable, ha restringido el flujo de la suspensión enriquecida en arcilla y la iluviación de la arcilla solo se ha podido realizar a través de las grietas entre los bloques estructurales, aunque es importante anotar que el horizonte *frágico* comúnmente se ha encontrado con evidencia de la arcilla iluviada (Bockheim y Hartemink, 2013). Además, en Karelia hay presencia de proceso *stágnico* en el suelo, evidente por las concreciones de Fe-Mn (capítulos 3.2 y 3.3), probablemente provocado por el mismo fragipán que es poco permeable. El clima actual dispone el suelo a los procesos criogénicos, que forman la estructura laminar en los horizontes superiores. Sin embargo, no llegan a perturbar el horizonte *frágico* y se queda intacto.

En Tlaxcala el clima favorece a desarrollo de perfil mucho más activo. Los procesos pedogenéticos han perturbado el horizonte *frágico* y se han formado los poros, que posteriormente se han rellenado de la arcilla iluviada, de tal manera que esto fue la segunda etapa de la compactación de este fragipán. Al igual que en Karelia, en Tlaxcala la presencia del fragipán provocó la formación de nódulos de Fe-Mn en el horizonte superior (proceso *stágnico)* pero este proceso tuvo lugar en el pasado durante la fase húmeda del Pleistoceno Tardío – MIS2. Sin embargo, desde que el clima se empezó a ser más cálido y árido en el Holoceno, el fragipán no ha tenido tanta influencia en el desarrollo del perfil. La influencia de este horizonte aumentó en el Holoceno Tardío porque su presencia ha provocado una drástica erosión en el área de estudio en la etapa antrópica del desarrollo del paisaje (los últimos 3000 años) causada por el uso del suelo.

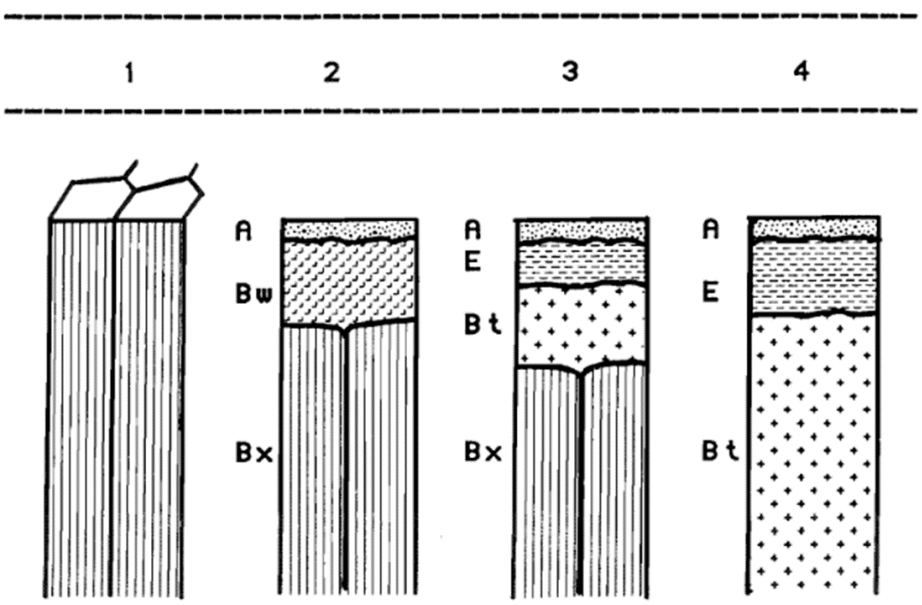

Fig. 1 Las fases del desarrollo del suelo sobre un fragipán (Citado por Ciolkosz et al.,1995). Los índices de horizontes están de acuerdo a la clasificación WRB.

Los resultados obtenidos nos permiten hacer unas conclusiones generales acerca de la interacción entre el desarrollo y la evolución de fragipanes y procesos de eluviación e iluviación de arcilla en los suelos con los horizontes *árgicos* (Bt). El esquema (Fig. 1) demuestra la secuencia del desarrollo de los perfiles con fragipán en Pennsylvania propuesta por Ciolkosz et al. (1995). Según este autor, el fragipán es un horizonte relicto que se encuentra en proceso de destrucción progresiva por la pedogénesis reciente. Este esquema no concuerda con los resultados obtenidos en Karelia y Tlaxcala, donde el fragipán se ha formado durante el desarrollo del perfil del suelo y no antes y los procesos pedogenéticos han provocado un aumento de la compactación del horizonte. En consecuencia, se puede considerar el fragipán como parte de la memoria edáfica y no solamente un relicto de procesos sedimentarios y/o criogénicos.

Conclusiones

En este trabajo se hizo el análisis de un suelo en Rusia y de los fragipanes de México Central, que se conocen como tepetate tipo fragipan.

1. Se determinó que la porosidad del fragipán en Karelia y Tlaxcala consiste mayormente de poros texturales, mientras que en Tlaxcala la compactación del fragipán se ha dividido en

dos fases: la compactación primaria con formación de poros texturales y posteriormente una etapa de illuviación de arcilla que ha tapado los poros grandes.

2. En condiciones contrastantes entre Karelia y Tlaxcala, a través de diferentes procesos pedogenéticos se ha formado el fragipán, lo que es un ejemplo de isomorfismo. Además, en los dos casos el fragipán se ha formado en un perfil tipo Luvisol, pero la secuencia de los procesos ocurridos ha sido diferente.
3. Los fragipanes forman parte de la memoria edáfica del desarrollo de un perfil con procesos de eluviación e iluviación, en condiciones de clima húmedo-templado, y sus rasgos permiten ver la secuencia de los procesos que han ocurrido en el perfil. En el caso de Karelia, se ha podido determinar las fase de iluviación durante el Optimo del Holoceno. En el caso de Tlaxcala, se ha podido distinguir la fase de formación del suelo durante el Pleistoceno Tardío (MIS 2).

Referencias

Acevedo-Sandoval, O.A., Flores-Román, D., 2000. Genesis of white fragipáns of volcanic origin: Revista Mexicana de Ciencias Geológicas, 17(2), 152-162

Assalay, A.M., Jefferson, I., Rogers, C.D.F., Smalley, I.J., 1998. Fragipán formation in loess soils: development of the Bryant hydroconsolidation hypothesis. Geoderma 83, 1–16.

Attou, F., Brua, A., 1998. Experimental study of 'fragipáns' formation in soils. Role of both clay dispersion and wetting–drying cycles. Earth and Planetary Science 326, 545–552.

Bockheim, J.G., Hartemink, A.E., 2013. Soils with fragipáns in the USA. Catena, 104, 233–242.

Bormann, H., Klaassen, K., 2008. Seasonal and land use dependent variability of soil hydraulic and soil hydrological properties of two Northern German soils. Geoderma 145, 295–302.

Brewer R., 1960. Cutans: their definition, recognition and classification. Soil Sci. 11, 280-292.

Bryant, R.B., 1989. Physical processes of fragipán formation. In: Smeck, N.E., Ciolkosz, E.J. (Eds.), Fragipáns: Their Occurrence, Classification and Genesis. SSSA Spec. Publ., 24. SSSA, Madison, Wisconsin, pp. 141–150.

Campos, A., Dubroeucq, D., 1990. Formación de tepetates en suelos provenientes de las alteraciones de materiales volcánico. Terra. 8(2), 137-141.

Chandrasekhar, P., Kreiselmeier, J., Schwen, A., Weninger, T., 2019. Modeling the evolution of soil structural pore space in agricultural soils following tillage. Geoderma 353, 401–414.

Ciolkosz, E.J., Waltman, W.J., Thurman, N.C., 1995. Fragipáns in Pennsylvania soils. Soil Survey Horizons 36, 5–20.

de Oliveira, J.A.T., Cássaro, F.A.M., Pires, L.F., 2021. Estimating soil porosity and pore size distribution changes due to wetting-drying cycles by morphometric image analysis. Soil and Tillage Research, 205, 104814.

Díaz-Ortega, J., Solleiro-Rebolledo, E., Sedov, S., Cabadas, H., 2010. Paleosuelos y tepetates del Glacís de Buenavista Morelos (México): testigos de eventos climáticos de la transición Pleistoceno-Holoceno. Boletín de la Sociedad Geológica Mexicana, 62, 469-486.

Dubroeucq, D., 1992. Los tepetates de la región de Xalapa, Veracruz (México): un endurecimiento de origen pedológico. Terra. 10, 233–240.

Duncan, M.M., Franzmeier, D.P., 1999. Role of free silicon, aluminum, and iron in fragipán formation. Soil Science Society of America Journal 63, 923–929.

Eghbal M.K., Givi J., Torabi H., Miransari M., 2012. Formation of soils with fragipán and plinthite in old beach deposits in the South of the Caspian Sea, Gilan province, Iran. Applied Clay Science 64, 44–52.

Etchevers, J.D., Hidalgo, C., Prat, C., Quantin, P., 2006. Tepetates of Mexico, in Encyclopedia of Soil Science: New York, USA, Marcel Dekker, 1745–1748.

Falsone, G., Bonifacio, E., 2009. Pore-size distribution and particle arrangement in fragipán and nonfragipán horizons. Journal of Plant Nutrition and Soil Science 172, 696–703.

FAO (1974). Soil map of the world. Volumes 1-10. Food and Agriculture Organization of the United Nations and UNESCO, Paris. 1:5,000,000.

Flores, R.D., A. Gonzalez, J.R., Alcala, J.E. Gama-Castro, J.E., 1991. Los tepetates. Revista de Geografía 3(4), 37-41.

Gutiérrez-Castorena Ma del C., Ortiz-Solorio C.A., Sánchez-Guzmán P., 2007. Clay coatings formation in tepetates from Texcoco, Mexico. Catena 71, 411-424.

Haulon M., G. Werner, G. Flores-García, A. Vera-Reyes y P. Félix-Henningsen. 2007. Assesment of erosion rates during rehabilitation of hardened volcanic soils (tepetates) in Tlaxcala. Revista Mexicana de Ciencias Geológicas 24:498-509.

Heidari, A., Mahmoodi, S., Roozitalab, M.H., Mermut, A.R., 2008. Diversity of clay minerals

in the Vertisols of three different climatic regions in western Iran. J. Agric. Sci. Technol.

10, 269–284.

Heine, K., Schönhals, E., 1973, Entstehung und Alter der "toba"-Sedimente in Mexiko: Eiszeitalter und Gegenwart, 23-24, 201-215.

Hessmann, R., 1992. Untersuchungen verhärteter Vulkanascheböden (Tepetate) in den Becken von Mexico und Tlaxcala (Mexico): Paris, Giessen, Bericht für die Kommission der Europäischen Gemeinschaft.

Hidalgo, C., 1995. Etude d'horizons indurés à comportement de fragipán, appelés tepetates, dans les sols volcaniques de la vallée de Mexico: contribution à la connaissance de leurs caractères et de leur formation. Universite´ Henri Poincare´, Nancy I, Nancy. 215 pp.

Hidalgo, M.C., Quantin, P., Zebrowsky, C., 1992. La cementación de los tepetates: estudio de la silificación. Terra 10, 192–201.

IUSS Working Group WRB. World Reference Base for Soil Resources 2014, update 2015 International soil classification system for naming soils and creating legends for soil maps. World Soil Resources Reports No. 106. FAO, Rome. 2015

Karathanasis, A.D., 1989. Solution chemistry of fragipáns—thermodynamic approach to understanding fragipán formation. In: Smeck, N.E., Ciolkosz, E.J. (Eds.), Fragipáns: Their Occurrence, Classification, and Genesis: SSSA Spec. Publ., 24. SSSA, Madison, Wisconsin, pp.113–139

Krasilnikov P., García-Calderón N., Pogosyan L., 2016. Polygenetic soils of montane cloud forest in Sierra Gorda. Geoderma Regional, 7(4), 366-375.

Krasilnikov, P.V., Gerasimova, M.I., 2004. Soil Classification 2004. Field Excursion Guide. 6-8 August 2004, Petrozavodsk, Karelia, Russia. Petrozavodsk. 34 p.

Leij, F.J., Ghezzehei, T.A., Or, D., 2002a. Modeling the dynamics of the soil pore-size distribution. Soil Tillage Res. 64, 61–78.

Lindbo, D.L., Veneman, P.L.M., 1993. Morphological and physical properties of selected fragipán soils in Massachusetts. Soil Science Society of America Journal 57, 429–436.

Miehlich, G., 1991. Chronosequences of volcanic ash soils: Hamburg, Hamburger Bodenkundliche Arbeiten, 15, 207 pp.

Miehlich G. 1992. Formation and properties of tepetate in the Central highlands of México. Terra. 10, 137-144.

Miller, F.P., Holowaychuk, N., Wilding, L.P., 1971a. Canfield silt loam, a Fragiudalf: I. Macromorphological, physical, and chemical properties. Soil Science Society of America Proceedings 35, 319–324.

Miller, F.P., Wilding, L.P., Holowaychuk, N., 1971b. Canfield silt loam, a Fragiudalf: II. Micromorphology, physical, and chemical properties. Soil Science Society of America Proceedings 35, 324–330.

Miller, M.B., Cooper, T.H., Rust, R.H., 1993. Differentiation of an eluvial fragipán from dense glacial till in Northern Minnesota. Soil Science Society of America Journal 57, 787–796.

Nikorych V., Szymański W., Polchyna S., Skiba M., 2014. Genesis and evolution of the fragipán in Albeluvisols in the Precarpathians in Ukraine. Catena 119, 154–165

Norfleet, M.L., Karathanasis, A.D., 1996. Some physical and chemical factors contributing to fragipán strength in Kentucky soils. Geoderma 71, 289–301.

Oleschko, K., Zebrowski, C., Quantin, P., Fedoroff, N., 1992. Patrones micromorfológicos de organización de arcillas en tepetates (México). Terra 10, 183–191.

Poetsch, T., 2004. Forms and dynamics of silica gel in a tuff-dominated soil complex: Results of micromorphological studies in the central highlands of Mexico. Rev. Mex. Cienc. Geol. 21, 195–201.

Poetsch, T., Arinkas, K., 1997. The micromorphological appearance of free silica in some soils of volcanic origin in Central Mexico. In: Zebrowski, C., Quantin, P., Trujillo, G. (Eds.), Suelos Volcánicos Endurecidos. III Simposio Internacional. Quito, Ecuador, pp. 56–64.

Prat C., Etchevers J.D., Baez A., Gallardo J.F., Padilla J., 2015. Habilitation agricole de tufs volcaniques indurés au Mexique: le cas des "tepetates" de l'altiplano central. In: Roose Eric (Eds.). Restauration de la productivité des sols tropicaux et méditerranéens: contribution à l'agroécologie. Montpellier: IRD, p. 519-533

Quantin, P., 1992. L´induration des materiaux volcaniques pyroclastiques en America Latine: processus geologiques et pedologiques. Terra. 10, 24-33

Rogers, C.D.F., Dijkstra, T.A., Smalley, I.J., 1994. Hydroconsolidation and subsidence of loess: studies from China, Russia, North America and Europe. Engineering Geology 37, 83–113.

Sedov, S., Solleiro-Rebolledo, E., Terhorst, B., Solé, J., Flores-Delgadillo, M.L., Werner, G., Poetsch, T., 2009. The Tlaxcala basin paleosol sequence: a multiscale proxy of middle to late Quaternary environmental change in central Mexico. Revista Mexicana de Ciencias Geológicas 26(2), 448-465.

Smalley I.J., Bentley S.P., Markovic S.B., 2016 Loess and fragipans: Development of polygonal-crack-network structures in fragipán horizons in loess ground. Quaternary International 399: 228-233

Smalley, I.J., Markovic, S.B., 2014. Loessification and hydroconsolidation: there is a connection. Catena 117, 94-99.

Soil Survey Staff, 2014. Keys to Soil Taxonomy, 12th edn.USDA-Natural Resources Conservation Service. (Washington, DC)

Solleiro-Rebolledo, E., Sedov, S., Gama-Castro, J.E., Flores-Román, D., Escamilla-Sarabia, G., 2003, Paleosol-sedimentary sequences of the Glacis de Buenavista, central Mexico: interaction of Late Quaternary pedogenesis and volcanic sedimentation. Quaternary International, 106-107, 185-201.

Steinhardt, G.C., Franzmeier, D.P., Norton, L.D., 1979. Chemical and Mineralogical Properties of the Fragipáns of the Cincinnati catena. Soil Science Society of America Journal 48, 1008–1013.

Suharta N. and Prasetyo B. H., 2009. Mineralogical and chemical characteristics of spodosols in Toba highland, North Sumatra. Indonesian Journal of Agricultural Science 10(2): 54-64

Svendsen, J.I., Alexanderson, H., Astakhov, V.I., Demidov, I., Dowdeswell, J.A., Funder, S., Gataullin, V., Henriksen, M., Hjort, C., Houmark-Nielsen, M., Hubberten, H.W., Ingolfsson, O., Jakobsson, M., Kjaer, K., Larsen, E., Lokrantz, H., Lunkka, J.P., Lysa, A., Mangerud, J., Matiouchkov, A., Murray, A., Möller, P., Niessen, F., Nikolskaya, O., Polyak, L., Saarnisto, M., Siegert, C., Siegert, M.J., Spielhagen, R.F., Stein, R., 2004. Late quaternary ice sheet history of northern Eurasia. Quaternary Science Reviews, 23(11-13), 1229-1271.

Targulian, V.O., Goryachkin, S.V., 2004. Soil memory: Types of record, carriers, hierarchy and diversity. Revista Mexicana de Ciencias Geológicas, 21, 1–8.

Tremocoldi, W.A., Steinhardt, G.C., Franzmeier, D.P., 1994. Clay mineralogy and chemistry of argillic horizons, fragipáns, and paleosol B horizons of soils on a loessthinning transect in southwestern Indiana, USA. Geoderma 63, 77–93.

Van Vliet, B., Langohr, R., 1981. Correlation between fragipáns and permafrost with special reference to silty Weichselian deposits in Belgium and northern France. Catena 8, 137–154.

Weisenborn, B.N., Schaetzl, R.J., 2005. Range of fragipán expression in someMichigan soils: II. A model for fragipán evolution. Soil Science Society of America Journal 69, 178–187.

Witty, J.E., Knox, E.G., 1989. Identification, role in soil taxonomy and worldwide distribution of fragipáns. In: Smeck, N.E., Ciolkosz, E.J. (Eds.), Fragipáns: Their Occurrence, Classification and Genesis. SSSA Spec. Publ., 24. SSSA, Madison, Wisconsin, pp. 1–9.

Anexo 1

Evidence for stages of landscape evolution in Central Mexico during the Late Quaternary from paleosol-pedosediment sequences

Svetlana A. Sycheva S[a], Lilit Pogosyan[b*], Sergey Sedov[c], Elizabeth Solleiro Rebolledo[c], Alexandra A. Golyeva[a], Hermenegildo Barceinas Cruz[d], Konstantin N. Abrosimov[e], Konstantin A. Romanenko[e]

[a] *Institute of Geography, Russian Academy of Sciences, Moscow, Russia,* 119017

[b] *Posgrado en Ciencias de la Tierra, Instituto de Geología, Universidad Nacional Autónoma de México, Ciudad Universitaria, CDMX, México, 04520*

[c] *Instituto de Geología, Universidad Nacional Autónoma de México, Ciudad Universitaria, CDMX, México, 04520*

[d] *Posgrado en Ciencias de la Tierra, Instituto de Geofísica, Universidad Nacional Autónoma de México, Ciudad Universitaria, CDMX, México, 04520*

[e] *V.V. Dokuchaev Soil Science Institute, Moscow Russia, 119017*

* Corresponding author

lilit-tos@yandex.ru

Abstract

Paleosols interbedded with pyroclastic deposits have been proven to be an important paleoenvironmental proxy for the Late Quaternary in Central Mexico. We studied a key upland section and several profiles on the slopes and lowlands of the Tlaxcala Block, assuming that the topographic variability of the soil-sedimentary mantle contains the complete record of the landscape history. The upland section included 3 paleosols separated by tepetates (compact volcanic pedosediments) and reflected a general trend of environmental evolution during the last 40 ka. Particle-size distribution, bulk chemical composition, magnetic characteristics, computed tomography and micromorphological observations demonstrated a strong seasonality of paleoclimate at the end of MIS3, followed by cool wet conditions during the Last Glacial Maximum, subsequent warming at the beginning of the Holocene and aridization during the last 3 ka. It was shown that tepetates had well-developed pedogenetic features that contribute to paleosol record. The studied slope and lowland profiles reflected the main phases of geomorphic activity in the Terminal Pleistocene and the early Holocene. These phases are linked to paleoclimate fluctuations in Central Mexico at the end of the last glaciation.

Keywords: landscape evolution, climate change, paleoenvironment, soil memory, paleo-catena, tepetate

Introduction

Landscape evolution is controlled by multiple factors such as changes in climate, volcanic eruptions, tectonism, erosion-sedimentation processes and human activity. During landscape development, there are periods of stable environmental conditions, when pedogenesis is active with soil cover development, and periods of dynamic instability, when landform evolution is driven by two groups of processes, i.e., sediment accumulation and erosion, which are interrelated

in space and time. The accumulation process produces new landforms while the erosion process transforms or eliminates them.

Both pedogenic and geomorphic processes coexist and actively impact landscape evolution. However, their relative importance may vary considerably in space and over time (Sycheva et al., 1998; Sycheva, 2003). Soil development is active during the periods of stable evolution of landscapes under closed vegetation cover (Glazovskaya, 1996, 2000). Pedosedimenary sequences can include sediments of highly variable composition and thickness, sedimentational gaps and erosional contacts between layers, which indicate a high rate of relief formation, frequent and dramatic changes in environments and occasional catastrophic events, respectively. Pedogenesis and soil erosion-redeposition are essentially antagonistic processes (Gerrard, 1981; Sycheva, 2008). High rates of relief-forming processes create extreme conditions for soil formation and can often completely inhibit it. When the conditions are optimal for soil development, the process of erosion and deposition are confined to steep slopes, valley floors, depressions, etc. An alternation of periods of geomorphic stability/soil development and geomorphic activity/intensive processes of erosion and deposition is controlled by global and regional environmental changes (Rohdenburg, 1970).

In Mexico, tepetates that are found in paleopedological sequences represent an additional source of information on past environmental changes (Solleiro-Rebolledo et al., 2003; Sedov et al. 2009; Diaz-Ortega et al., 2010, 2011). Tepetate (a Nahuatl term meaning a stone bed) refers to a variety of hard, dense or cemented subsoil horizons, which are frequently formed on volcanic deposits (Miehlich, 1992; Zebrowski, 1992; Gama-Castro et al., 2007). A fragipan type of tepetate is a non-cemented, dense and compacted layer with a very low hydraulic conductivity (Nimlos and Hillery, 1990), which promotes lateral soil drainage and rapid erosion (Gama-Castro et al., 2007). For this reason, a tepetate relief has a well-developed gulley network, which was clearly observed in the study area. It is usually described in literature as a BC or C horizon of soil. However, Aeppli (1973) considers the tepetate as a direct result of soil formation. Other specialists consider it as a pedosediment developed as a result of soil erosion and redeposition associated with volcanic eruptions and extreme climatic events (Solleiro-Rebolledo et al., 2003). Another important question relates to whether these compacted materials are the product of past environments, as some authors propose (Fölster et al., 1977; Solleiro-Rebolledo et al., 2003; Díaz-Ortega et al., 2010), or are the result of geological and pedological processes (Quantin, 1992; Miehlich, 1992; Oleschko et al., 1992). There is no unambiguous answer to the question about the origin of tepetate, so the subject is still debatable (Poetsch, 2004). In this manuscript, based on our findings, we further speculate about tepetates as compact pedosediments, which have been involved in pedogenetic processes after their deposition. Although in the studied profiles, there are not only tepetates, but also loose colluvial sediments.In this paper, we describe soil-sedimentary sequences, which included tepetates developed in different topographic positions within the Tlaxcala 'Block' (Mexican Plateau), from the very end of the Pleistocene to the late Holocene. Specifically, we investigated trends and dynamics of the landform and soil evolution in the Tlalpan region (Fig. 1). The aim of the present study is to identify the stages of stability (soil formation) and instability (geomorphic evolution) of regional landscapes based on radiocarbon dating of paleosols, tepetates, and colluvial deposits in order to reconstruct paleoenvironments.

As geomorphic evolution involves erosion and sedimentation (sediment reallocation), we analyzed the sequences located in near-watershed ('upland') positions and on slopes and valleys ('lowlands') within the ravine network as complementary information sources. A comprehensive study of surface soils and the sedimentary mantle is important in order to have access to the most complete "soil memory", as has been shown by Kozlovskii and Goryachkin (1996). Parts of the

sedimentary mantle that have developed in low geomorphic positions (e.g., footslopes and depressions) often provide more detailed soil-sedimentary records with a higher temporal resolution for certain chronological intervals, as compared to the sections developed in more upland watershed areas (Sycheva 2006, 2008).

Background

Previous studies of paleoclimatic records of the Holocene in Central Mexico

Over recent decades extensive paleoenvironmental reconstruction has been undertaken in Central Mexico. Most of these studies have been based on lacustrine, glacial and fluvial or soil-sedimentary records. Lacustrine sediments reveal the history of closed basins and lower landscape positions, whereas glaciers are limited to the highest volcanic elevations. As a result, we have information on extreme landscape positions (high and low). In intermediate positions, not covered by glaciers or lake sediments, the processes of soil formation, soil erosion and soil redeposition represent another important source of information.

The most detailed paleoenvironmental reconstructions have been obtained from lacustrine sediments within the Basin of Mexico. Drilling of the Chalco Lake has allowed for dating of the oldest sediments, up to 400 ka (Brown et al., 2019), as well as detailed studies of Marine Isotope Stages (MIS), from MIS 6 to MIS 2 (Torres-Rodríguez et al., 2015; Martínez-Abarca et al., 2021). However, the lacustrine basin has a hiatus from 14.5 to 3.3 ka (Caballero et al., 1999).

The history of glaciations has been studied on the volcanoes of Iztaccihuatl, Nevado de Toluca, Popocatepetl and La Malinche (White, 1962; Heine, 1984; Vázquez-Selem and Heine, 2004), where different glacier advances and retreatments have been recorded during MIS 6 and from 25 to 12 ka, with some episodes during the Holocene (Vázquez-Selem and Heine, 2011).

Fluvial archives, as well as preserving the history of relief-forming processes in valleys and on interfluves, also record the rhythmically alternating phases of stable landscape evolution (pedogenic phases) and dynamic morpholithogenic phases, unfavorable for soil formation. Borejzca and Frederick (2010) performed studies of fluvial sequences in several large gullies in Tlaxcala.

The paleopedological record has also contributed to the reconstruction of past landscapes. Specifically, in Tlaxcala, we have studied the most complete paleosol-sedimentary sequence, which documents the environmental history from the middle Pleistocene (900 ka) to the late Holocene (Sedov et al., 2009; Sycheva et al., 2013). In addition, tephra-paleosol sequences have provided information on landscape development from MIS 5 to MIS 2, giving us an opportunity to establish the stages of volcanic activity interrupted by pedogenetic phases (Sedov et al., 2001; Solleiro-Rebolledo et al., 2004; Jasso et al., 2006). The sequences from the Teotihuacan Valley contain evidence of climate change since MIS 3 (Solleiro-Rebolledo et al., 2006) as well as a detailed record of human activities during the last 3000 years (Sánchez-Pérez et al., 2013). However, these archives allow for only a fragmented reconstruction of the history of geomorphic evolution linked to pedogenesis-erosion-sedimentation cycles, which can be associated with climate change. Therefore, it is important to study the paleosol and paleo-catena records, which may contain the missing information. In consequence, we expected that the present study of gulley sequences would reveal important knowledge on the environmental evolution.

Landscape and environmental setting

The study area is located within the Transmexican Volcanic Belt (Fig. 1a), specifically within the Tlaxcala Block which is surrounded by several volcanic structures (Fig. 1b). The Tlaxcala Block is an elevated part of a horst-graben system originated during the Miocene by a normal fault (Mooser et al., 1996; Lermo-Samaniego and Bernal-Esquia, 2006). In the grabens, there are closed depressions infilled by lacustrine sediments. Volcanic activity was intense and, perhaps, synchronous to tectonic movements in the main stratovolcanoes of Popocatepetl, Iztaccihuatl and La Malinche (with altitudes ranging from 4461 to 5426 masl) as well as smaller volcanoes (altitudes around 2500 to 2700 masl). In the study region, lava flows have been identified in the Blanca gulley, dated by potassium-argon method to 2.4 Ma (Sedov et al, 2009). We have also found lavas at the floor of the Concepcion gulley (Fig. 1). The region is heavily dissected with numerous linear erosional landforms such as rills, ravines, and deeply incised gullies, which are locally named barrancas, with slopes ranging from 3 to 60% (Alvarado-Cardona et al., 2007). These slopes have been cultivated for around 3000 years, since the pre-Hispanic period (Lauer, 1979). As a consequence, the territory represents a dramatic example of environmental impact of intensive agriculture and deforestation since the Preclassic period (2500–100 BC). The agricultural system included the construction of terraces to avoid or control the erosion in the area (Whitmore et al., 2001; Borejsza et al., 2008). This is why, cross-slope terraces (*zanja-bordo* or dich-and-border terraces) are a prominent landscape feature (LaFevor, 2014; Borejsza et al., 2008).

The climate is characterized by the alternation of dry and wet seasons. The wet season is mostly confined to summer months (June to September) and causes most of the erosion phenomena (Haulon, 2007). The study area has a mean annual precipitation of 812 mm and a mean annual temperature of 14°C (García, 2004). The soil cover of the Tlaxcala Block is mostly dominated by Cambisols with profile differentiation into A1-AB-B horizons (Werner et al., 1988). Most of the tepetate formations correspond to BC-C horizons. Fluvisols are occasionally found on lacustrine and fluvial sediments within gullies. Both Cambisols and Fluvisols of the study area may alternatively be classified as Anthrosols, as they have been ploughed since ancient times and often contain pottery fragments in the uppermost 20-25 cm.

Our study was carried out within drainage basins of the gullies ('barrancas') of Concepcion, Tlalpan and Young. The Concepcion Barranca included profiles from the upland area, terraces, slopes, and the valley floor (Figure 1c). The Concepcion Barranca represents a large ramified system of gullies originating from a watershed of around 2600 masl. Along the Tlalpan Barranca, a paleopedological study had previously been conducted in the locality named Tlalpan (Sedov et al. 2009), where tepetates are widely exposed (Alliphat-Fernández and Werner, 1994), as well as in the Young Barranca (Fig. 1c). Sedov and co-authors identified several paleosol units separated by tepetates. According to their morphology, the materials were grouped into Gray, Brown, and Red units (from the younger to the older one). The Gray Unit developed during the MIS 3 to 1 which is evidence for the climate shift from cool and humid to drier and warmer conditions (Solís-Castillo et al., 2012).

Materials and Methods

Field survey

As part of the field work, we carried out a reconnaissance survey to determine the main relief-forming processes and to identify the most active ones as well as to estimate the scale of eroded objects (surfaces). During the survey, special attention was given to sites with evidence of

local catastrophic events such as fires, water breaks through natural dams, etc.; sites of ancient settlements; and areas of former ephemeral lakes (lakelets). We also described sedimentary sequences in various parts of the Concepcion, Tlalpan and Young Barrancas (Fig. 1c). In particular, sections 19 and 20 are at the head of the Young gulley: sections 7, 8 and 11 contain sediments infilling an older ('paleo') gulley deposits. Sections 12, 13a and 28 are located in the lower part of the Tlalpan Barranca downstream of the Young Barranca mouth (Fig. 1c). The sections in the Concepcion Barranca are arranged as follows: 5 – at its head, on the remnant of the former floor at the confluence of several tributaries entering the main valley; 30, on the gulley terrace in the middle part of the long profile; and 31, the main gulley terrace downstream from the Tlalpan Barranca mouth (Fig. 1c). We collected samples of soil organic matter, charcoal, carbonates, and bones from the sections presented in Figure 1c, in order to establish the chronological frame. In addition, we re-sampled the Gray Unit at Tlalpan section, previously studied by Sedov et al. (2009) and Pogosyan et al. (2019). During the morphological description, new indexations of the profile horizons were done, and soils were classified following the IUSS Working Group WRB system (2015) (Fig. 2). Therefore, we divided the modern soil into A and AB horizons; the first paleosol into 2Ah-2AB-2B horizons; then follows 3EBg(k)-3BCxt horizons which previously were marked as 2Bk and TG1 respectively; the next paleosol level has 4ABi-4Bti horizons (3ABi previously); in the lowermost part of the section, there are two tepetate horizons 5BCxt and 6BCxt (TG2 and TP1 respectively). In this new description, the tepetate layers were considered as BCx horizons differently to our previous observations where they were named as Cx horizons (Sedov et al., 2009) or described as TG (Tepetate of the Gray Unit) and TP (Tepetate of the Brown Unit) (Sycheva et al., 2013). However, the studied profiles on the gulley slopes have no direct analogies with the Tlalpan profile, making correlation difficult, thus we still use the indexation TG and TP for those profiles. Additionally, samples for magnetic studies, bulk chemical composition, pore space distribution and biomorphs were taken every 10 cm throughout the Tlalpan profile.

Analytical methods

Particle-size distribution analysis and micromorphological observations of each genetic horizon were conducted (Fig. 2). Particle-size distribution was determined using an Analysette 22 Comfort laser analyzer (FRITSCH, Germany) and the parameters of calculation proposed by Sochan et al. (2014); the upper limits of fraction sizes were determined by Schoeneberger et al. (2012). The samples were pre-treated with an ultrasonic disruptor (Stepped Solid Horn 1/2'', Digital Sonifier S-250D, Branson Ultrasonics, USA) following North (1976). Fraction sizes were defined as sand (63-1000 μm), silt (2-63 μm) and clay (< 2 μm) following the FAO guidelines (2006). Thin sections for micromorphology were prepared using a polyester resin, cut and polished to obtain a 30 μm section. For the micromorphological descriptions, an Olympus petrographic microscope was used, following the terminology of Bullock et al. (1985).

Magnetic susceptibility was used as an indicator of pedogenic vs. lithogenic processes. Each sample was air dried, gently crushed and then tightly packed into 8 cm^3 cubical diamagnetic boxes. The mass of each sample was measured to calculate mass-normalized magnetic susceptibility (χ). Magnetic susceptibility in low (0.47 kHz) and high (4.7 kHz) frequencies (χlf and χhf) was measured with a Bartington MS2B susceptibility meter with a dual sensor. Also, we calculated the frequency dependent magnetic susceptibility (χfd), which is the percentage difference between low and high frequency magnetic susceptibility ($\chi fd = 1 - \chi hf/\chi lf$).

The bulk chemical composition was measured for major (Ca, Fe and K) and trace (Ti) elements. For this analysis, 5 g of soil were crushed in agate saddle stone and sieved with sieve

number 60. Then, the samples were placed in plastic bags and measurements made using a NITON XL3t Thermo Scientific portable analyzer.

Pore space was studied by computed tomography to describe the pore distribution and connectivity. The porosity may contain a significant element of soil memory in the shape and orientation of pores (Romanis et al., 2021) and preserves the original forms for a long time (López-Prat et al., 2021). Tomographic scanning of soil samples was performed using a Bruker SkyScan 1172G 3D X-ray scanner. The resolution of obtained images is 3.15 µm. Image reconstruction was performed using nRecon software (Bruker, 2018a). The images were segmented manually by global thresholding. Morphometric analysis was performed using CTAn software (Bruker, 2018b). We obtained the following morphometric data: porosity (open and closed), pore size distribution, connectivity of solid phase. Porosity is the ratio of volume of pores (black voxels after segmentation) to whole volume of interest. Rendering of soil 3D images was performed using CTVox (Bruker, 2018b).

The detritus, phytoliths, sponge spicules and other remains of biomorphs were studied under the microscope. A 50 g sample was treated with a hot 30% solution of H_2O_2; sand and clay fractious were separated from silt, which was subjected to flotation in a heavy liquid (cadmium iodide and potassium iodide with a specific gravity of about 2.3 g/cm^3). After 10 min-centrifugation, the floating siliceous particles and other biomorphs were collected into a tube and washed with distilled water several times, and dried. Then the sample was immersed in oil (silica oil or glycerine) and studied under the optical microscope at magnifications varying from 200 to 900 times. The morphotypes were counted in specimens prepared with an approximate volume of 1.9 mm^3 each. Analyzing the entire complex of soil microbiomorphs enables the entire spectrum of particles from one sample to be determined. Ecological and environmental interpretation of the phytolith assemblages was undertaken according to Golyeva (2007).

Dating of the materials

The dating of materials was performed using the vacuum pyrolysis method (^{14}C dating of small-size samples with the use of an accelerator). The dated material was mostly presented by humic acids separated from soils, tepetate, and colluvial deposit samples. In addition, there were also dated charcoal and bone remains from slope deposits and carbonate concretions recovered from tepetate. Calibration was done by using the OxCal 4.4 calibration program (https://c14.arch.ox.ac.uk/oxcal.html) and the Northern Hemisphere Radiocarbon Age Calibration Curve IntCal 20 (Reimer et al., 2020). As for the Tlalpan sequence, the datings have been presented earlier (Sedov et al., 2009).

Results

Key profile Tlalpan

The macromorphological description of the modern soil and the Gray Unit of the Tlalpan profile has been previously published by Sedov et al. (2009) and Solís-Castillo et al. (2012) and updated by Pogosyan et al. (2019). The studied sequence consists of the modern soil, two paleosols and three tepetate layers (marked here as BCtx horizons) which correspond to different events of sedimentation and separate soil formation cycles (Fig. 2). The modern soil (Regosol Technik) is grayish, vastly eroded and preserves many obsidian artifacts. The soil below it (Protovertic Cambisol) is darker and has a better aggregate structure in the 2Ah horizon. Below the first paleosol there is another paleosol (Stagnik Luvisol) which starts with a 3EBg(k) horizon. This

horizon is characterized by the presence of 1300-year-old carbonate concretions and thick iron nodules (0.5 cm in diameter). The first tepetate 3BCtx horizon underlies the 3EBg(k) horizon and has typical fragipan morphological properties. Below there is the dark-colored clayey paleo-Vertisol with well-defined angular (wedge-shaped) aggregates. At the bottom of the profile there are two tepetate layers, 5BCtx and 6BCtx, with properties similar to those of the 3BCtx tepetate, but the lower one belongs to the older Brown stratigraphic Unit (Sedov et al., 2009).

Micromorphological observations have shown that the modern soil is characterized by a dark compact groundmass with a subangular blocky structure, few channel voids (Fig. 3a) and the presence of microartefacts: charcoal and ceramic fragments. The 2Ah horizon has a clayey groundmass and angular blocky structure; sometimes microaggregates have a wedge-like shape (Fig. 3b). Below, within the 3EBg(k) horizon, the groundmass has more coarse sand and silt material and incorporates large rounded ferruginous nodules (Fig. 3c). Thick illuvial clay coatings are a prominent feature of the first tepetate (3BCxt horizon). They partly fill the few original large channels leaving only small, isolated pores (Fig. 3d). Most of them have a dotted morphological pattern caused by multiple inclusions of fine silt particles. In this horizon we observed evidence of moderate weathering of volcanogenic minerals, in particular – etching of pyroxenes (Fig. 3e). Clay coatings are also present in the underlying 4ABi horizon, however here they are more limpid and frequently fragmented and deformed (Fig. 3f). The 4Bi horizon shows the most clear Vertic micromorphological pattern: compact clayey groundmass has striated b-fabric with strong birefringence areas along thin fissures (stress-cutans) (Fig. 3g). The lower gray tepetate - 5BCtx horizon also contains clay coatings (Fig. 3h) and infillings which occupy large channels – as in 3BCtx horizon. Their color is brownish-yellow due to slight ferruginous pigmentation – thus their morphology differs from all other illuvial pedofeatures within the overlying sequence (Fig. 3g).

The studied paleosol sequence showed variations in the particle-size distribution, which clearly differentiate each soil/paleosol unit. The first pattern corresponds to the modern soil (Au horizon) with a predominance of the silt fraction (Fig. 4a). The particle-size distribution of the first paleosol, particularly the 2Ah horizon, was characterized by a higher amount of the coarse fractions (coarse silt and sand) (Fig. 4b). The 3EBg(k) and 3BCtx horizons (first gray tepetate) have a similar pattern (Fig. 4c) to that observed in the modern soil (Fig. 4a), but here the amount of sand is higher. The vertic paleosol horizons (4ABi and 4Bti horizons) have a higher proportion of clay and the highest content of the fine sand fraction (Fig. 4d). The second level of the tepetate (5BCtx horizon) shows a bimodal distribution, where sand and fine silt-clay fractions are more abundant (Fig. 4e). Similarly, the pattern found in the 6BCtx horizon also presents a bimodal distribution, but here the clay content is lower (Fig. 4f).

Concerning the magnetic properties, the χlf values are more or less homogeneous in the paleosols horizons, but an enhancement is clearly observed in the modern soil (Fig. 5) although there is not a high amount of superparamagnetic particles, given by the χfd proportions, ranging from 2-3%. In paleosols, χfd values are low in general and exhibit some abrupt variations along the profile, even within a single horizon. The highest χfd values are observed in the 2Ah, 2B horizons, in the transitional zone from 3EBg(k) horizon to the 3BCtx horizon and at the 4ABi horizon.

The Fe and Ti distribution shows a similar pattern throughout the profile, with higher concentrations in the 2Ah and in the lowermost 4Bti, 5BCtx and 6BCtx horizons (Fig. 5). The profile distribution of K is the opposite to that of Ti and Fe and has minimal and maximal values in opposite points. Ca has its maximum value in the upper part of the modern soil and gradually

decreases with depth, but there is also a small peak at the depth of 185 cm within the 4ABi horizon and in the first brown tepetate.

The computed tomography showed differences in the pore distribution of the different horizons (Fig. 6). The topsoil horizon is characterized by big and connected channel biogenic pores (Fig. 6a). The 3EBg(k) horizon showed a compact structure and low presence of pore-channels (Fig. 6b). In the 3BCtx horizon the pore space is represented by interaggregate and intergrain packing pores and there are many small vesicular pores homogeneously distributed in all the samples (Fig. 6c). All tepetate horizons are similar in their pore space organization pattern, which is shown in Figure 6c (3BCtx horizon). The 3D image of vertic horizons showed that they are more compact, and their pore space is constituted by planar fissures where slickensides are shown (Fig. 6d, 4ABi horizon).

The whole sequence shows a high abundance of phytoliths (Fig. 7) except in the lowermost tepetate layers (5BCxt and 6BCxt) where their quantities decrease. Unexpectedly in the upper tepetate, 3BCxt, phytoliths are as abundant as in the underlying and overlying paleosol horizons. The distribution of the main botanical groups in general shows irregular variations of a relatively low amplitude. However, the following tendencies could be clearly identified: (i) forms typical for cereals related to agricultural land use were detected only in the uppermost Ah horizon; (ii) conifers were only slightly increased in the 3EBg(k)-3BCtx horizons; (iii) on the contrary, meadow grasses were more abundant in the 2Ah-2AB and 4ABi-4Bti horizons. However, the highest content of meadow grasses was in found in 5BCtx horizon. We were surprised to find in this currently dry and well drained position some opaline microfossils indicative of hydromorphic conditions or even water bodies: those are phytoliths of reed and diatom shells (many of them fragmented). Diatoms tended to increase in the upper part of the sequence. SEM images of some typical forms encountered within the profile are shown in the Fig. 8.

Sections at the head of gullies

Head (sections 19 and 20) and eroded slope (section 8) at the Young Barranca

At the topographically highest levels, sections 19 and 20, several stratigraphical differences were detected, in the comparison to the Tlalpan section (Fig. 9). In those sections we also observed the basal brown tepetate (TP), but not the TG2 (5BCtx), thus the 4Bti horizon rests directly on TP. However, TG1 was found in two levels: one directly on the surface (TG1-1) and another one (TG1-2) overlying the 4Bti horizon. Between these two tepetate layers, a well-developed paleosol was found, which has redoximorphic features. The Ah horizon organic matter of this paleosol has a date of 16068±222 cal yr BP (Fig. 9, Table 1). TG1-1, in section 19, has an age of 14576±349 cal yr BP. A few calcitic concretions were found on the surface of the profile and dated by ^{14}C to 4707±136 cal yr BP (Table 1). An additional observation is the occurrence of a depression, that nowadays is covered with water (Fig. 9, 10), similar to the one of section 20. Here, a gleyed Luvisol (with 3Btg horizon) occurs under the tepetate TG1-1. This Luvisol varies to a Gleysol in the deeper part of the depression, where compact thin laminae (sand alternating with clay) are also observed, formed most probably in a small lakelet. The underlying distinctly pronounced dark-colored soil TX2 (Sedov et al., 2009) labelled here as 4Bti, is seen in both sections. Additionally, the section shows a cultural layer of an ancient settlement under the modern colluvium which contains numerous flakes and blades of obsidian together with ceramic fragments. On the eroded part of the slope (section 7), the described layers of the barranca´s head decrease in thickness. In consequence, TP is exposed on the surface or covered with a thin layer of colluvium (Fig. 11a).

The incised landform of Young Barranca appears as a rill at its uppermost part and then transforms to a canyon-like 3-5 m deep gulley.

Incised valley of the Young Barranca (sections 8, 11)

The uppermost part of the sequence in the incised valley of the Young Barranca is composed of colluvial deposits, which cover a dark-colored soil. The age of this soil, sampled in section 8, is 7153±124 cal yr BP (Table 1). Alluvial and colluvial deposits fill the paleo-gulley, which cuts through all the inclined layers of the Brown Unit of the Pleistocene age (Sedov et al., 2009). They are complex in structure and occur discordantly in reference to the present-day surface. The erosional paleo-landform (paleo-gulley) is also filled with pedosediments of brown and grayish-brown colors, horizontally stratified (Fig. 9). The stratification is clear and shows an alternation of layers of compact ("tepetized") loams and of loose brownish loam and horizons of soils. Interlayered with the sediments filling the paleo-gulley, a buried soil can be recognized in sections from 8 to 11 (Fig. 11a), overlain by TP1 and a colluvium. The ages of TP1 (sample taken within the paleo-gulley) and of the paleosol are dated by ^{14}C at 9198±139 cal yr BP and 9012±187 cal yr BP respectively (Table 1).

Sequences of the terraces and gulley floors

In the Concepción barranca (Fig. 1), the tepetate surface is mostly inclined at an angle of 3-5° to 7-10°. Section 5, at the head of the Barranca, is close to the confluence of several gullies and opens a small remnant of a former gulley floor, which at present is a terrace. Section 5 displays the thickest and most complete Holocene soil and tepetate series overlying the eroded surface. The soil-tepetate series consists of four paleosols separated by tepetates (labeled here as Tep1 to Tep 4). In the lower part of the series, the best preserved and developed Luvisol appears, with the following horizons: 5E-5Btk-5Btg. The paleosol is overlain by a light-colored tepetate Tep 4 composed of pyroclastic material and fragments of an eroded eluvial horizon. The higher levels are constituted by paleosols, with only the following horizons detected (from the bottom to the top of the series): 4EB, Tep 3, 3ABhg, Tep 2, 2Ah-2ABth. The series ends with the accumulation of weakly humified, undifferentiated deposits, separated by a more compact tepetate layer (Tep 1) composed of humified pedosediments which include pyroclastic and organic materials. The ages of such tepetates are shown in Table 1: Tep 1-1995±104 cal yr BP, Tep 2-3367±83 cal yr BP, Tep 3-4866±121 cal yr BP. Practically all the tepetates were affected by the soil forming processes including clay and humus illuviation (TP 2 in particular), probably, gleization in the lower part of the profile (Tep 1) and carbonate accumulation (Tep 2 and Tep 3).

Section 12, situated in the lower part of the Tlalpan Barranca downstream of the Young Barranca mouth (Fig. 1), exposes three-layered gray fluvial and colluvial deposits overlying a dark-colored paleosol. The paleosol is the same as that occurring in the deposits filling the paleo-gulley, observed in section 11, and dated by ^{14}C at 9012±187 cal yr BP.

Section 13a in theTlalpan Barranca, the Holocene colluvial deposits occur as a continuous three-layered mantle. At the boundary between the layers 2 and 3, a fossil bone was found, whose collagen was dated at 9012±187 cal yr BP (Table 1). In section 28, situated lower down the slope, colluvial sediments are also present, where brown and gray layers are intercalated. A charcoal sample taken at a depth of 2.4 m gave a ^{14}C age of 16438±165 cal yr BP (Table 1). In between the colluvial sediments, a gray-colored tepetate is observed, which corresponds to the upper Gray tepetate of the Tlalpan profile (TG1).

A the middle part of the Concepcion Barranca, there are three alluvial layers exposed in a fresh scarp cut into the former floor of the Concepcion Barranca (section 30) (Fig. 11b). The sequence is about 5 m thick and has similarities with section 13a. It also includes three layers distinguishable by color: the lower one ~1 m thick is brownish yellow, the middle layer (~2 m) is grayish yellow, and the upper one, about 2 m thick altogether, begins with dark gray humus interlayer 0.2-0.3 m in thickness.

At the lower part of a slope of the Concepcion Barranca, section 31, near a sharp bend of this gulley, several terrace deposits were found. Samples for radiocarbon dating were taken from the depths of 3.5 m (tepetate) and 4.0 m (loose material of a redeposited Ah horizon). The results showed an inversion of ^{14}C ages (Table 1): 7684±87 cal BP for tepetate and 6385±134 cal yr BP for the redeposited Ah horizon.

Various combinations of pedogenesis, deposition and denudation processes result in a complex soil-depositional series - representing a kind of record of past process interactions and terrestrial environment evolution (Glazovskaya, 1996). The paleosols and other deposits with different origins were found to appear repeatly in the studied sections and to form certain combinations known as cyclites. The recorded cyclic changes are related to variations in environments and reflect rhythms of various duration that were mostly controlled by climate changes. Each of the cyclite constituents corresponds to a certain ecological phase of the rhythm. Among the studied cyclites in the sequences the following combinations have been identified:

1. Soil – tepetate is the most typical combination which represents two kinds of environmental conditions: one favorable for soil and vegetation development (warm and humid phase marked by soil formation) and another – unfavorable, when a tepetate develops. Specifically, the sequence is as follows: the soil forms first, then later the overlying tepetate develops above the soil from its own pedosediment. This is supported by the recorded inversion of dates and by phytoliths analysis of the 'soil–tepetate' sequence of the Tlalpan profile. The radiocarbon age of tepetate is somewhat greater than that of the underlying soils, which suggests that the tepetate was formed immediately after the soil formation (as a result of a destabilization of the relief-forming processes and deterioration of environments), so the soil and tepetate might be related to the two opposite phases of the same rhythm.

No chronological inversion has been recorded in the radiocarbon ages of dark paleosol (~16 ka BP) and the overlying tepetate (~14.5 ka BP) described in sections 19 и 20. Besides, the considerable difference in their ages – about one thousand years – suggests that the horizons not only developed in different phases of a single rhythm, but most probably belonged to different rhythms. The tepetate could be formed of pedosediment of a paleosol younger than 16 ka BP.

No inversion was found in section 5. The recorded differences in radiocarbon ages of tepetate and soils belonging to three cyclites are indicative of three separate rhythms, their duration being ~1400-1500 years on average.

2. Colluvium – tepetate. Cyclites of this type show the prevalence of sedimentation over soil formation and alternating faster and slower processes of the relief formation. Such cyclites dated to the Holocene occur in the lower reaches of the gullies Tlalpan and Concepcion (see section 31). There is a notable inversion of radiocarbon dates documented in the section 31, which exposed the sequence in the Concepcion Barranca terrace (the tepetate overlying the sequence is dated to 7684 BP, while the age of the underlying colluvium is 6385 BP), which gives grounds to assigning them to different rhythms.

3. Colluvium – soil. Such an order of layers is typical of sediments filling paleo-channels and suggests an alternation of accelerated erosion phases and short-term episodes of soil formation; in such cases the soils are rather immature, while the colluvial series are thick and display a complicated stratified texture.

4. Colluvium – soil – tepetate. Such a combination is also typical of sediments filling older erosional landforms. While the colluvium was deposited by rapid flows and served as a parent material for the soil, the tepetate is formed by slower lahar flows that include eroded soil and bury the soils in lower positions. There may be thin soils and tepetate found in colluvial series that correspond to short-term rhythms.**Discussion**

Main stages of landscape development: paleopedological record of the Tlalpan key profile

The Tlalpan key profile holds information regarding several of the main stages of environmental changes in Central Mexico. In comparison with previous investigations (Sedov et al., 2009; Solís-Castillo et al., 2012), in this paper we analyzed not only the memory from the soil horizons, but also the memory contained within the tepetate horizons. We consider tepetates as pedosediment layers which indicate unstable and changeable landscapes. The presence of such tepetates means that soil formation had been interrupted by a short-term sedimentation process.

Based on the morphological descriptions as well as on the analyses (Fig. 3, 4, 5, 6, 7, 8), we distinguished 6 paleosol-sedimentary units which reflect stages of soil formation interrupted by deposition events. At the bottom of the sequence, we observed the TP (Brown tepetate) layer, which was named as the 6BCtx horizon. This tepetate shows signs of strong clay illuviation, which is associated with a period of humid climate. After that, pedogenesis was interrupted by catastrophic events, which cause the erosion of the complete soil profile (except for its lower layer, i.e., the 6BCtx horizon). Then there is evidence of sedimentation with the occurrence of the Gray tepetate (TG1), and the formation of the 5BCtx horizon, under similar conditions as at the previous stage. The next cycle resulted in the formation of a well-developed Vertisol (4ABi-4Bti) with antient clay coatings that are superimposed by slickenside formation and with strong humus accumulation (Fig. 2, 3, 6). We suggest warm and humid conditions for the beginning of this soil development, and then a change to a contrasting seasonal climate with wetting/drying cycles. Consistently, phytoliths provided evidence for the presence of meadow grasses (Fig. 7). The soil development is intensive, as evidenced by the strong weathering of primary minerals with lower values of K and higher percentages of Ti and Fe (Fig. 5), as well as by an increased contribution of ultrafine magnetic particles, indicated by the high χfd values (Fig. 5). Ortega-Guerrero et al. (2004) consider that these superparamagnetic particles are formed by pedogenesis in the volcanic paleosols of Tlaxcala. The pedogenesis of this unit had been interrupted by the deposition of the next lithologic group that includes the upper Gray tepetate i.e., the 3BCtx horizon. The pore shape and distribution studied in detail with the use of computed tomography and micromophological methods (Pogosyan et al., 2019) showed that the consolidation of the tepetate horizon occurred before the clay illuviation. Concerning the soil development after the tepetate consolidation, we detected two main processes: clay illuviation (with thick clay illuvial coatings in the 3BCtx horizon) and surface redoximorphic (Stagnic) processes (with the accumulation of stagnic iron nodules in the 3EBg(k) horizon as well as of diatoms at the top of the 3BCtx horizon). It is probable that the water stagnation is derived from the presence of the low permeable tepetate. These main processes responsible for profile differentiation are accompanied by moderate weathering of primary minerals. We assume that conditions were wet but cool during this stage of pedogenesis. Regarding the carbonate nodules observed in this soil, as was mentioned by Sedov et al. (2009),

the carbonate nodules found here have a much younger age and do not correspond to the third paleosol formation.

The next lithological group refers to the upper paleosol, which is presented by the 2Ah, 2AB and 2B horizons. From the morphological observations it is evident that this soil had a strong humus accumulation and, at the micromorphological level, incipient slickenside formation. The paleosol is relatively low in K content and rich in ultrafine magnetic minerals, considered as a sign of strong weathering and pedogenesis in a warm environment, but not humid, so the soil developed vertic properties. The last stage of pedogenesis is presented in the upper, modern soil. The soil cover is thin and despite the presence of biogenic pores shown by the computed tomography, the soil is not as rich in organic material as the underlying paleosol. We explain such a poor development of this soil by a long-term human-induced erosion. Remains of this anthropogenic activity are distributed on the soil surface in the form of ceramic and stone fragments as well as obsidian flakes. Heine (2003) has documented several erosional phases for the last 3500 years and assumed this was a human-induced process. The enhancement of the magnetic susceptibility observed in this layer (Fig. 6) can also be evidence of the charred material produced by human activities. Additionally, the carbonate nodules found in the 3EBg(k) horizon correspond to this modern stage of pedogenesis due to the young age of 1.3 ka (Sedov et al., 2009). We further speculate that the six stages described in the Tlalpan profile development are related to the specific environmental evolution during the Late Quaternary, as described below.

Until now there is no data on the ages of both lower tepetate layers (TG2 and TP: 5BCtx and 6BCtx horizons, respectively). However, the age of the fourth stage which corresponds to a paleo-Vertisol (4ABi-4Bti), named as TX2, ranges from 30189 to 51798 ka (Sedov et al., 2009). Therefore, this soil is related to MIS 3. The next paleosol (Stagnic Luvisol) which includes the upper Gray tepetate (TP1- 3BCtx horizon) correlates with TX1b paleosol from the Mamut section, which also contains iron nodules. This paleosol was developed during a colder climate, most probably during MIS 2 (Sedov et al., 2009; Solís-Castillo et al., 2012). It also coincides with data published by Metcalfe at al. (2000), who suggest cool and wet conditions for the same time period. At the end of MIS 2, a dynamic landscape development was recorded by the presence of 16068±222 cal yr BP-tepetate found in slope sections of the Young Barranca (Fig. 9). The formation of Stagnic Luvisol was interrupted and the paleosol was buried by the sediments, which later became parent materials of the youngest paleosol of the Tlalpan section. That paleosol was most probably formed during the early to middle Holocene, and correlates to paleosols/pedosediments and alluvial-colluvial sediments found in the eroded slope (section 8), the incised valley and the terrace of the studied barrancas, whose ages range from 9 to 3 ka (Table 1, Fig. 9). The modern soil with the evidence of a long human occupation was formed during the late Holocene under a dry climate and with anthropogenically induced erosion. This soil corresponds to the soil from slope sections of the age of 2 ka.

Detailed soil-sedimentary records for the Late Pleistocene and Holocene in slope sections and correlation of the sections

The record oflandscape evolution in this study was not only established from the Tlalpan profile located at the highest relief position, but also from the slope sequences. In this way we have accessed more detailed records, i.e., a higher time-scale resolution, with more stages of formation being detected. The ages from the paleosol samples reveal their approximate age near their burial time. In the case of colluvial sediments, the obtained ages should be interpreted cautiously, as they can incorporate old materials. Therefore, the radiocarbon ages may not coincide with the time of sedimentation.

In the small paleo-depressions, there are indicators of pedogenesis-sedimentation processes. In the lakelet at the head of the Young Barranca, section 20 (Fig. 9, 10), we were able to reconstruct the succession of events from the observed changes in the stratigraphy: formation of the dark-colored paleosol (Luvisol) TX2 -4Bti→ erosion of the surface and development of a depression → flooding of the depression and the small lake formation (marked by accumulation of stratified sediments) → lake shallowing and drying-up → sedimentation and tepetate development → sedimentation, soil formation with the formation of the pedogenic carbonates (dated to 4707±136 cal yr BP) → erosion. As the age of this tepetate is 14576±349 cal yr BP, it is most probably an equivalent of the upper Gray tepetate from the Tlalpan section (3BCtx horizon).

The cultural layer of section 19 documents an erosional stage. In this way, the soil material is eroded leaving the artifacts on the surface of the Gray Unit tepetate. The abundance of artifacts suggests that this is a site of a large ancient settlement that was occupied by people over a long period and could not have existed without a permanent water source. As there wasn't any permanent stream at the site, the local population could have used one of the small lakes. It is worth noting that such lakelets may be still found in villages in the region, some of them being sustained by earthen dams (Fig. 9). The age of small lakes could vary from the Late Glacial to the Late Holocene.

We suggest that the bottom of the oldest erosional landform (i.e., the beginning of the gulley incision) was formed at the end of the Pleistocene. This suggestion is confirmed by the age of the tepetate layer cut by the incision, 14576±349 cal yr BP. In addition to this evidence, the age of a bone fragment found in the alluvial-colluvial deposits in section 28 is 16438±165 cal yr BP. This bone was transported downslope at the time of the paleo-gulley initiation.

Therefore, we assume that the deep downcutting of the gulley occurred at the final stage of the last (Wisconsin) glaciation. The deposition proceeded at maximal rates at the first stage of the paleo-depression filling. It may be safely concluded that the environments changed drastically towards a cooler climate and an increase in humidity. Two intervals of reduced erosion were identified in the development of two levels of paleosols separating alluvial-colluvial layers, differing in age. The upper paleosol was dated in the Young Barranca by radiocarbon at 9012±187 cal yr BP (Table 1). This paleosol is buried under a tepetate of approximately the same age (9198±139 cal yr BP), so we suggest a continuous sequence of events: soil formation, followed by soil burial under the tepetate formed of redeposited pedosediment of the same soil from the upper locations. Most probably, the soil burial was a result of environmental deterioration. The second soil is ^{14}C dated to 7153±124 cal yr BP. Perhaps, the deposition rate decreased in the Middle Holocene.

The well-developed Luvisol found in section 5 (5E-5Btk-5Btg) has been formed under forest ecosystems, mostly coniferous, over a long time, as seen from its mature, well differentiated profile. The burial of the Luvisol could be a consequence of deforestation and subsequent erosion resulting from a volcanic eruption or a drought (the pyroclastic material detected in the overlying tepetate (Tep 4) favors the hypothesis about volcanic activity). We have no unambiguous evidence indicative of the soil age. The rest of the sequence, documented by the ages of the tepetates (Tep 3 to Tep 1), was formed during the Middle to Late Holocene, when the area was densely occupied by humans (Heine, 2003; Borejsza et al., 2008, Borejsza and Frederick, 2010).

The present-day Young and Concepcion gullies follow older valleys filled with brown alluvial-colluvial deposits overlain with well-developed paleosols, one of which was dated by radiocarbon at 9012±187 cal yr BP in the Young Barranca. The downcutting processes and gulley

growth were particularly active at the time of gulley initiation and the formation of the paleo-ravine bed. At first the filling of the erosional landform proceeded at a high rate. The lower layer of the brown colluvium M3 occasionally includes thin tepetate units and immature paleosols. Later, the erosion processes became less active, a rather well-developed soil formed on the colluvium (9012±187 cal yr BP) and was soon buried under the dentate tepetate composed of cemented pedosediment of approximately the same age. After that the deposition of colluvium continued until a new phase of soil formation around 7684±87 cal yr BP.

Correlation of landscape evolution records for the Holocene and the Late Pleistocene in Central Mexico and other regions

The correlation of the key profile Tlalpan formation with the main environmental changes has been suggested previously by Sedov et al. (2009) and with new details presented in this paper. Below we provide the correlation for the slope section profiles, as a proxy of higher resolution records of Holocene and Late Pleistocene conditions.

The oldest colluvial sediments and paleosols, documented in the studied sections of gulley slopes and bottom, are dated to an age of over 16 ka, which means there was a period of stability when the bottom paleosols were developed. According to Sedov et al. (2009), these paleosols are: TX2 (4Bti) formed during the MIS 3 and TX1a and TX1b, developed during MIS 2 (the youngest age for this unit is around 20000 cal yr BP). The tepetate TG-1 contains fragments of the A horizon of a paleosol which was formed after the erosional activity dated to 16 ka. During the late Glacial (14.70-12.9 ka BP) the strongest and long-lasting volcanic eruptions occurred (Mooser, 1967). It was during that interval that gullies were initiated, and the oldest erosional landforms developed. Global climate change was also involved in the landscape development processes. As suggested by Heine (1994), the deglaciation of the Laurentide Ice Sheet at the end of the Younger Dryas discharged cold meltwater to the Gulf of Mexico, which is also a reason for the cold and unfavorable environment for soil formation.

The observations of the Holocene climate evolution follow the new global Holocene subdivisions scale (Walker et al., 2019). The significant glacier advances recorded on La Malinche and Nevado de Toluca volcanoes (Palacios et al., 2020), about 10–8 ka BP in Mexico correspond to the Greenlandian stage. At that time, extremely strong eruptions were followed by extensive glaciation leaving three moraines on La Malinche and other volcanoes. It is not inconceivable that the strongest eruptions of Popocatepetl and other volcanoes in the Late Glacial and the beginning of the Holocene caused the sizeable mountain glaciations in the region recorded on La Malinche and other summits 10-8 ka BP (Heine, 1988, 1994; Vázquez-Selem and Heine, 2004). That, in turn, extended the glacial influence into the early Holocene and contributed to the prolonged existence of cold and wet conditions in Tlaxcala and adjacent regions. The sections 11 to 13a revealed three ^{14}C dates at 9 ka. One of these ages was obtained for a Luvic Andosol-type paleosol, which requires warm and humid climatic conditions and more than a thousand years for its formation (Miehlich, 1992; Sedov et al., 2003; Solleiro-Rebolledo et al., 2015). The deepest and most active downcutting and the channel formation happened at the end of the Pleistocene – beginning of the Holocene. At first the landform infilling proceeded at a high rate. After the deposition rate was somewhat lessened and the lower soil developed (9012±187 cal yr BP), the erosion resumed. The soil is buried under the tepetate consisting of cemented pedosediment ^{14}C-dated at the similar age (9198±139 cal yr BP). That tepetate development is related to the cooling related to the previously mentioned glacial events.

The transition from the cold and unstable Greenlandian epoch to warmer and more stable Northgrippian Stage did not leave any notable evidence in the Tlaxcala paleosol sequence. The younger Andosol with some characteristics of Luvisols, which was dated to 7 ka, was formed after the 8.2 ka event and probably on the colluvial sediment produced because of this event. After that, the accumulation of alluvial-colluvial deposits continued until a new phase of stability and soil formation; the radiocarbon age of the second paleosol (in the deposits filling paleo-channels) is 7153±124 cal yr BP. The most humus-rich soils, colluvial layers and tepetate are confined to the middle part and the beginning of the Holocene. That could have been brought about by the climate amelioration and less active processes of sheet and rill erosion on the forested slopes. Our data for the 7 ka paleosol are in good correlation with pollen assemblages for Central Mexico (Caballero et al., 2010). Thus, favorable (warm and wet) conditions for soil (Luvisol) formation existed in the upper reaches of gullies at the end of the first half of the Holocene (section 5). Even at that time, during repeated erosion, alluvial-colluvial deposits accumulated and tepetate developed in the lower reaches of gullies (section 31). The interruption of paleosol formation at the age of 6 ka may be related to the fourth Bond cycle (5.9 ka) for the North Atlantic (Bond et al., 1997; 2001).

Bernal et al. have suggested that the influence of North Atlantic climatic changes decreased since the beginning of Meghalayan epoch due to the greater importance of the El Niño-Southern Oscillation studied in the speleothems of southwestern Mexico (Bernal et al., 2011). They expect that this restricted the advection of humidity from the Caribbean area and provoked dryer conditions in southwest Mexico during the end of the Holocene, which means it would have affected Central Mexico as well.

The radiocarbon age of the lower humified tepetate in section 5 is 4866±121 cal yr BP, and the uppermost one – 1995±104 cal yr BP. This leads us to conclude that the overlying alluvial-colluvial series is a result of man-induced erosion and to date it to the Preclassic period (2500–100 BC). We are of the opinion that the human impact imposed on the arid climate essentially aggravated the effect of the latter. The lakelets surrounded with settlements gradually shallowed and dried up, and the people had to look for better habitat. The soil-forming processes were suppressed by the processes of erosion, deposition and tepetate formation. Accelerated man-induced erosion developed in several stages (at least, three): 1) formation of eroded sites at the heads of gullies; 2) initiation of gullies within the area of paleo-depressions filled with older deposits; 3) development of badlands. At present, formation of gullies proceeds on a large scale. The present-day gullies are a relatively new phenomenon, largely attributable to the natural trend in the relief evolution superimposed on the man-induced accelerated erosion. In the upper reaches they are incised into the older soil-tepetate series, and downstream they cut into alluvial-colluvial deposits accumulated during the earlier stages of gulley evolution. During the last 2000 years the principal process was the accumulation of synsedimentary, poorly sorted colluvial deposits.

Anthropogenic effects in the soil erosion during the late Holocene (approximately last 3000 years) in the Central Mexican Highlands and in particular in Tlaxcala is still a controversial issue. There is a large spread opinion that the agricultural practices of the ancient Mesoamerican civilizations were environmental-friendly and protective and that intensive soil erosion started only in the colonial period when ploughing and cattle breeding were installed (García-Cook, 1986). However, Heine who studied colluvial sequences in the downslope and valley bottoms positions in Tlaxcala showed extensive accumulation of pedosediments already before colonial time indicative of strong soil mobilization and redeposition upslope (Heine, 2003). Borejsza et al. (2008) investigated surface slope sediments in La Laguna, Tlaxcala state and documented intensive soil erosion already during the Formative period, which resulted in the exposure of tepetate at the surface. Later during the Classic and Colonial periods terraces were constructed on

the slopes to control soil loss. We conclude that intensive human-induced colluviation event took place since the beginning of agriculture also at the studied site.

Our results are also in agreement with materials published by Borejsza and Frederick (2010) who distinguished three differently aged terraces and the modern bottom in the studied gullies of Tlaxcala. The oldest terrace is dated to the Late Pleistocene (most probably, MIS 2), the next one formed at the end of Pleistocene – early Holocene (as suggested by the presence of the early Holocene hydromorphic humified alluvial deposits at its base); the young terrace and bottom developed in the late Holocene.

Conclusions

This study has shown that tepetate horizons hold a significant record of the landscape evolution and the main trends of Central Mexican Plateau paleoenvironmental history. The combination of higher and lower located profiles of the gulley range helped us to increase the time-scale resolution for the paleo-environmental reconstruction in the Holocene part of the section.

For the Late Pleistocene period we have found humid and warm conditions for the lowest two tepetate horizons and for the first stage of the formation of a Luvisol, which probably happened during the MIS3. Later the climate became arid and the same paleosol (4Bti horizon) was modified to a Vertisol. After that we identified a period of dynamic landscape development, when a tepetate horizon was formed. The tepetate formation, that is the compaction and hardening, occurred before pedogenesis. This compaction contributed to the formation of the redoximorphic features observed in the 3EBg(k) horizon. It is likely that the next paleosol was formed at the end of MIS2 in humid and cold conditions which were characteristic for the end of MIS2 period in general. For the end of the Pleistocene and its transition to the Holocene we distinguished only two incipient paleosols and only in slope sections, so we assume that the environmental conditions were not favorable for soil formation.

For the Holocene we distinguished a stage of stable environment for the paleosol formation at the beginning of the Holocene (9 ka paleosol), as well as during the Middle Holocene (6 and 5 ka paleosols). Those three paleosols were found in slope sections, but most likely they are correlated to the youngest paleosol from the Tlalpan section, for which we can say that it was formed in a warm but not humid environment. However, this paleosol formation was interrupted several times and the erosional processes left three different records of that.

The last stage of the environmental evolution we found is related to the soil with strong anthropic influence. The soil formation recorded dryer conditions than those of Middle Holocene environments. The modern soil development is restricted by human-induced erosion.

Acknowledgements

This work has been supported by the Russian Science Foundation, grant N 14-27-00133 and PAPIIT grant IN106616. Additional support was provided by the Russian State Task Program No. 0148-2016-0003. The Authors are grateful to N.N. Kovalyukh and V.V. Skripkin for the radiocarbon dating, which was performed at the Institute of Radiogeochemistry and Environments of the National Academy of Sciences of Ukraine, and to Dr. Beatriz Ortega-Guerrero for the permission to analyze the samples at the laboratory of Magnetic Susceptibility of the Institute of Geophysics, UNAM, Mexico. We thank Jaime Diaz for the help in preparation of the thin sections and Anna Yudina for help with texture analysis. Lilit Pogosyan and Hermenegildo Barceinas Cruz

708 gratefully acknowledge CONACyT for the PhD scholarship (51849333-2) and a scholarship of
709 researcher's helper file 19134. Authors thank UNAM's Academic Writing Program for its
710 important suggestions in improving of this manuscript.

711 **References**

712 Aeppli, H., 1973. Barroböden und Tepetate. Untersuchungen zur Bodenbildung in vulkanischen
713 Aschen unter wechselfeuchtem gemässigtem Klima im zentralen Hochland von México: Diss.
714 Beim Fachbereich Umweltsicherung, Justus-Liebig-Universität. Giessen. 172 p.

715 Alvarado-Cardona, M., Colmenero-Robles, J.A., Valderrábano-Almegua, M.L., 2007. La erosión
716 hídrica del suelo en un contexto ambiental, en el Estado de Tlaxcala, México. Ciencia Ergo Sum,
717 14, 3, 317-326.

718 Bernal, J.P., Lachniet, M., McCulloch, M., Mortimer, G., Morales, P., Cienfuegos, E. 2011. A
719 speleothem record of Holocene climate variability from southwestern Mexico. Quaternary
720 Research, 75, 104–113.

721 Bond, G., Kromer, B., Beer, J., Muscheler, R., Evans, M.N., Showers, W., Hoffmann, S., Lotti-
722 Bond, R., Hajdas, I., Bonani, G., 2001. Persistent solar influence on north Atlantic climate during
723 the Holocene. Science 294, 2130–2136.

724 Bond, G., Showers,W., Cheseby, M., Lotti, R., Almasi, P., deMenocal, P., Priore, P., Cullen, H.,
725 Hajdas, I., Bonani, G., 1997. A pervasive millennial-scale cycle in north Atlantic Holocene and
726 glacial climates. Science 278, 1257–1266.

727 Borejsza, A., Frederick, C.D., 2010. Fluvial response to Holocene climate change in low-order
728 streams of central Mexico. Journal of Quaternary Science 25(5), 762-781.

729 Borejsza, A., Rodríguez-López, I., Frederick, C.D., Bateman, M.D., 2008. Agricultural slope
730 management and soil erosion at La Laguna, Tlaxcala, Mexico. Journal of Archaeological Science,
731 35, 1854-1866.

732 Brown, E. T., Caballero, M., Cabral Cano, E., Fawcett, P. J., Lozano-García, S., Ortega, B., Pérez,
733 L., Schwalb, A., Smith, V., Steinman, B. A., Stockhecke, M., Valero-Garcés, B., Watt, S., Wattrus,
734 N. J., Werne, J. P., Wonik, T., Myrbo, A. E., Noren, A. J., O'Grady, R., Schnurrenberger, D., and
735 the MexiDrill Team, 2019. Scientific drilling of Lake Chalco, Basin of Mexico (MexiDrill). Sci.
736 Dril., 26, 1–15.

737 Bruker (2018a) Micro-CT software support. Available at
738 https://www.bruker.com/service/support-upgrades/software-downloads/micro-ct.html

739 Bruker (2018b) Micro-CT software. Available at
740 https://www.bruker.com/products/microtomography/micro-ct-software.html

741 Bullock, P., Fedoroff, N., Jongerius, A., Stoops, G., Tursina, T. & Babel, U. 1985. Handbook for
742 soil thin section description. – 152 p., Wolverhampton, United Kingdom (Waine Research
743 Publications).

744 Caballero, M., Lozano, S., Ortega, B., Urrutia, J., and Macias, J. L., 1999. Environmental
745 characteristics of Lake Tecocomulco, northern Basin of Mexico, for the last 50,000
746 years. Journal of Paleolimnology, 22, 399–411.

747 Caballero, M., Lozano-García, S., Vazquez-Selem, I., Ortega, B., 2010. Evidencias de cambio
748 climatico y ambiental en regisros glaciales y en cuencas lacustres del centro de Mexico durante el
749 ultumo maximo glacial. Boletin de la Sociedad Geologica Mexicana, 62, 359-377.

750 Díaz-Ortega, J., Solleiro-Rebolledo, E., Sedov, S., 2011. Spatial arrangement of soil mantle in
751 Glacis de Buenavista, Mexico as a product and record of landscape evolution. Geomorphology,
752 135, 248-261.

753 Díaz-Ortega, J., Solleiro-Rebolledo, E., Sedov, S., Cabadas, H., 2010. Paleosuelos y tepetates del
754 Glacís de Buenavista Morelos (México): testigos de eventos climáticos de la transición
755 Pleistoceno-Holoceno. Boletín de la Sociedad Geológica Mexicana, 62, 469-486.

756 FAO. 2006. Guidelines for soil description. 4th edition. Rome

757 Fölster H., Hetsch W., Schrimpff E., 1977. Late quaternary paleosols in the Western and Central
758 Cordillera of Colombia. Palaeog Palaeoclim Palaeoecol 21, 245–264

759 Gama-Castro, J., Solleiro-Rebolledo, E. Flores-Román, D., Sedov, S., Cabadas-Báez, H., Díaz-
760 Ortega, J., 2007. Los tepetates y su dinámica sobre la degradación y el riesgo ambiental: el caso
761 del Glacis de Buenavista, Morelos. Boletín de la Sociedad Geológica Mexicana LIX(1), 133-145.

762 García, E., 2004. Modificaciones al sistema de clasificacion climatica de Köpen. México, Instituto
763 de Geografía UNAM, 5th edition. 90 p

764 García-Cook, A.G., 1986, El control de la erosión en Tlaxcala; un problema secular: Erdkunde,
765 40, 251-262.

766 Gerrard A.J., 1981. Soils and Landforms. An Integration of Geomorphology and Pedology.
767 London: George Allen & Unwin, Boston, Sydney. 202 p.

768 Glazovskaya**,** M.A., 1996. Pedolithogenesis and organic carbon fossilization in the Quaternary
769 deposits of the Eurasian plains. Izvestiya. Russian Academy of Sciences. Ser. Geogr. 6, 21–33 (in
770 Russian).

771 Glazovskaya, M.A., 2000. Denudational-aggradational patterns of the soil cover as the
772 manifestations of pedolithogenesis. Eurasian Soil Science, Interperiodica Publishing (Russian
773 Federation), 33 (2), 114-126.

774 Golyeva, A., 2007. Various phytolith types as bearers of different kinds of ecological information.
775 In: M. Madella, D. Zurro (Eds.), Plants, People and Places. Recent Studies in Phytolith Analysis,
776 Oxbow books, pp. 196-201.

777 Haulon, M., Werner, G., Flores-García, G., Vera-Reyes, V., Felix-Henningsen, P., 2007.
778 Assessment of erosion rates during rehabilitation of hardened volcanic soils (tepetates) in Tlaxcala.
779 Revista Mexicana de Ciencias Geológicas, 24, 3, 498-509.

780 Heine, K., 1984. The classical late Weichselian climatic fluctuations in Mexico. In: Mörner, N.-
781 A., Karcén, W.D. (Eds.), Climatic changes on a yearly to millennial basis. Geological, historical
782 and instrumental records. Riedel Publishing Company. Dordrecht/ Boston/ Lancaster, pp. 95–115.

783 Heine, K., 1988. Late Quaternary glacial chronology of the Mexican volcanoes. Die
784 Geowissenschaften 6/7, 197-205.

785 Heine, K., 1994. The late – glacial moraine sequences in Mexico, is there evidence for Younger
786 Dryas. Palaeogeography, Palaeoclimatology, Palaeoecology, 112, pp. 113-123.

787 Heine, K., 2003. Paleopedological evidence of human-induced environmental change in the
788 Puebla-Tlaxcala area (Mexico) during the last 3,500 years: Revista Mexicana de Ciencias
789 Geológicas, 20(3), 235-244.

790 IUSS Working Group WRB. World Reference Base for Soil Resources 2014, update 2015
791 International soil classification system for naming soils and creating legends for soil maps. World
792 Soil Resources Reports No. 106. FAO, Rome. 2015

793 Kozlovskii, F. I. and Goryachkin, S. V. 1996. Soil as a mirror of landscape and the concept on
794 informational structure of soil cover. Eur. Soil Sci. 29, 255–263

795 LaFevor, M.C., 2014. Conservation Engineering and Agricultural Terracing in Tlaxcala, Mexico.
796 PhD dissertation, Faculty of the Graduate School of The University of Texas at Austin.

797 Lauer, W., 1979. Medioambiente y desarrollo cultural en la región de Puebla-Tlaxcala. Fundación
798 Alemana para la Investigación Científica, Puebla, México. Comunicaciones, 16, 29-54.

799 Lermo-Samaniego, J., Bernal-Esquia, I., 2006. Zonificación sísmica del Estado de Tlaxcala,
800 México: Boletín de la Sociedad Geológica Mexicana. 57(2), 215–221.

801 López-Prat M., Agostino R.G., Bandyopadhyay S.R., Carrascosa B., Crocco M.C., De Luca R.,
802 Filosa R., Formoso V., Lancelotti C., Noori N.A., Pecci A., Simón-Cortés J., Miriello D., 2021.
803 Architectural Terracruda Sculptures of the Silk Roads: New Conservation Insights Through a
804 Diagnostic Approach Based on Non-Destructive X-ray Micro-Computed Tomography, Studies in
805 Conservation, DOI: 10.1080/00393630.2020.1862605

806 Martínez-Abarca, L.R., Lozano-García, S., Ortega-Guerrero, B., Chávez-Lara, C.M., Torres-
807 Rodríguez, E., Caballero, M., Brown, E.T., Sosa-Nájera S., Acosta-Noriega, C., Sandoval-Ibarra,
808 V., 2021. Environmental changes during MIS6-3 in the Basin of Mexico: A record of fire, lake
809 productivity history and vegetation. Journal of South American Earth Sciences, 109, 103231.

810 Metcalfe, S.E., O'Hara, S.L., Caballero, M., Davies, S.J. 2000. Records of Late Pleistocene-
811 Holocene climatic change in Mexico - a review. Quaternary Science Reviews, 19, 699-721.

812 Miehlich, G., 1992. Formation and properties of tepetate in the central highlands of Mexico.
813 TERRA, 10, 137-144.

814 Mooser F., 1967. Tefracronologia de la Cuenca de México para los úlltimos treinta mil años.
815 Boletín INAH, 30, 12-15.

Mooser, F., Montiel, A., Zúñiga, A., 1996, Mexico, CFE, Nuevo mapa geológico de las cuencas de México, Toluca y Puebla.

Nimlos, T.J., Hillery, P.A. 1990. The strength/moisture relations and hydraulic conductivity of Mexican tepetate. Soil Science, 150, 425-430.

Oleschko, K., Zebrowski, C., Quantin, P., Fedoroff, N., 1992. Patrones micromorfológicos de organización de arcillas en tepetates (México). Terra 10, 183–191.

Ortega-Guerrero, B., Sedov, S., Solleiro-Rebolledo, E., Soler, A., 2004. Magnetic mineralogy in the Barranca Tlalpan exposure paleosols, Tlaxcala, Mexico: Revista Mexicana de Ciencias Geológicas, 21(1), 120-132.

Palacios D., Stokes C.R., Phillips F.M., Clague J.J., Alcalá-Reygosa J., Andrés N., Angel I., Blard P.-H., Briner J.P., Hall B.L., Dahms D., Hein A.S., Jomelli V., Mark B.G., Martini M.A., Moreno P., Riedel J., Sagredo E., Stansell N.D., Vázquez-Selem L., Vuille M., Ward D.J., 2020. The deglaciation of the Americas during the Last Glacial Termination. Earth-Science Reviews, 203, 103113

Poetsch, T., 2004. Forms and dynamics of silica gel in a tuff-dominated soil complex: Results of micromorphological studies in the Central Highlands of Mexico. Revista Mexicana de Ciencias Geológicas 21, 195-201.

Pogosyan L., Gastelum A., Prado B., Marquez J., Abrosimov K., Romanenko K., Sedov S. 2019. Morphogenesis and quantification of the pore space in a tephra-palaeosol sequence in Tlaxcala, central Mexico. Soil Research, 57, 559-565.

Quantin, P., 1992. L´induration des matériaux volcaniques pyroclastiques en America Latine: processus geologiques et pedologiques. Terra ,10, 24-33.

Reimer, P., Austin, W.E.N., Brad, E., Bayliss, A., Blackwell, P.G., Bronk Ramcey, C., Butzin, M., Edwards, R.L., Friedrich, M., Grootes, P.M., Guilderson, T.P., Hajdas, I., Heaton, T.J., Hogg, A., Kromer, B., Manning, S.W., Muscheler, R., Palmer, J.G., Pearson, C., van der Plicht, J., Reim Richards, D.A., Scott, E.M., Southon, J.R., Turney, C.S.M., Wackel, L., Adolphi, F., Büntgen, U., Fahrni, S., Fogtmann-Schulz, A., Friedrich, R., K¨ohler, P., Kudsk, S., Miyake, F., Olsen, J., Sakamoto, M., Sookdeo, A., Talamo, S., 2020. The IntCal20 Northern Hemisphere radiocarbon age calibration curve (0-55 cal kB). Radiocarbon, 62 (4), 725–757.

Rohdenburg, H., 1970. Morphodynamische Aktivitäts- und Stabilitätszeiten statt Pluvial- und Interpluvialzeiten. Eiszeitalter und Gegenwart, 21, 81–96.

Romanis T., Sedov S., Lev S., Lebedeva M., Kondratev K., Yudina A., Abrosimov K., Golyeva A., Volkov D., 2021. Landscape change and occupation history in the Central Russian Upland from Upper Palaeolithic to medieval: Paleopedological record from Zaraysk Kremlin. Catena, 196, 104873.

Sánchez-Pérez, S., Solleiro-Rebolledo, E., Sedov, S., McClung de Tapia, E., Golyeva, A., Prado, B., Ibarra-Morales, E., 2013. The Black San Pablo paleosol of the Teotihuacan Valley, Mexico: pedogenesis, fertility, and use in ancient agricultural and urban systems. Geoarchaeology, 28, 249-267.

Schoeneberger, P.J., Wysocki, D.A., Benham, E.C., Soil Survey Staff, 2012. Field Book for Describing and Sampling Soils. Version 3.0. Natural Resources Conservation Service. National Soil Survey Center, Lincoln, NE.

Sedov, S., Solleiro-Rebolledo, E., Gama-Castro, J.E., Vallejo-Gómez, E., González-Velázquez, A., 2001. Buried paleosols of Nevado de Toluca: an alterative record of Late Quaternary environmental change in Central Mexico: Journal of Quaternary Science, 16(4), 375-389.

Sedov, S., Solleiro-Rebolledo, E., Gama-Castro, J., 2003. Andosol to Luvisol evolution in central Mexico: timing, mechanisms and environmental setting. Catena 54, 495-513,

Sedov, S., Solleiro-Rebolledo, E., Terhorst, B., Solé, J., Werner, G., Poetsch, T., 2009. The Tlaxcala Basin paleosol sequence: multiscale proxy of the Middle to Late Quaternary environmental change in central Mexico. // Revista Mexicana de Ciencias Geológicas 26, 448-465.

Sochan, A., Polakowski, C., & Łagód, G. 2014. Impact of optical indices on particle size distribution of activated sludge measured by laser diffraction method. Ecological Chemistry and Engineering S, 21(1), 137-145.

Solís-Castillo, B., Solleiro-Rebolledo, E., Sedov, S., Salcido-Berkovich, C., 2012. Paleosuelos en secuencias coluvio-aluviales del Pleistoceno – Holoceno en Tlaxcala: registros paleoambientales del poblamiento temprano en el centro de México. Boletín de la Sociedad Geológica Mexicana, 64, 91-108.

Solleiro-Rebolledo E., Sedov S., McClung de Tapia E., Cabadas H., Gama-Castro J., Vallejo-Gómez E., 2006. Spatial variability of environment change in the Teotihuacan Valley during the Late Quaternary: Paleopedological inferences. Quaternary International 156–157, 13–31.

Solleiro-Rebolledo, E., Macías, J.L., Gama-Castro, S., Sedov, S., 2004. Quaternary pedostratigraphy of the Nevado de Toluca volcano. Revista Mexicana de Ciencias Geológicas, 21, 101-109.

Solleiro-Rebolledo, E., Sedov S., Cabadas-Báez H., 2015. Use of soils and palaeosols on volcanic materials to establish the duration of soil formation at different chronological scales. Quat. Int. 376: 5-18.

Solleiro-Rebolledo, E., Sedov, S., Gama-Castro, J.E., Flores-Román, D., Escamilla-Sarabia, G., 2003. Paleosol-sedimentary sequences of the Glacis de Buenavista, Central Mexico: interaction of Late Quaternary pedogenesis and volcanic sedimentation: Quaternary International 106/107, 185-201.

Sycheva, S.A., 2003. Evolution of erosional landforms of the Moscow-Valday age on the interfluves of the Central Russian Upland. Geomorphologiya 3, 72-91. (in Russian).

Sycheva, S.A., 2006. --Long-term pedolithogenic rhythms in the Holocene. Quaternary International, 152-153. P. 181-191.

Sycheva, S.A., 2008. Morpholithopedogenesis in accumulative and trans-accumulative landscapes as a specific mechanism of the soil- and pedogenic memory. In: Targulyan, V.O.,

Goryachkin, V.S. (Eds), Soil memory: Soil as a record of biosphere-geosphere-anthroposphere interactions. LKI Press, Moscow, pp. 128-161. (in Russian).

Sycheva, S.A., Daineko, E.K., Sulerzhitskiy, L.D., Usyanov, A.A., Chichagova, O.A., 1998. Stages of erosion on the Central Russian Upland in the Holocene. Geomorphologiya 3, 12-20. (in Russian).

Sycheva, S.A., Sedov, S.N., Solleiro-Rebolledo, E., 2013. Evolution of landscapes and relief of the Central Mexican Plateau in the late Glacial and Holocene. Geomorphologiya 2, 97-112. (in Russian).

Torres-Rodríguez, E., Lozano-García, S., Roy, P., Ortega, B., Beramendi-Orosco, L., Correa-Metrio, A., and Caballero, M., 2015. Last Glacial droughts and fire regimes in the central Mexican highlands. J. Quaternary Sci., 30, 88–99.

Vázquez-Selem L., Heine K., 2004. Late Quaternary glaciation of Mexico. In: Ehlers, J., Gibbard, P.L. (eds.), Quaternary glaciations – extent and chronology, Part III. Developments in Quaternary Science, 2, Elsevier, pp. 233-242.

Vázquez-Selem, L., Heine, K., 2011. Late Quaternary Glaciation in Mexico. Developments in Quaternary Science, 15, pp. 849–861.

Walker, M., Gibbard, P., Head, M., Berkelhammer, M., Björck, S., Cheng, H., Cwynar, L., Fisher, D., Gkinis, V., Long, A., Newnham, R., Rasmussen, S.O., Weiss, H. 2019. Formal Subdivision of the Holocene Series/Epoch: A Summary. Journal of the Geological Society of India, 93(2), 135-141.

Werner, G., Lückoff, A., Moll, W., 1988. Die Böden des Staates Tlaxcala im zentralen Hochland von Mexiko. Das Mexiko-Projekt der Deutschen Forschungsgemeinschaft. Stuttgart. Bd. 20.

White, S.E, 1962. Late Pleistocene glacial sequence for the West side of Iztaccihuatl, Mexico. Geological Society of America 73, 935-958.

Whitmore, T.M., Turner II, B.L., 2001. Cultivated Landscapes of Middle America on the Eve of Conquest. Oxford University Press, Oxford.

Zebrowski, C., 1992. Los suelos volcanicos endurecidos en America Latina. TERRA, 10, 15-23.

Table headings

Table 1. Results of radiocarbon dating of soils and deposits.

Figure captions

Fig. 1 Location of study area and investigated profiles: a) the general scheme; b) positions of main volcanoes in relation to the study site (red mark) and the gulley of Blanca (green mark); c) the map of locations of the studied profiles within the gulley network. Orange numbers correspond to the Concepcion gulley (profiles 5 and 30), red and blue ones to the Tlalpan (12, 13a, 28 and 31) and Young gullies (7, 8, 11, 19 and 20). The green arrow shows the direction to the gulley of Blanca, which is located at a distance of about 8 km from the study site.

Fig. 2 Photo of the Tlalpan profile with main morphological units and its horizons scheme.

Fig. 3 Micromorphological photographs of main horizons of the Tlalpan profile: a) biogenic aggregation and pores in the Au horizon, PPL; b) wedge-shaped aggregates typical for Vertisols in the 2Ah horizon, PPL; c) compact matrix organization and complex ferruginous nodule in the 3EBg(k) horizon, PPL; d) illuvial impure clay coatings occupy a significant part of pore-channels in the 3BCtx tepetate horizon, PPL; e) Moderately weathered grain of pyroxene with serrated edges in the 3BCtx tepetate horizon, PPL; f) deformed illuvial clay coatings in the 4ABi horizon, PPL; g) porostriated b-fabric (stress cutans) in the 4Bti horizon, N+; h) compact matrix, thick undisturbed illuviated clay coating in the pore-channel of the 5BCtx tepetate horizon, PPL. PPL - plain polarized light; N+ - crossed polarizers.

Fig. 4 Six general patterns of the particle-size distribution of the Tlalpan profile. Type A corresponds to the Au horizon; type B includes AB, 2Ah, 2AB, 2B horizons; type C includes the 3EBg(k) and the 3BCtx horizons; type D corresponds to the 4ABi and 4Bti horizons; type E to the 5BCtx horizon and type F to the 6BCtx horizon. Texture classes were defined as sand (63-1000 μm), silt (2-63 μm) and clay (< 2 μm) following the gradation proposed by the FAO guidelines (2006), the horizontal (x) axis is presented in logarithmic scale.

Fig. 5 Diagrams of magnetic susceptibility in low (0.47 kHz) frequencies (χlf), frequency-dependent magnetic susceptibility (χfd) and distribution of major elements (Ca, Fe and K) and trace elements (Ti) in the Tlalpan profile. For the diagrams of element distribution, the horizontal (x) axis is presented in logarithmic scale.

Fig. 6 Pore space distribution from CT of Tlalpan profile horizons: a) rounded interconnected biogenic pore-channels in the Au horizon; b) compact structure of the 3EBg(k) horizon; c) a homogeneous distribution of different pore size types in the 3BCtx tepetate horizon and irregular-shaped pore-channels being filled and separated from each other by illuviated clay (see Fig. 3d,g,h); d) a compact structure of the vertic 4ABi horizon with well-defined slickenside surfaces, large pore-channels are almost absent.

Fig. 7 Distribution of biomorphs in the Tlalpan profile.

Fig. 8 SEM micrographs of phytolits from the Tlalpan profile that originated from: a) reed; b) coniferous species; c) dicotyledonous herb; d) meadow grass.

Fig. 9 Geomorphological scheme of correlation of main stratigraphic layers of the Tlalpan profile and the profiles of Young Gulley, and picture of the small lakelet, which was observed during field work at this location for more than 20 years. Legend of the main scheme: 1 - modern soil; 2 - A horizon; 3 - Bt horizon; 4 - redoximorphic features; 5 - tepetate horizon; 6 - lacustrine deposits; 7 - colluvial deposits.

Fig. 10 Stages of the lakelet evolution and formation of the TG1-1 horizon at the head of the Young Barranca: I - formation of Luvisol, II – formation of the lake basin by stream and wind erosion, III – functioning of the lakelet – accumulation of laminated sediment, IV – the break-through or drying of the lake and filling of the depression by redeposited material of humus horizon (Ah), V – transformation of colluvium (Ah) into tepetate (TG1-1).

Fig. 11 Photos of the gullies' profiles: a) the Young Barranca, profiles 9, 10 and 11; b) stratigraphy of the Concepcion gulley terrace (section 30).

Table

Table 1. Results of radiocarbon dating of soils and deposits.

Geomorphic position, section number	Depth, cm	Soil, sediment, horizon,	Laboratory No	Dated material	^{14}C-age, yr BP	^{14}C-age, cal BP (yrs) (2σ)	^{14}C-age, cal BP (yrs)	Deviation
Concepcion Barranca, 5	1.25	TP1	Ki-10869	Humic acids	2340±70	2298-2261 (2.7%) 2155-1819 (91.8%) 1809-1793 (0.6%) 1759-1751 (0.3%)	**1995±104**	1σ 521-355 BC 2σ 561-345 BC
	1.9	Soil S2	Ki-10870	Humic acids	3160±70	3558-3526 (2.1%) 3510-3503 (0.4%) 3495-3207 (92.2%) 3193-3180 (0.8%)	**3367±83**	1σ 1517-1387 BC 2σ 1603-1553 BC 1637-1261 BC
	2.8	TP3	Ki-10871	Humic acids	4300±70	5264-5245 (0.6%) 5236-5189 (1.9%) 5053-4788 (78.1%) 4765-4617 (14.8%)	**4866±121**	1σ 3023-2875 BC 2σ 3099-2837 BC 2817-2665 BC
Young Barranca, 19	1.8	Dark soil Ah	Ki-14387	Humic acids	13350±150	16523-15640 (95.4%)	**16068±222**	1σ 14450-13750BC 2σ 14800-13100BC
Young Barranca, 20	0.1	At the top of TP1	Ki-14588	Carbonates	4190±100	4963-4504 (90.9%) 4494-4437 (4.2%) 4431-4425 (0.3%)	**4707±136**	1σ 2890-2620 BC 2σ 3050-2450 BC
	0.2	TP1	Ki-14392	Humic acids	12400±200	15255-14000 (94.0%) 13933-13865 (1.4%)	**14576±349**	1σ 13100-12150BC 2σ 13600-12100BC
Young Barranca, 8	1.8	Ah	Ki-14386	Humic acids	6260±100	7422-7377 (3.7%) 7364-6937 (91.5%) 6914-6907 (0.3%)	**7153±124**	1σ 5330-5060 BC 2σ 5500-4900 BC
Young Barranca, 11	2.7	TP1	Ki-14472	Humic acids	8220±100	9472-8990 (95.4%)	**9198±139**	1σ 7350-7080 BC 2σ 7530-7040 BC
Young Barranca, 11	2.9	Ah	Ki-14391	Humic acids	8100±110	9401-9364 (1.9%) 9309-86412 (93.5%)	**9012±187**	1σ 7200-6980 BC 2σ 7450-6650 BC
	4.0	Colluvium	Ki-14389	Humic acids	5580±120	6666-6176 (93.0%)	**6385±134**	1σ 4550-4320 BC

The Concepcion Barranca terrace, 31/07		(A1)				6146-6116 (1.5%) 6044-6019 (0.9%)		2σ 4750-4050 BC
	3.5	TP (A1)	Ki-14390	Humic acids	6830±90	7918-7902 (1.1%) 7860-7563 (91.6%) 7538-7513 (2.7%)	**7684±87**	1σ 5800-5630 BC 2σ 5900-5600 BC
Tlalpan Barranca, 13a/07	3.4	TP (Ah)	Ki-14586	Bone	8190±100	9461-8978 (92.2%) 8915-8895 (0.8%) 8882-8864 (0.7%) 8830-8784 (1.8%)	**9163±147**	1σ 7330-7060 BC 2σ 7550-6800 BC
Tlalpan Barranca «, 28/07	2.4	Colluvium (A1)	Ki-14587	Charcoal	13600±100	16796-16105 (95.4%)	**16438±165**	1σ 14650-14100BC 2σ 15000-13800BC

Figure 1

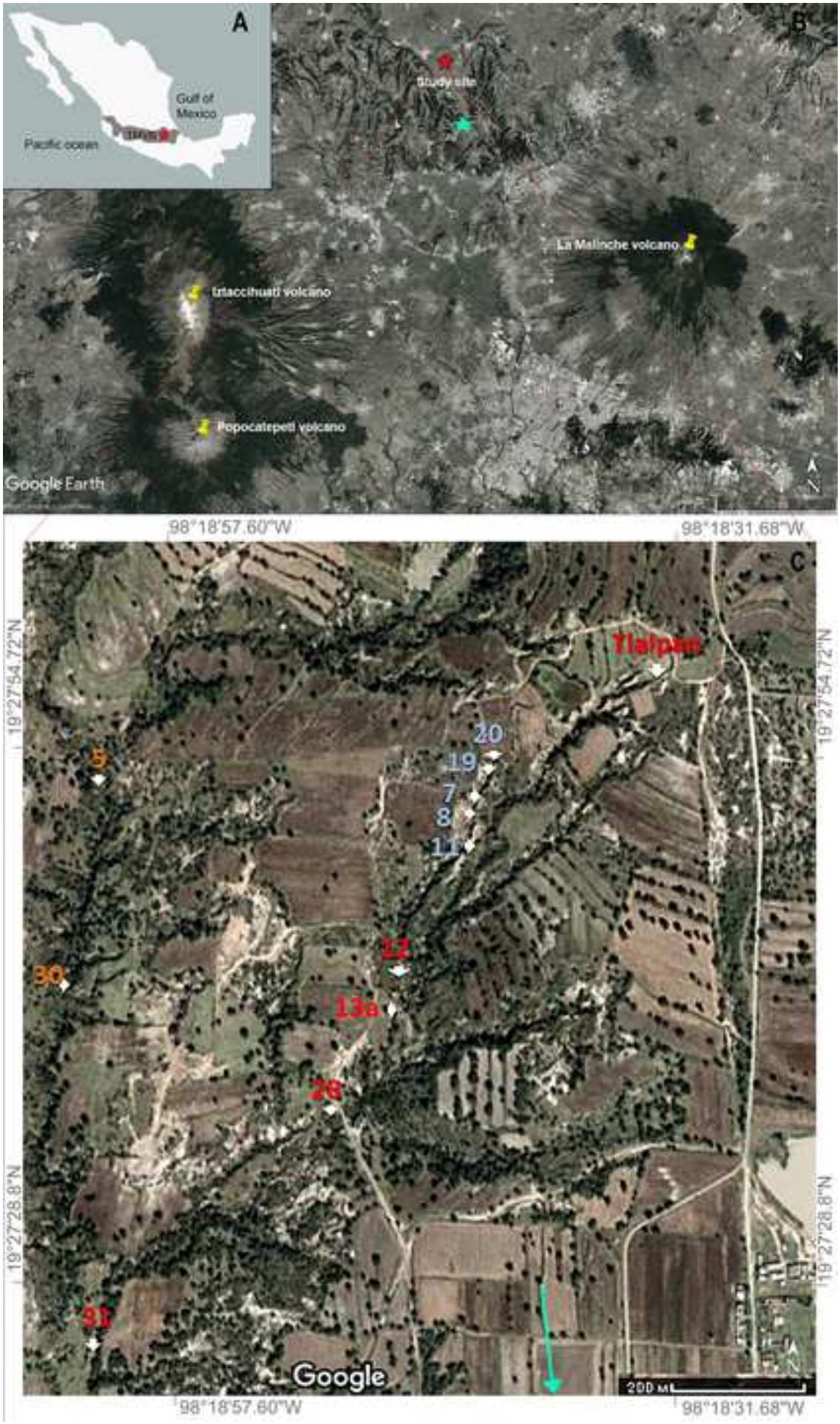
A
Gulf of Mexico
Pacific ocean
B
Study site
La Malinche volcano
Iztaccihuatl volcano
Popocatepetl volcano
Google Earth
98°18'57.60"W
98°18'31.68"W
C
Tlalpan
20
19
7
8
11
5
12
30
13a
28
31
19°27'54.72"N
19°27'28.8"N
Google
200 m

Figure 2

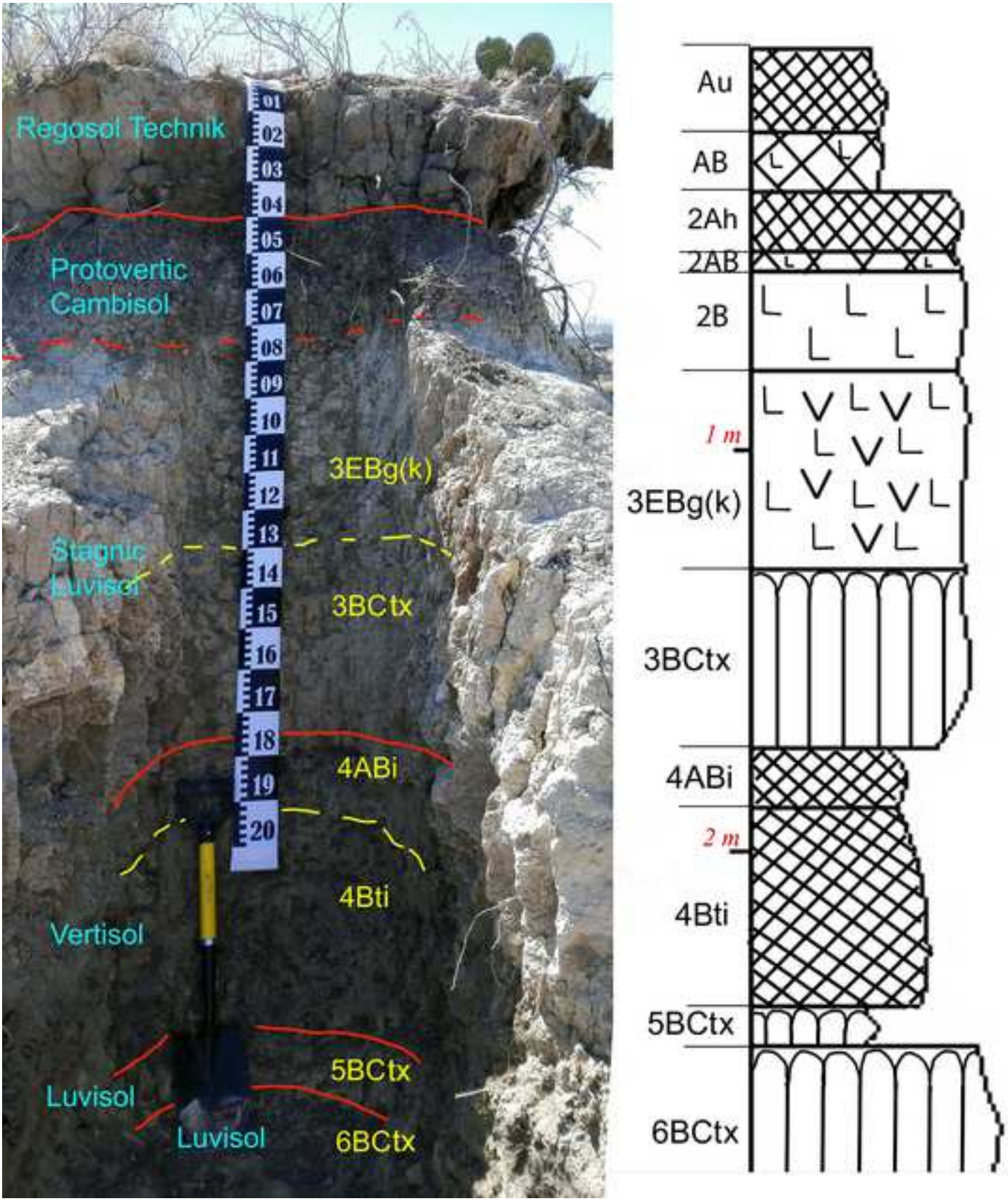
Regosol Technik
Protovertic Cambisol
Stagnic Luvisol
Vertisol
Luvisol
Luvisol
3EBg(k)
3BCtx
4ABi
4Bti
5BCtx
6BCtx
Au
AB
2Ah
2AB
2B
1 m
3EBg(k)
3BCtx
4ABi
2 m
4Bti
5BCtx
6BCtx

Figure 3

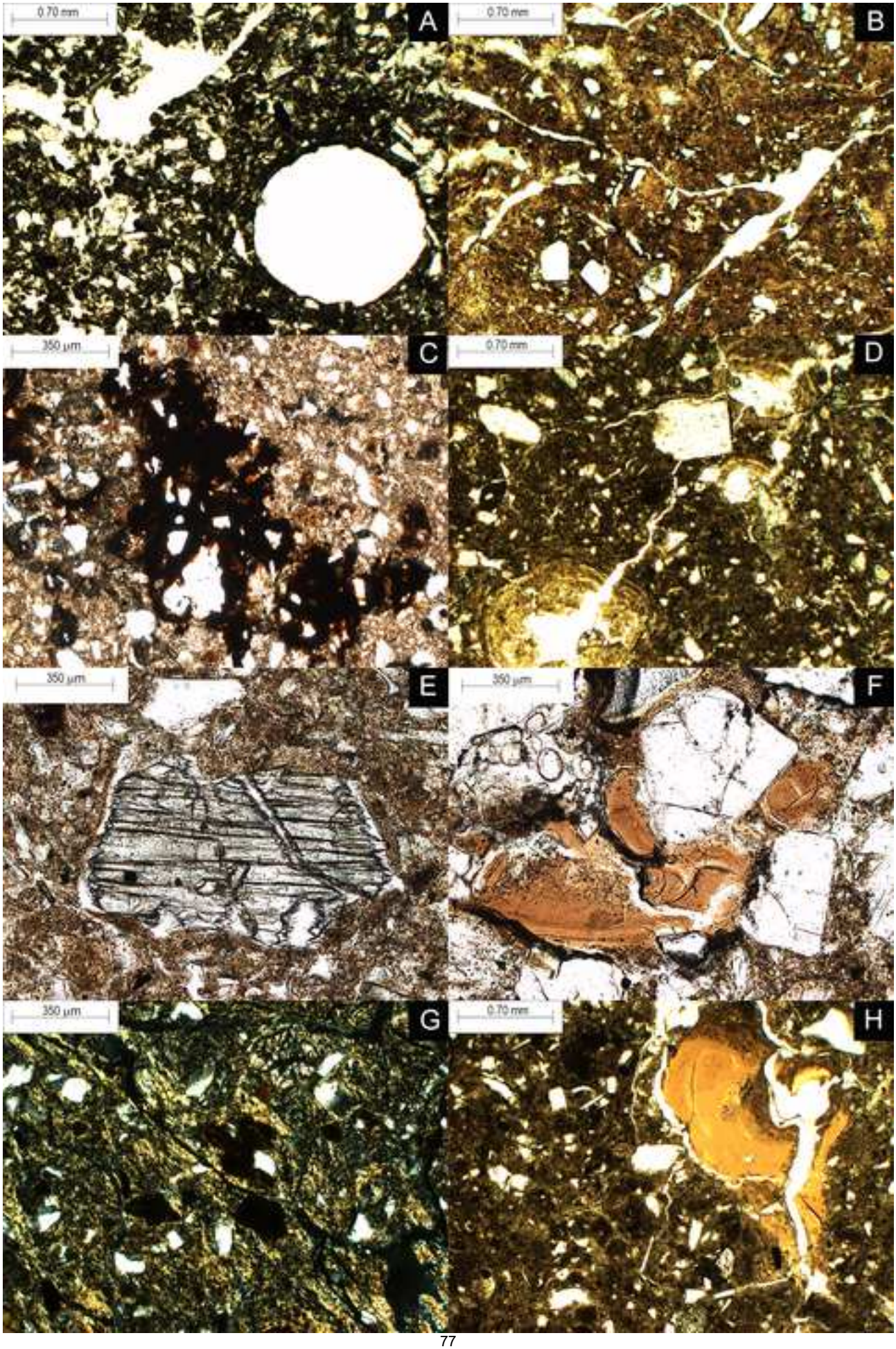

Figure 4

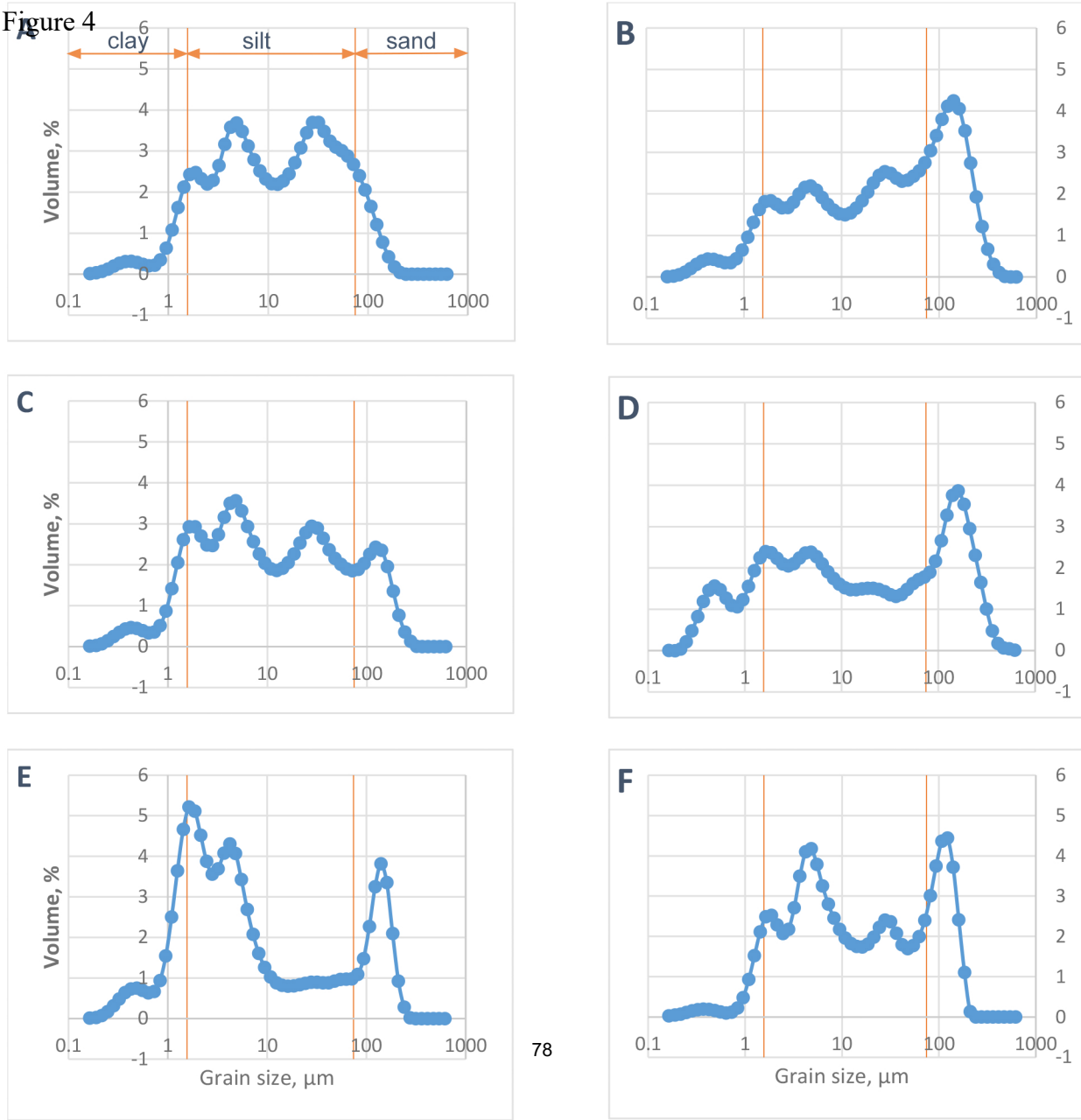
A
clay
silt
sand
Volume, %
B
C
D
E
F
Grain size, µm
0.1
1
10
100
1000
-1
0
1
2
3
4
5
6

Figure 5

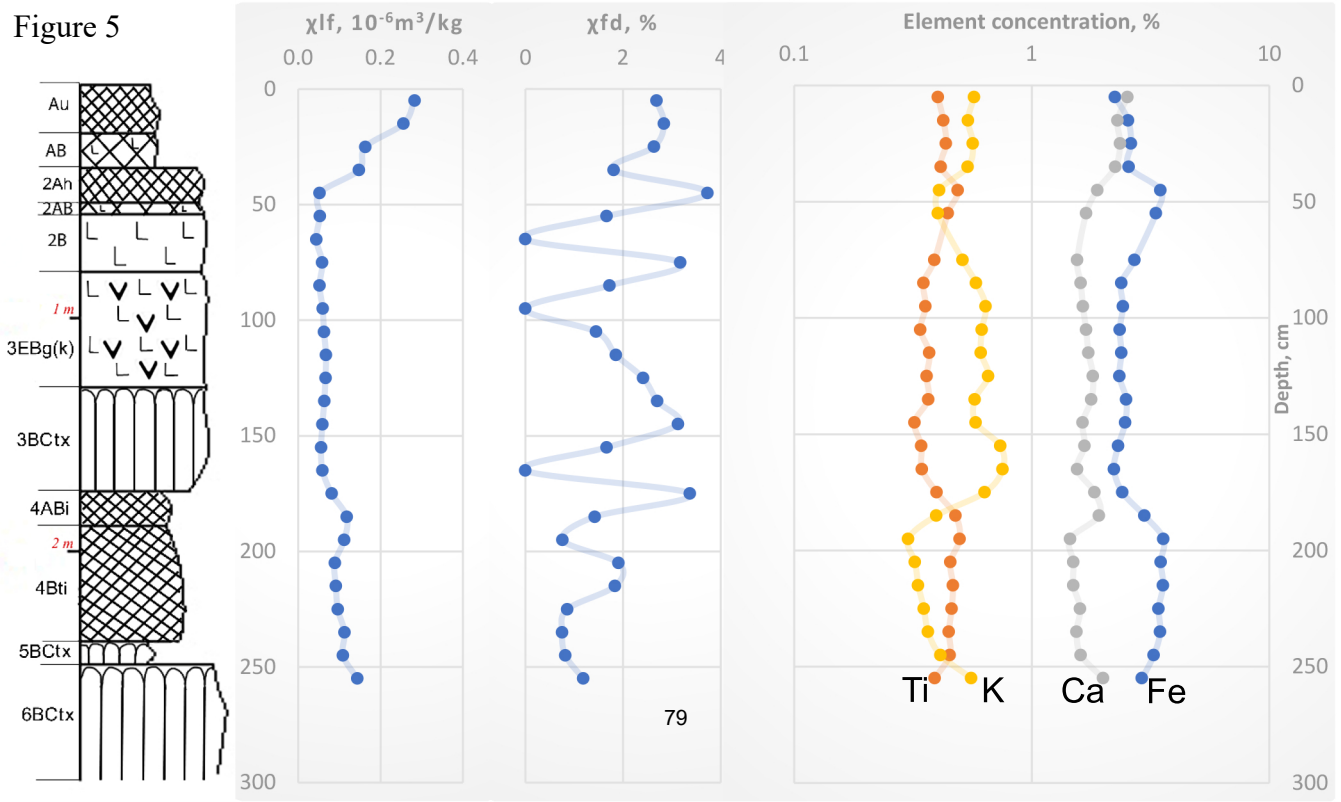
Au
AB
2Ah
2AB
2B
1 m
3EBg(k)
3BCtx
4ABi
2 m
4Bti
5BCtx
6BCtx
χlf, 10⁻⁶m³/kg
0.0
0.2
0.4
χfd, %
0
2
4
Element concentration, %
0.1
1
10
0
50
100
150
200
250
300
Depth, cm
Ti
K
Ca
Fe
79

Figure 6

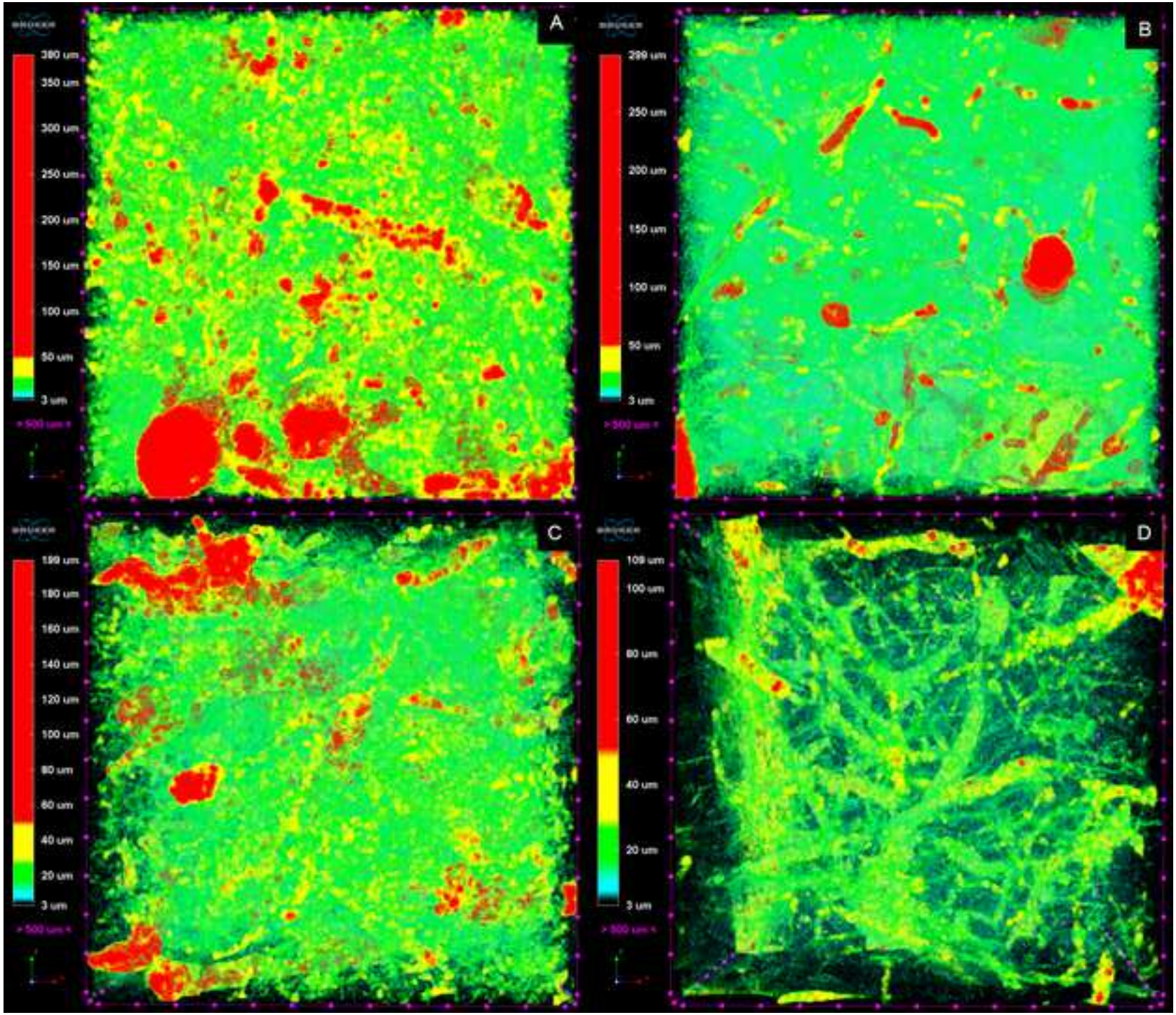
A
380 um
350 um
300 um
250 um
200 um
150 um
100 um
50 um
3 um
B
299 um
250 um
200 um
150 um
100 um
50 um
3 um
C
199 um
180 um
160 um
140 um
120 um
100 um
80 um
60 um
40 um
20 um
3 um
D
109 um
100 um
80 um
60 um
40 um
20 um
3 um

Figure 7

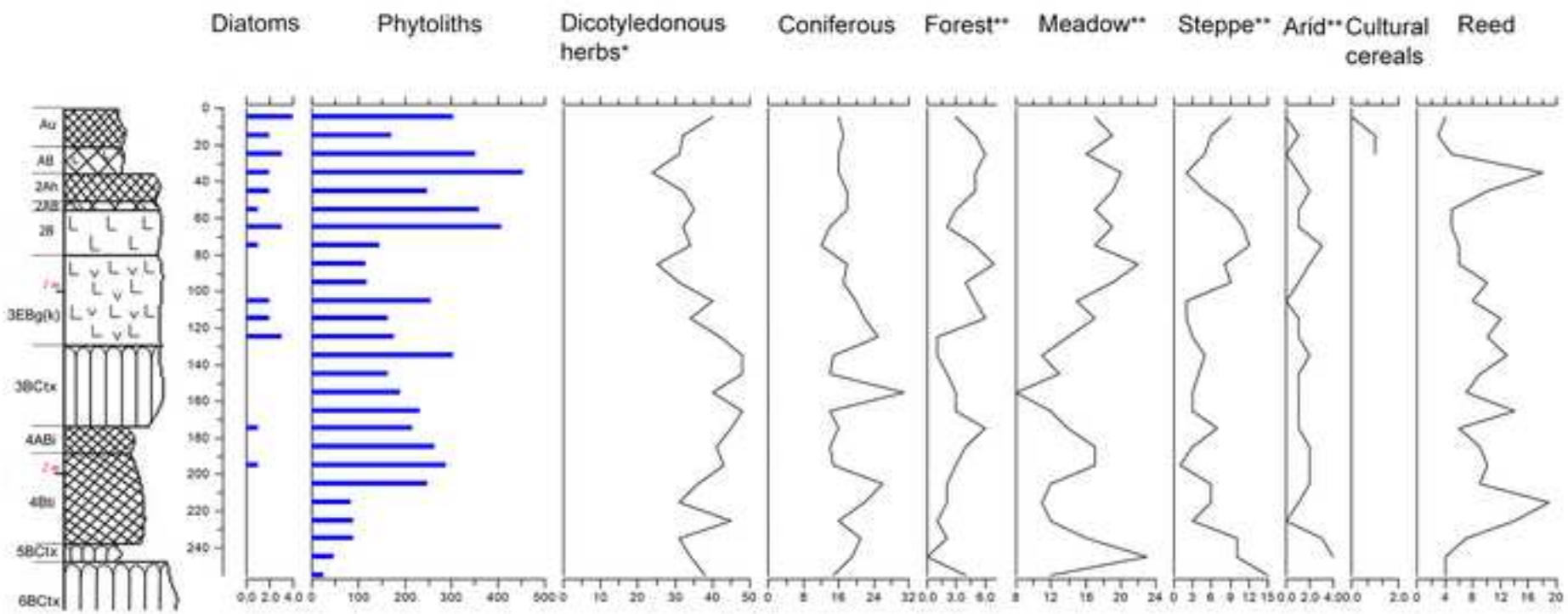
Diatoms
Phytoliths
Dicotyledonous herbs*
Coniferous
Forest**
Meadow**
Steppe**
Arid**
Cultural cereals
Reed
Au
AB
2Ah
2AB
2B
3EBg(k)
3BCtx
4ABi
4Bti
5BCtx
6BCtx

Figure 8

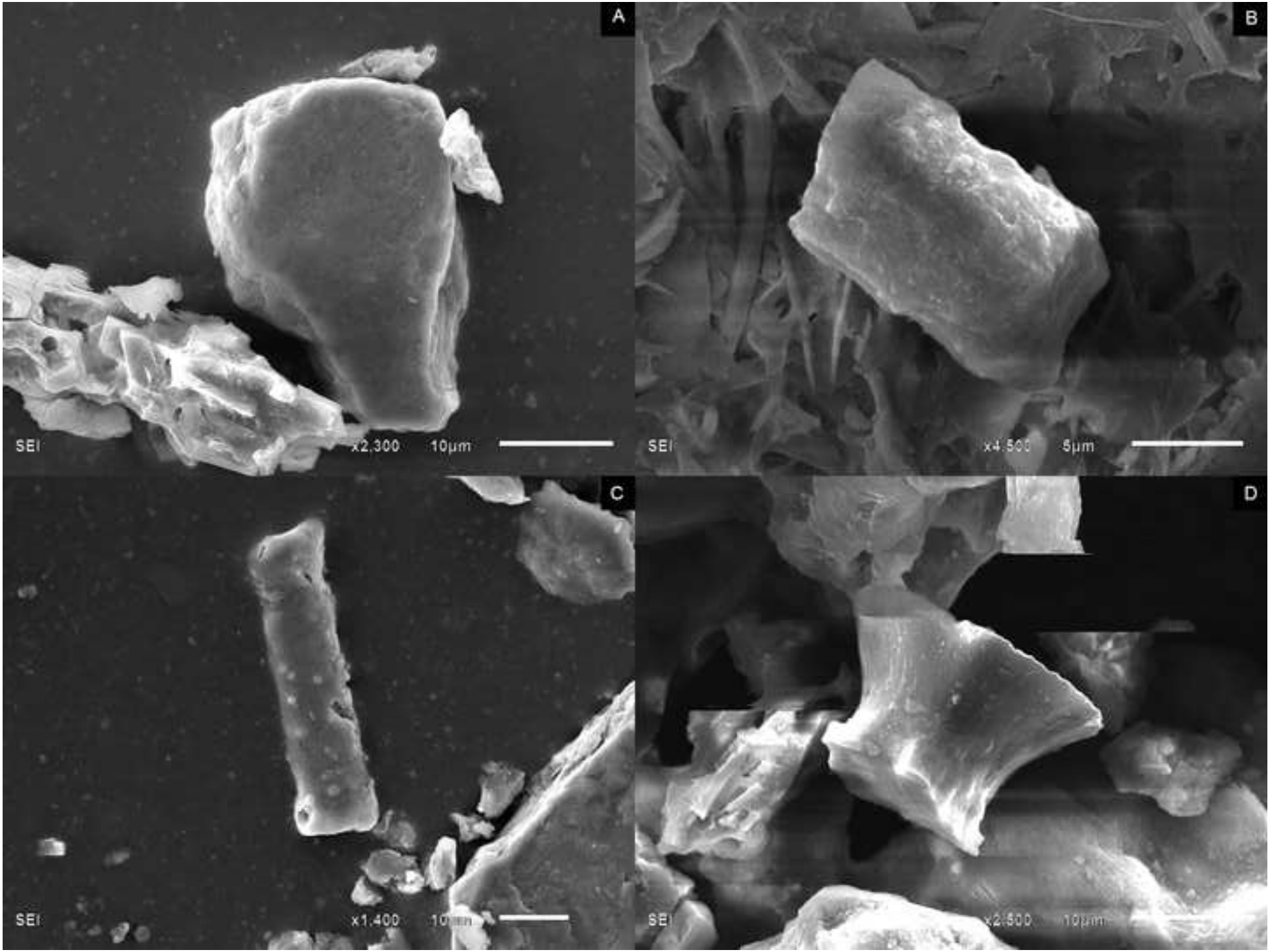

Figure 9

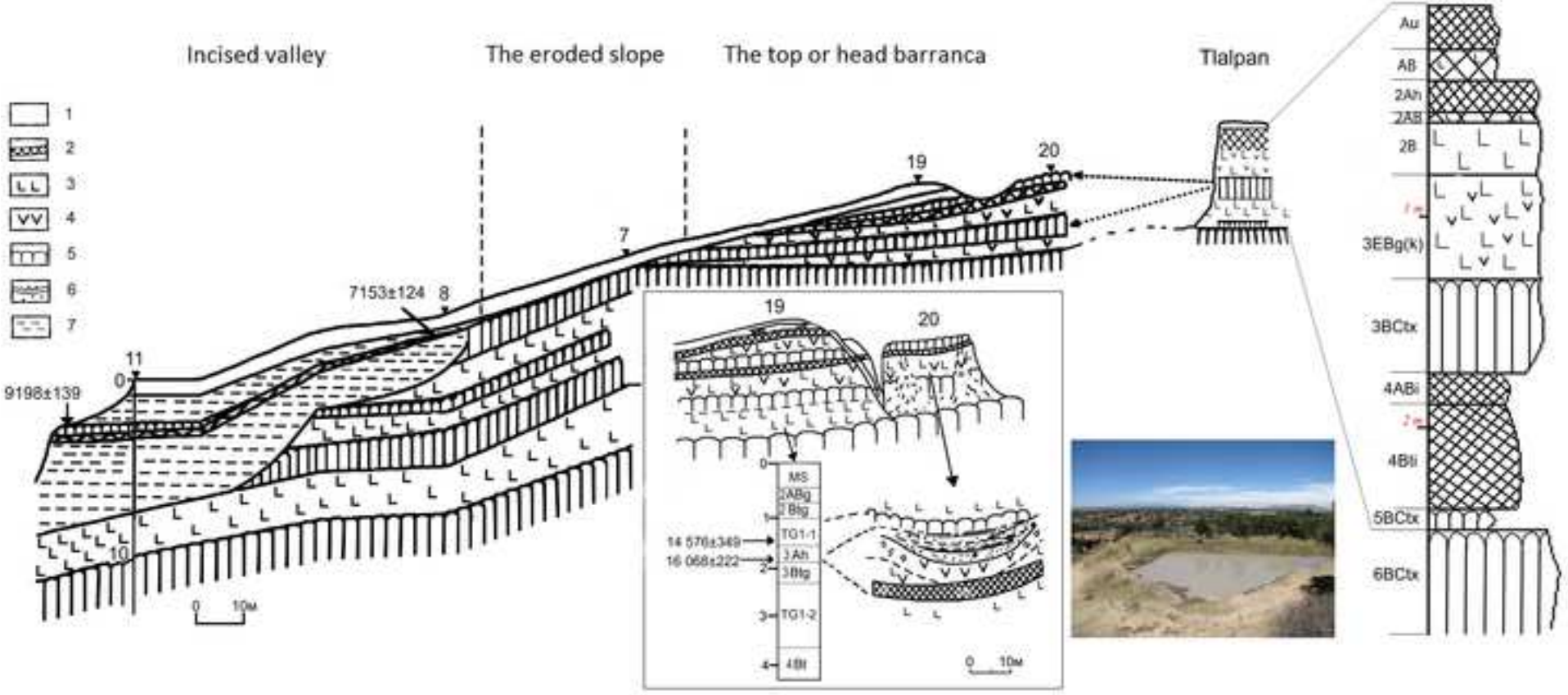
Incised valley
The eroded slope
The top or head barranca
Tlalpan
1
2
3
4
5
6
7
11
0
9198±139
10
7153±124
8
7
19
20
0 10м
MS
2ABg
2 Bfg
TG1-1
3 Ah
3Bfg
TG1-2
4Bl
14 576±349
16 068±222
Au
AB
2Ah
2AB
2B
3EBg(k)
3BCtx
4ABi
4Bti
5BCtx
6BCtx

Figure 10

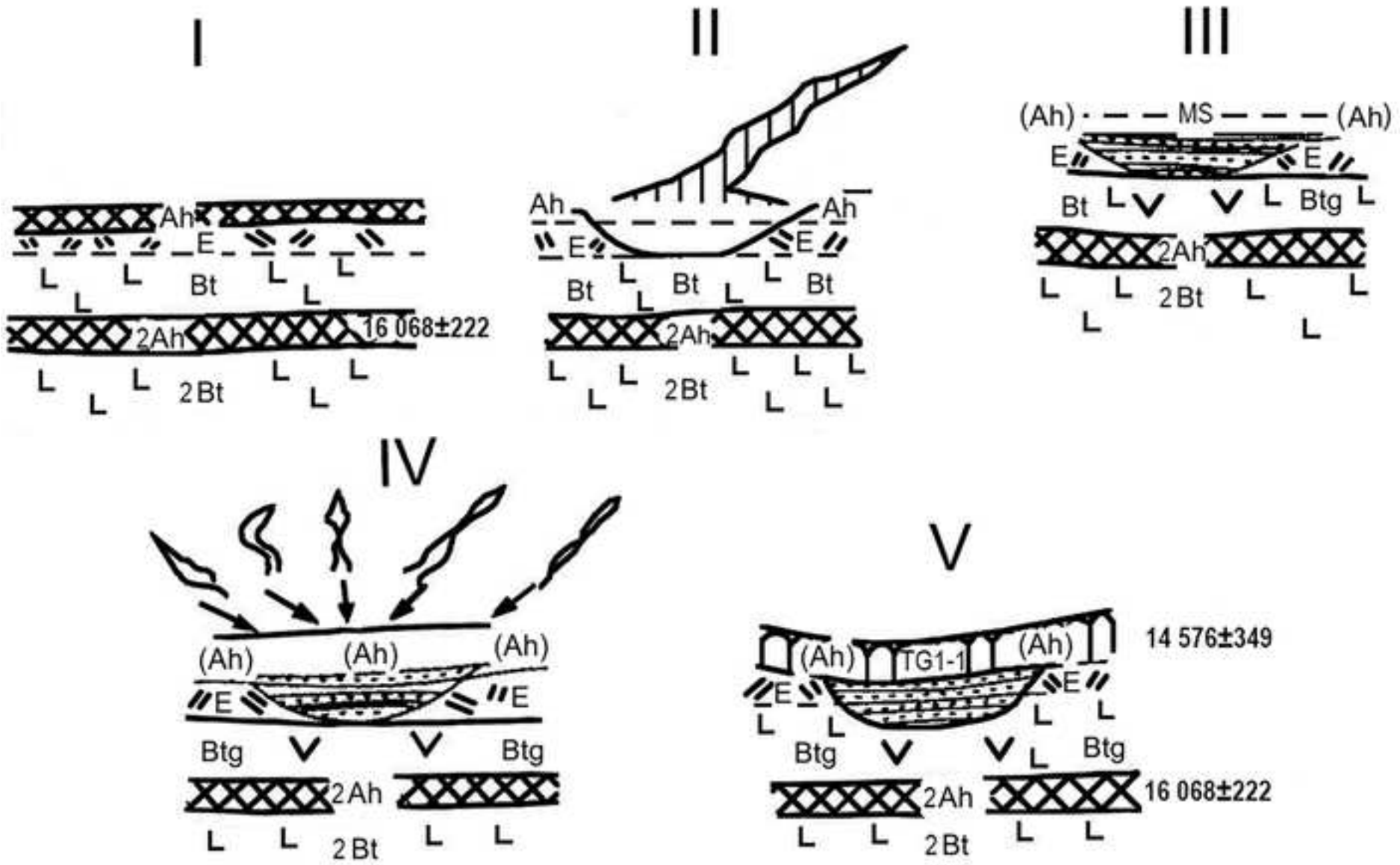
I
Ah
E
Bt
2Ah
16 068±222
2 Bt
II
Ah
Ah
E
E
Bt
Bt
Bt
2Ah
2Bt
III
(Ah)
MS
(Ah)
E
E
Bt
Btg
2Ah
2 Bt
IV
(Ah)
(Ah)
(Ah)
E
E
Btg
Btg
2Ah
2 Bt
V
(Ah)
TG1-1
(Ah)
14 576±349
E
E
Btg
Btg
2Ah
16 068±222
2 Bt

Figure 11